Method development for the analysis of bioactive lipids by liquid chromatography tandem mass spectrometry (LC-MS/MS)

Dissertation

zur Erlangung des Doktorgrades der Naturwissenschaften (Dr. rer. nat.)
der Naturwissenschaftlichen Fakultät IV-Chemie und Pharmazie – der
Universität Regensburg

vorgelegt von

Max Scherer

aus Hamburg

2010

Die vorliegende Arbeit entstand in der Zeit von November 2007 bis September 2010 in der Abteilung für Klinische Chemie und Laboratoriumsmedizin des Klinikums der Universität Regensburg unter der Anleitung von Prof. Dr. G. Schmitz.

Das Promotionsgesuch wurde eingereicht im September 2010

Tag der mündlichen Prüfung: 9.11.2010

Prüfungsausschuss:

Prof. Dr. J. Wegener   (Vorsitzender)

Prof. Dr. O. S. Wolfbeis   (Erstgutachter)

Prof. Dr. G. Schmitz   (Zweitgutachter)

Prof. Dr. F.-M. Matysik   (Drittprüfer)

Danksagung

Zum Gelingen dieser Arbeit haben viele Leute beigetragen durch wertvolle Ratschläge, wissenschaftliche Diskussionen, tatkräftige Unterstützung und einer gehörigen Portion Geduld:

Schließlich danke ich auch allen Freunden und Bekannten für ihre Unterstützung während dieser Zeit.

TABLE OF CONTENTS

1   General Introduction

1.1   Mass spectrometry of lipids

Complex lipids such as glycerophospholipids and sphingolipids, in contrast to proteins, are composites of a wide range of building blocks. Permutations that may arise from lipid building blocks give rise to more than a dramatic number of structures that can be present in a given cell or tissue extract (1). Today about 1000 lipid species can be quantified from the postulated 9000 – 10000 that may exist in mammalian systems. This multitude of lipid species can't be currently identified due to either a lack of sensitivity of MS-methods and preanalytics, or a lack of specificity of the current methods. The need to develop analytical tools that can readily tackle such a diverse range of molecular structures is a key reason that lipidomics has lagged behind her sister discipline proteomics. In lipidomics, mass spectrometry has been deployed in two ways, namely targeted lipidomics, which focuses on the identification and quantification of a single lipid class or subset of lipids in a tissue or cellular extract, and the untargeted lipidomics, which aims to identify and quantify all the lipids in a given biological matrix (2). The present work focuses on the targeted lipidomics approach for the analysis of minor, regulatory sphingolipid and glycerophospholipid species as well as for bile acid analysis.

1.1.1   Electrospray Ionization (ESI)

Early analysis of complex, high-molecular-weight lipids was conducted by fast atom bombardement (FAB) MS. FAB has made a major contribution to lipid MS, but was fundamentally limited by low overall sensitivity, the presence of matrix ions, and significant in-source fragmentation that precluded quantitative analysis (3). The application of ESI-MS to the analysis of lipids solved these problems. In contrast to FAB, ESI is a soft ionization technique. It produces protonated, deprotonated or adduct ions (e.g. Na^+, Li^+, NH_4^+) and only a negligible percentage of in-source fragmentation. Additionally, ESI-MS shows an increase of two to three orders of magnitude in sensitivity over FAB (4). Therefore, ESI has given rise to two main approaches for lipid analysis, namely online high-performance liquid chromatography-mass spectrometry (HPLC-MS) and direct infusion ESI-MS (shotgun

lipidomics). HPLC-MS is the technique of choice for the analysis of low-abundance signaling lipids such as sphingosine-1-phosphate (S1P), ceramide-1-phosphate (Cer1P) and lysophosphatidic acid (LPA).

In summary, the application of ESI-MS as a soft ionization technique, originally developed for macromolecules (5), was an important breakthrough in the analysis of lipids. Especially, limits of detection were diminished to the femto molar rrange, using ESI-MS.

1.1.2 Tandem mass spectrometry in lipidomics

Triple quadrupole tandem MS is the most commonly used technique in the field of targeted lipidomics. The combination of soft-ionization methods such as ESI with tandem MS has undoubtedly been the most significant contribution to recent advances in lipidomics. Tandem MS is a reliable diagnostic tool for the structural elucidation of lipids, and the use of related scanning approaches [e.g., precursor ion and neutral loss scans and multiple reaction monitoring (MRM) (Fig. 1)] has significantly enhanced analytical sensitivity in both targeted and untargeted lipidomics (3).

In targeted lipidomic approaches, the infusion of crude lipid extracts into the MS and the ionization via ESI can result in mass spectra with isobaric species and a high chemical noise. The specific fragmentation pattern by collision induced dissociation (CID) allows specific determination of each lipid class and species with significantly reduced noise (Fig. 1). Brugger et al. (6) demonstrated that the use of specific precursor ion and neutral loss scans on triple quadrupole mass spectrometers is a powerful tool for the analysis of phospholipids in complex lipid extracts. Subsequent investigations of the fragmentation behavior of ionized lipids have led to a broad array of potential precursor ion and neutral loss transitions.

a Normal

Quadrupole$_1$ Quadrupole$_2$ Quadrupole$_3$
                       (collision cell)

| All ions transmitted | → | All ions transmitted | → | Scan |

b Product ion

| Fixed | → | CID | → | Scan |

c Precursor ion

| Scan | → | CID | → | Fixed |

d Neutral loss or neutral gain

| Scan | → | CID | → | Scan |

e Multiple reaction monitoring

| Fixed | → | CID | → | Fixed |
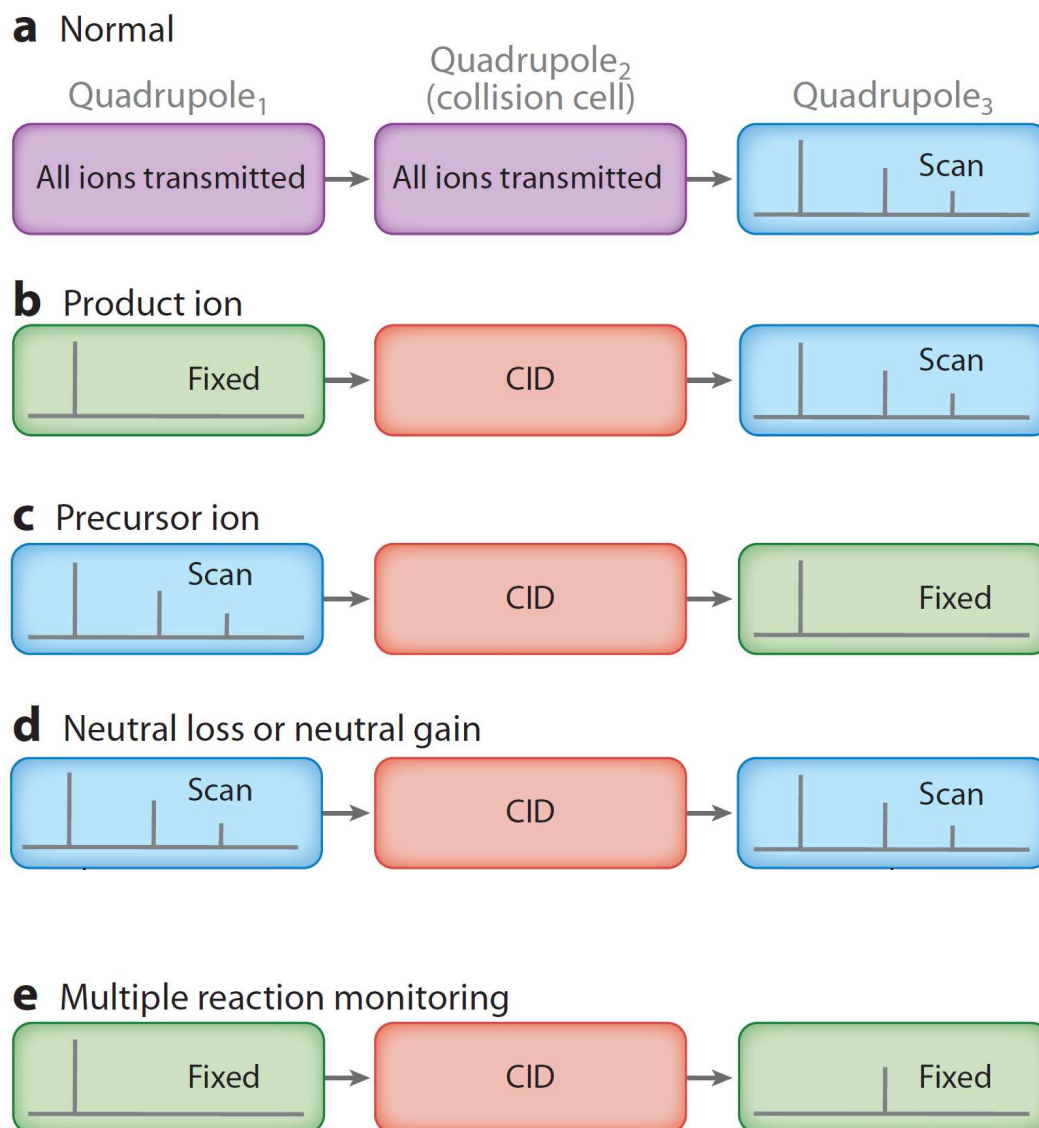
Fig. 1. Schematic representation of the configuration of a triple quadrupole MS for scan types commonly employed in lipidomic analysis, including (a) normal, (b) product ion, (c) precursor ion, (d) neutral loss or neutral gain, (e) multiple reaction monitoring (MRM) Adapted from Blanksby et al. ([3])

The specificity and sensitivity of online HPLC-MS applications are enhanced significantly by the use of MRM, in which a triple quadrupole MS is programmed to a mass transition that is specific to target lipid species. In MRM experiments, a signal is detected only if an ionized lipid has the prescribed *m/z* ratio for both the precursor and the product ion, thus minimizing chemical noise. In this configuration, up to 100% of the target ions entering the instrument can be detected, leading to increased sensitivity and allowing detection and quantification of lipids at femto molar levels.

Therefore a large number of MRM transitions are necessary to monitor all lipid species in a single chromatogram.

1.1.3 Linear ion trap mass spectrometry

Due to their versatility, quadrupole linear ion trap (QLIT) mass spectrometers are becoming more and more popular in the growing field of lipidomics. The combination of triple quadrupole MS with LIT technology is particularly interesting, because Q_3 (Fig. 1) can be either used in the classical scan-mode or as a trapping device. Q_0, which is generally used to focus ion before entering Q_1, can be also used as ion trap. Ions accumulate in the Q_0 region while the Q_3 trap is scanning ions during ion trap experiments. Thus, all specific scan functions of the triple quadrupole such as product ion, neutral loss, precursor ion, and MRM mode (Fig. 1) are maintained along with and in combination with the trap scan modes ([7]). The term 'enhanced' is always used when Q_0 accumulate ions and Q_3 is operated as an LIT. Basically QLIT exhibits no new scan functions, however scan combinations of triple quadrupole mode and trap mode can be performed in the same LC-MS run leading to increased sensitivity and specificity. In lipidomics analysis the linear ion trap is used for qualitative analysis ([8]), whereas quantitative analysis is performed in the MRM-mode ([9-11]). The following QLIT scan modes are the most commonly used for lipidomic analysis.

Enhanced MS mode

The enhanced MS (EMS) mode also produces a conventional mass spectrum but with increased sensitivity as a result of ion trapping in Q_3 while ions accumulate in Q_0. Typically, ions within a defined mass range are collected in Q_3 for a specified time and are then scanned at specific scan rates. Trap fill times in practice are in the range of 100 - 500 ms. Scanning rates of the LIT are 250, 1000 and 4000 Da/s, with the resolution being dependent on the scanning speed. The EMS scan is particularly interesting for lipid species identification using information dependent acquisition and it is often performed before the enhanced product ion scan (see Chapter 2.3.5.).

Enhanced product ion mode

In the enhanced product ion mode (EPI), the selection of the precursor ion is performed in Q_1 (Fig. 1). Afterwards, CID occurs in the collision cell (Q_2), and fragment ions are trapped in Q_3, operated as LIT. These fragment ions are scanned at specific scan rates in Q_3, resulting in increased sensitivity compared to classical product ion spectra.

MS^3 mode

In the MS^3 mode, accelerated precursor ions selected by Q_1 are fragmented in the collision cell (Q_2). The fragments and the residual precursor ions are transmitted into Q_3, where they are trapped for several ms. The next-generation precursor ion is then isolated within the LIT. Fragmentation in the LIT occurs via excitation by a distinct frequency to give the sequential product ion spectrum.

Information-dependent acquisition

IDA is a procedure, that combines two or more different scan modes in a sequential fashion for the same LC-MS run. The first scan is defined as the survey scan (e.g. EMS), where data are processed to determine the ions of interest based on predefined selection criteria. If the selection criteria are fulfilled, a second scan (e.g. EPI) is performed. Ions of interest can then be further processed through an additional IDA by a third MS scan mode (e.g. MS^3) (for an example see chapter 2.3.5.).

1.2 Chromatography

Although shotgun or direct infusion MS offers some advantages for the analysis of lipids from complex mixtures, there are limitations in its use. The presence of isobaric species, ion suppression, and exact lipid identification requires a different analytical approach. Some of these problems can be solved by interfacing HPLC with on-line ESI-MS.

Generally, the the selection of an appropriate chromatographic strategy is a major challenge in targeted lipid species. A set of non-naturally occurring internal standards is used for quantification. Frequently, non-naturally occurring short-chain lipid species are applied, since stable-isotope-labeled internal standards are not commercially available. Co-elution of analytes and internal standards is of major

importance, especially if gradient elution is applied. Basically, HPLC-MS analysis of lipid species can be categorized into three chromatographic principles. These are discussed in the following.

Reversed-phase chromatography

A combination of reversed phase (RP) HPLC and MS allows detailed analysis of individual molecular species with a high precision in a targeted approach. However, since RP-chromatography shows chain-length dependent lipid species separation within a lipid class, co-elution of analytes and internal standards may not be accomplished (12-16). Additionally, RP-chromatographic MS methods suffer from long run times. These exclude such methods from high sample throughput.

Normal-phase chromatography

The opposite chromatographic strategy is normal phase (NP) chromatography. 'Classical' normal phase chromatography offers polar head group specific separation, which leads to co-elution of lipid species within each lipid class. However, classical NP chromatography may be impaired by limited reproducibility and insufficient peak shapes. Moreover, the use of apolar solvents may not provide optimal ionization conditions for ESI.

Hydrophilic interaction chromatography

Hydrophilic interaction chromatography (HILIC) combines the separation principle of 'classical' NP-chromatography with the use of polar solvents, which are commonly used for RP-chromatography. These two key features provide polar head group specific separation of lipid classes i.e. co-elution of lipid species within each lipid class. Furthermore, polar solvents for chromatographic separation provide optimal ionization conditions for ESI and therefore an increase in sensitivity.

1.3 Biological background

All eukaryotic cells are surrounded by a membrane composed of a lipid bilayer, whose chemical nature and essential role in cell permeability were first proposed around a hundred years ago. Today it is known that there are four major classes of lipids, i) neutral lipids, such as triacylglycerols, which serve primarily to store energy; ii) glycerolipids, the major component of plasma membrane lipids that serve as substrates for bioactive lipids including diacylglycerol (DAG) and phosphoinositides; iii) sphingolipids, which also serve membrane and singnaling functions; and iv) sterols, which function in membrane structure and fluidity, as well as hormone production and cell and organism regulation ([17]) (Fig. 2).

Glycerolipid   **Sphingolipid**   **Sterol**

R^{1-3} = Fatty acid; H

R^1 = e.g. phosphate, choline, H
R^2 = fatty acid
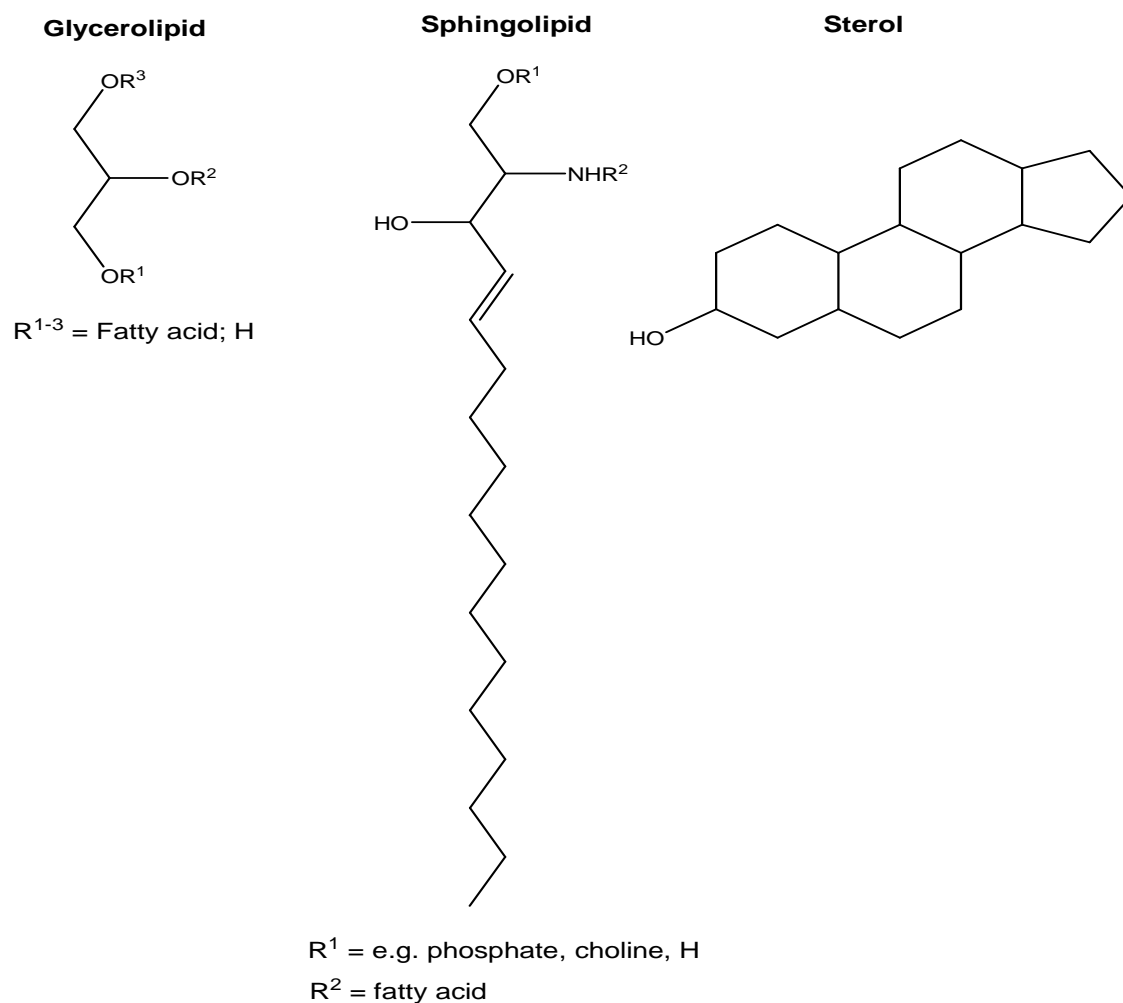
Fig. 2. General chemical structures of the three major classes of lipids in an eukaryotic cell membrane

However, intensive research on lipid metabolism and function has revealed that imbalances of the major lipid signaling pathways contribute to disease progression in chronic inflammation, autoimmunity, cancer, atherosclerosis hypertension, heart hypertrophy, and metabolic and degenerative diseases ([18]).

1.3.1 Glycerophospholipids

Glycerophospholipids (GP) are among the principal structural components of cells, and contain a highly diverse group of biological active molecules with a large number of molecular species. Beside their cell membrane barrier function, some members of the GP subclasses are mediators of molecular signaling for numerous cellular functions ([19]). A third and usually overlooked function is energy storage in the form of fatty acyl components, which is important under extreme conditions such as starvation ([20]). The present work focuses on a subclass of GPs, the so called polyglycerophospholipids, including phosphatidylglycerol (PG), bis(monoacylglycero)phosphate (BMP) and cardiolipin (CL) (Fig. 3).
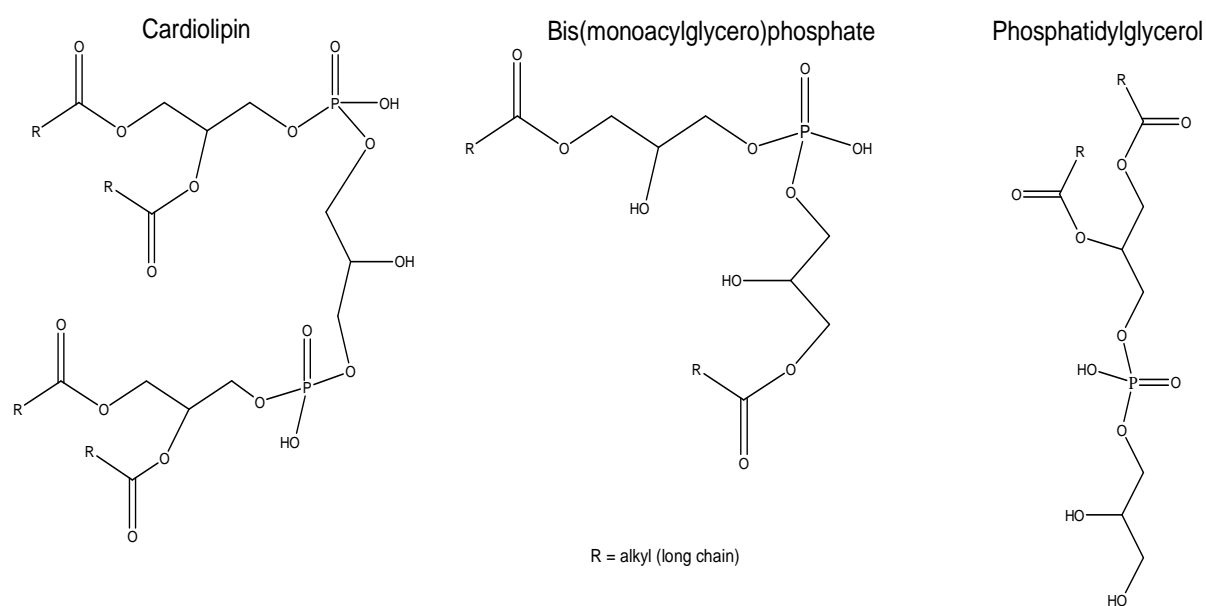
Fig. 3. Structures of polyglycerophospholipids

1.3.1.1 The metabolism of polyglycerophospholipids in mammalian cells

Phosphatidylglycerol is synthesized at the cytosolic side of the endoplasmatic reticulum (ER) and mitochondria as a common precursor for BMP synthesis in endolysosomes and CL synthesis in inner mitochondrial membranes.

Biosynthesis of PG in mammalian cells occurs via the cytidinediphosphate-diacylglycerol (CDP-DG) pathway, first elucidated by Kennedy and coworkers in 1963 (21). Phosphatidic acid (PA) serves as precursor for PG biosynthesis. The first step is the conversion of PA to CDP-DG by the enzyme CDP-DG synthase, which is localized in both mitochondria and microsomes (Fig. 4) (22). Subsequently, glycerol-3-phosphate and CDP-DG are converted to phosphatidylglycerophosphate (PGP) by the sequential action of PGP synthase, followed by dephosphorylation by a yet unknown phosphatase to form PG (22). Finally, CL is synthesized by condensation of PG and one molecule CDP-DG at the mitochondrial inner membrane, a reaction catalyzed by the enzyme CL-synthase. In contrast, the biosynthetic pathway of BMP remains unknown and needs to be investigated.
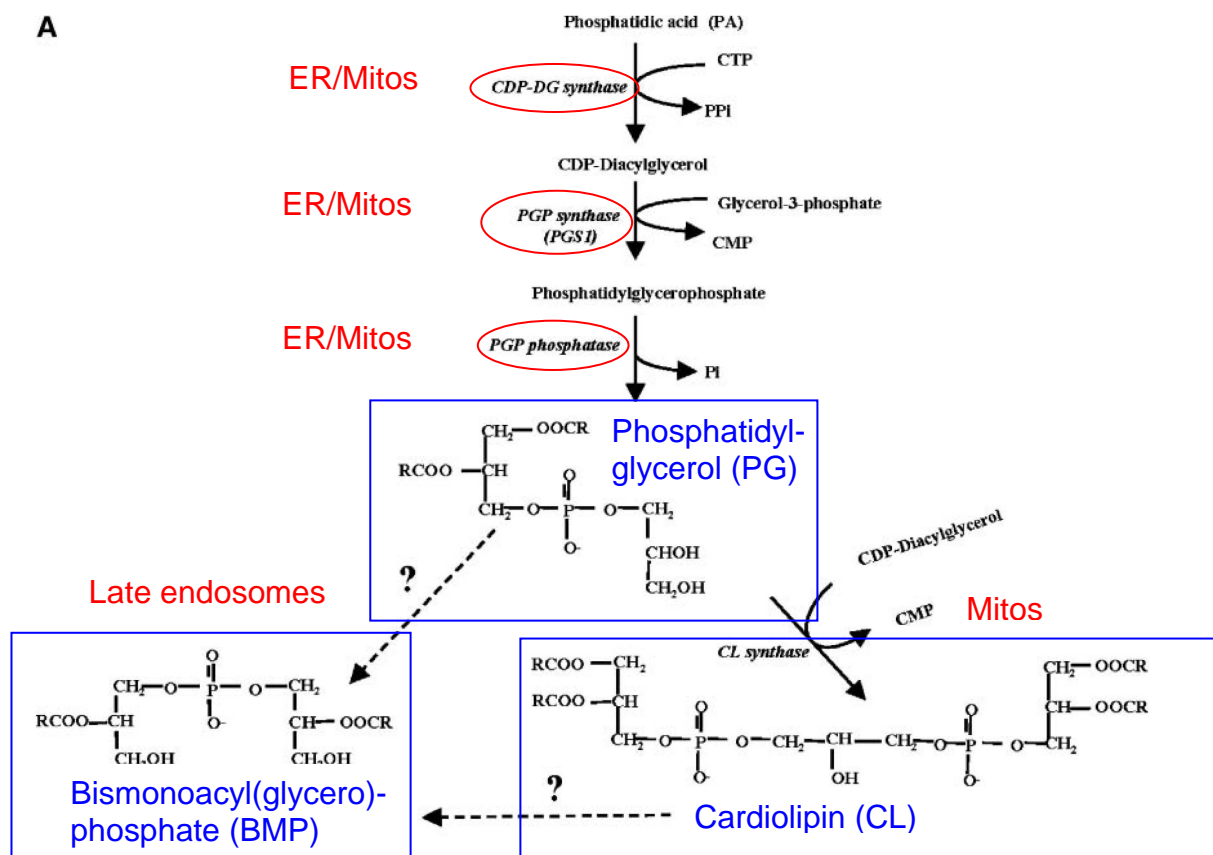
Fig. 4. Biosynthetic pathway of polyglycerophospholipids in mammalian cells. Adapted and modified from Hullin-Matsuda et al. (23).

Fig. 5. Possible remodeling pathways of CL in mitochondria. Adapted and modified from Hullin-Matsuda et al. ([23](#)).

Two enzymatic activities acting in CL remodeling have been described to date in the mitochondria (Fig. 5): 1) Tafazzin (TAZ) is a mitochondrial Coenzyme A (CoA)-independent, acyl-specific phospholipid transacylase with a substrate preference for CL and phosphatidylcholine (PC), 2) MLCL AT is a mitochondrial monolysocardiolipin (MLCL) acyltransferase requiring acyl-CoA (preferentially unsaturated acyl-CoA, like linoleoyl-CoA in the transfer of acyl chain to MLCL).

The remodeling pathway also involves phospholipase A activity (like mitochondrial phospholipase A2) to deacylate CL into MLCL and acyl-CoA: lysophosphatidylcholine acyltransferase (LPCAT) to reacylate lysophosphatidylcholine (LPC) ([22;23](#)).

1.3.1.2 The function of polyglycerophospholipids

Phospholipids play an important role to maintain the structural integrity of biological membranes. These membranes compartmentalize the cell, which is essential to create different environmental conditions, such as pH and ion gradients, required for enzyme specificity and substrate/product specificity.

Polyglycerophospholipids are widely distributed in animals, plants and microorganisms. PG can be found as a minor component of cellular phospholipids, mostly at the cytosolic side of the ER and mitochondria. BMP depicts less than 1% of total phospholipids in animal tissues, except for alveolar (lung) macrophages where it

makes 14-18% of total phospholipids (20). It is found at high concentrations in the lysosomal compartment, especially in late endosomes and in the acidic vesicular transport complexes (endosomal sorting complex required for transport (ESCRTs)), where BMP is involved in the formation of multivesicular membranes characteristic of late endosomes (23). Furthermore, BMP plays an important role during SL degradation. SL degradation occurs on the luminal surface of intra-endosomal and intra-lysosomal membrane structures (Fig. 6). During endocytosis, intra-lysosomal membranes are formed, and prepared for digestion by a lipid-sorting process during which their cholesterol content decreases and the concentration of the negatively charged BMP increases. Hence, SL degradation requires anionic phospholipids like BMP, and therefore SL and GL metabolism is linked (24). BMP has also been shown to regulate cholesterol transport by acting as a collection and distribution device (25). BMP plays an important role in the efficient partitioning of cholesterol in lipid membranes and the subsequent transport of cholesterol out of the internal membranes of the multivesicular bodies. Accumulation of cholesterol within BMP-rich internal membranes is predicted to alter membrane properties (26). Thus, BMP is a critical component of the endosomal/lysosomal network and essential for the correct function of this system (26).
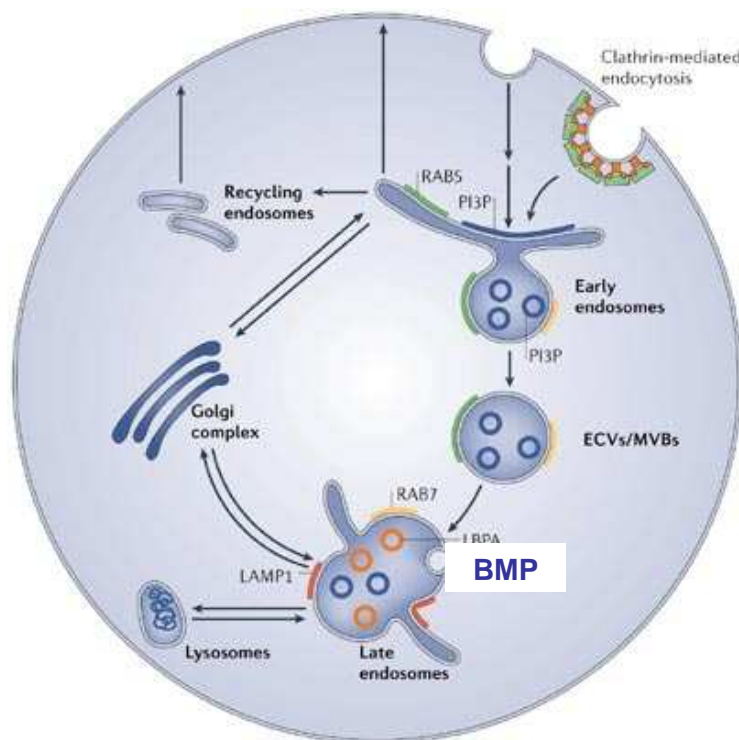
Fig. 6. Endocytosis and role of BMP. Adapted and modified from Matsuo et al. (27).

In animals, CL is found in highest concentrations in cardiac muscle, hence this lipid class was called cardiolipin, and is exclusively found in the mitochondria (28). CL is intimately involved in different cellular processes including stabilization of the electron transfer complex and therefore preventing mitochondrial apoptosis (28).

CL is involved in the transduction of electrons and the production of ATP via a complex mechanism (29). Recent studies by Jiang et al. (30) demonstrated that complete absence of CL in yeast mitochondria results in a partially defective protein import into mitochondria and a decreased mitochondrial membrane potential. These deficiencies are partially compensated by high levels of the precursor PG. However, the deficient ADP/ATP carrier activity and decreased mitochondrial membrane potential can not be restored through elevated levels of PG (30). Moreover, the unique structure of CL is suggested to function for the maintainance of the electron transfer complex for physiological ATP production (31).

Beside its function in energy metabolism, CL serves as a central switch in the mitochondrial apoptotic program, controlling the initiation of this process at different levels. CL is closely associated with cytochrome *c* at the outer leaflet of the mitochondrial inner membrane. While CL peroxidation may be crucial for enabling cytochrome *c* dissociation from the mitochondrial inner membrane, cytochrome *c* itself catalyzes CL peroxidation. Moreover, peroxy-CL directly activates the release of cytochrome *c* and other apoptogenic factors from the mitochondria. CL is also directly involved in mitochondrial outer membrane permeabilization by enabling docking and activation of pro-apoptotic Bcl-2 proteins. It appears therefore that CL has multiple roles in apoptosis and that CL metabolism contributes to the complexity of the apoptotic process. This makes CL a potentially interesting target for therapeutical intervention in diseases in which cell death is deregulated, such as cancer (28;32;33).

1.3.1.3   *Role of polyglycerophospholipids in specific pathologies*

Peter Barth and his colleagues described about a quarter of a century ago, a Dutch family with a three-generation history of infantile cardiomyopathy, in which abnormal mitochondria were implicated (34). The disorder showed an X-linked recessive mutation in the taffazin gene, clinically characterized by heart failure, myopathy, neutropenia and abnormal growth (35). This disorder, known today as Barth syndrome, is characterized by an alteration in CL remodeling.

At the biochemical level, Barth syndrome is characterized by decreased levels of CL ([28](#)). Under normal conditions, CL is degraded to MLCL and then converted back into CL in order to exchange its fatty acids (Fig. 4). Barth fibroblasts and taffazin-deficient yeast showed highly increased levels of MLCL. In addition, a shift is observed in the degree of unsaturation of CL acyl chains ([36;37](#)). This observation in conjunction with the low CL levels suggested a decline in the rate of reacylation relative to the rate of deacylation ([34](#)). Therefore, the abberrations in CL are used as a diagnostic marker, which can be used to quickly screen for Barth syndrome ([28](#)). In addition Barth lymphoblasts, showed changes in the composition of all major mitochondrial phospholipids, PC, phosphatidylethanolamine (PE) and CL ([38](#)). The complementary nature of the fatty acid alterations in CL and PC suggested that fatty acid transfer between these two lipids was inhibited in Barth syndrome ([38](#)).

The pathogenesis of Barth syndrome is still not well understood. It has been demonstrated that the activity of selected respiratory chain complexes is reduced in muscle biopsies of Barth syndrome patients. Recent studies have confirmed these findings and have shown that the reduced respiratory chain activity is caused by reduced stability of the oxidative phosphorylation supercomplexes, and therefore the loss of ATP production. This reduction in energy production is likely to be the primary cause of the (cardio)myopathy ([28](#)).

Beside the Barth syndrome, no other pathological conditions have been described which have a primary deficiency in CL metabolism due to mutations in a single gene. Several pathological conditions, however, have been linked to CL abnormalities, including Tangier disease, diabetes and heart disease ([39](#)).

Tangier disease (TD) is an inherited disorder of lipid metabolism characterized by very low high density lipoprotein (HDL) plasma levels, cellular cholesteryl ester accumulation and reduced cholesterol excretion in response to HDL apolipoproteins. Molecular defects in the ATP binding cassette transporter 1 (ABCA1) have recently been identified as the primary cause of TD. ABCA1 plays a key role in the translocation of cholesterol across the plasma membrane, and defective ABCA1 causes cholesterol storage in TD cells. Phospholipid analysis showed a three- to fivefold increase in the levels of CL, MLCL and dilysocardiolipin ([40](#)). Therefore, it is suggested, that increased CL levels result in decreased mitochondrial cholesterol oxidation via the enzyme cholesterol 27-hydroxylase, and thereby a reduction of oxysterols which enhances cholesterol solubility and stimulate cholesterol efflux.

The Niemann Pick disease (NPD) is another cholesterol storage disorder. Patients with NPD Types A and B have an inherited deficiency of acid sphingomyelinase activity, which leads to accumulation of sphingomyelin in late endosomes/lysosomes (41). However, also other lipids particularly BMP has been found to accumulate in fibroblasts from patients with NPD (41). Genetic analysis revealed loss-of-function mutations in NPC1 and NPC2 genes as the molecular triggers for the disease. Although the precise function of these proteins has not yet been clarified, recent research suggests that they orchestrate cholesterol efflux from late endosomes/lysosomes. NPC protein deficits result in impairment in intracellular cholesterol trafficking and deregulation of cholesterol biosynthesis. Disruption of cholesterol homeostasis is also associated with deregulation of autophagic activity and early-onset neuroinflammation, which may contribute to the pathogenesis of NPC disease (41).

1.3.1.4 *Quantitative analysis of cardiolipin and metabolites by tandem mass-spectrometry*

Electrospray ionization mass spectrometry (ESI-MS) has emerged as a powerful tool for the qualitative and quantitative analysis of complex phospholipids (2;42). A number of methods were described for CL analysis based either on direct MS (43-45) or LC-MS (8;22;46;47). Since BMP and PG are structural isomers (Fig. 4), a chromatographic separation for the simultaneous, mass spectrometric analysis for these lipids in the presence of each other is required (25). 'Classical' NP-chromatography may be hampered by limited reproducibility, insufficient peak shapes and solvent mixtures incompatible for ESI-MS-analysis. Therefore RP-chromatography up to date was prevalent for the simultaneous analysis of BMP and PG species (25) or CL (8;22). However, since RP- chromatography shows chain length-dependent separation, co-elution of analytes and internal standards may not be accomplished. Nevertheless, co-elution is of major importance for compensation of matrix effects and varying ionization efficiencies, especially during gradient elution. Due to the fact that up to now, methods for the combined analysis of BMP, CL, PG, and PA species are lacking, and RP-chromatography might not solve this problem, development of novel methods are essential.

Additionally, MS-analysis of GP species may exhibit an isotope overlap due to a variable number of double bonds. A correction of this overlap is especially

important for high molecular weight lipids like CL. Most assays published up to now quantified CL from MS spectra which may be corrected by the isotope pattern of the molecular ion (2). Isotopic overlap in MS/MS experiments is more complex since isotope distributions of charged fragments and neutral fragments have to be considered (48). Omission of isotopic correction leads not only to mis-quantification but also to mis-identification of species.

Taken together, it is imperative to use structure specific and sensitive LC-MS/MS methods including isotopic correction, to investigate alterations in polyglycerophospholipid metabolism in patients.

1.3.2 Sphingolipids

1.3.2.1 Structure and metabolism

Sphingolipids (SLs) are structurally distinguished from other lipid classes by their sphingoid long chain base backbone, from which SLs derive their name (Fig. 2). As is the case for all membrane lipids, SLs are amphiphatic molecules that have both hydrophobic and hydrophilic properties. The biochemical pathways of SLs are well described (49;50). The intracellular sites of biosynthesis take place in the endoplasmic reticulum (ER), Golgi apparatus and lysosomes (49-51). De novo SL biosynthesis starts with the condensation of palmitoyl-CoA and serine (alternatively alanine and glycine can be transferred) catalyzed by three diefferent serine palmitoyl transferase (SPTLC 1-3) resulting in 3-ketosphinganine (Fig. 7). 3-Ketosphinganine is subsequently reduced to form sphinganine (SPA), which is then N-acylated by (dh)ceramide-synthases to form dhCer (50;51). In addition, Ceramide (Cer) can also be formed through the hydrolysis of more complex SLs, such as sphingomyelin (SM). Cer is the key molecule in the SL pathway and is the precursor for the following products:

- Cer can be glucosylated by the transfer of a UDP-glucose or UDP-galactose donor to form glucosylceramide (GluCer) or galactosylceramide (GalCer) from which higher glycosylated SLs are formed (50).
- Cer can be linked to phosphocholine via the enzyme SM synthase to form SM
- Cer is phosphorylated to form ceramide-1-phosphate (Cer1P).

- Cer can be deacylated to sphingosine (SPH) by ceramidases, from which various forms are known, acting either at neutral, acid or alkaline pH (52).

SPH produced from Cer can be phosphorylated to sphingosine-1-phosphate (S1P) by sphingosine-kinase (SK). Two mammalian isoforms of SKs are known, SK1 and SK 2 (53;54). Since S1P is an important signaling lipid, serving as first and second messenger, regulation of its intracellular level is critical. Thus S1P can be either degraded by S1P-phosphatase to form the precursor SPH, or by S1P-lyase, which yields hexadecenal and phospohethanolamine (55;56) (Fig. 3). However, platelets lack S1P-lyase activity (57) and have highly active SK, so they accumulate high concentrations of S1P (58).

HSAN1 is an inherited neuropathy found to be associated with several missense mutations in the SPTLC1 subunit of serine palmitoyltransferase. HSAN1 mutations induce a shift in the substrate specificity of SPT, which leads to the formation of the two atypical deoxysphingoid bases (DSBs) 1-deoxy-sphinganine and 1-deoxymethyl-sphinganine. Both metabolites lack the C1 hydroxyl group of sphinganine and can therefore neither be converted to complex sphingolipids nor degraded. Consequently, they accumulate in the cell (59).

In summary, the biochemical pathway of SL biosynthesis and degradation have been fully described (50;51;55;60;61). Since disturbances within the SL pathway are associated to several diseases (17), the next challenge in this area is to understand how these pathways are regulated and integrated in metabolism.
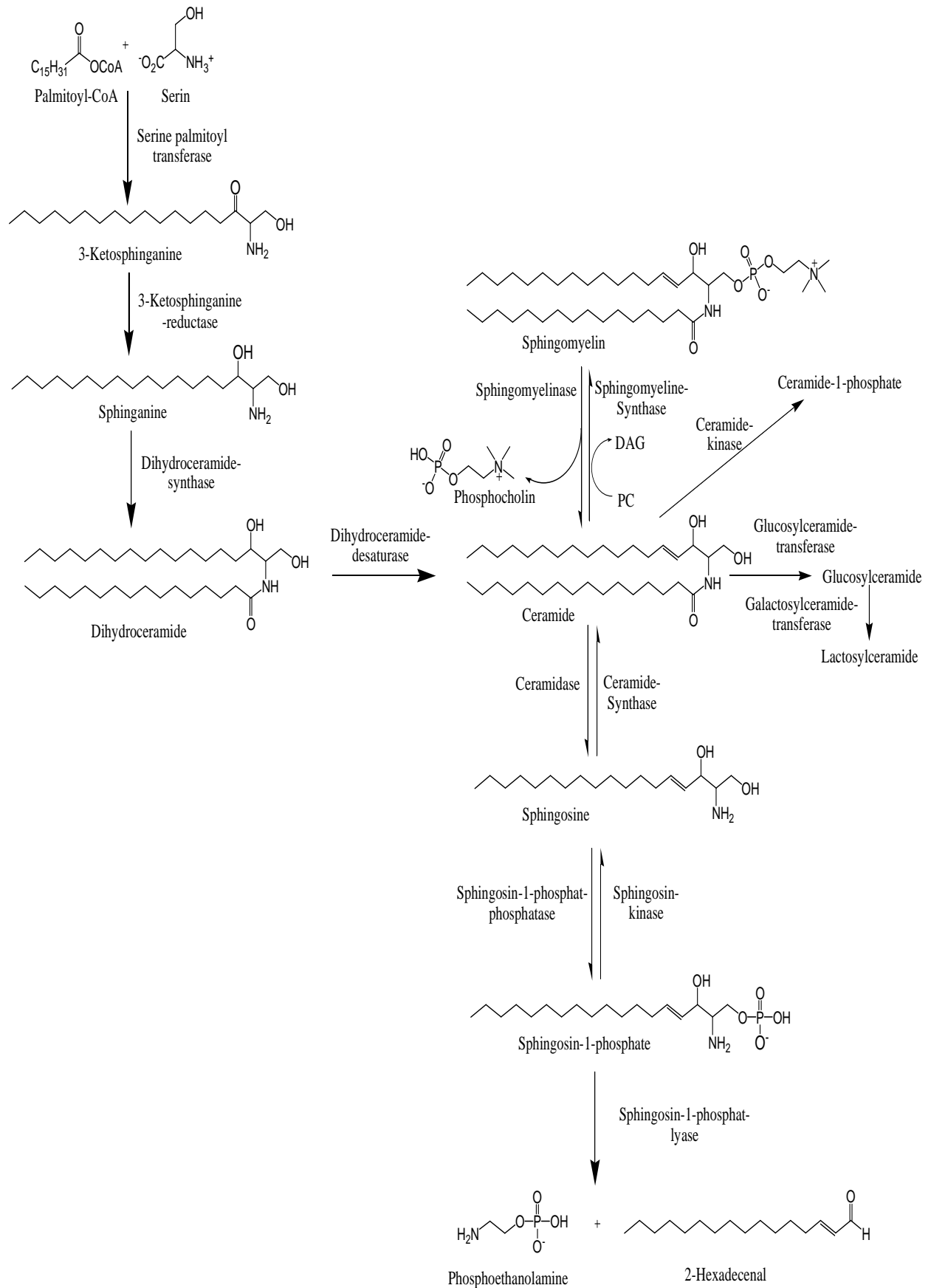
Fig. 7. Biosynthesis and metabolism of SLs

PC: Phosphatidylcholine; DAG: Diacylglycerol

1.3.2.2   Sphingolipids as bioactive molecules

The structural diversity of SLs is associated with equally diverse functions. Part of the reason for the recent explosion in SL biology is the role of these lipids in intracellular signaling, particularly of SPH, Cer, S1P, Cer1P and sphingosylphophorylcholine (SPC) (62). Cer, SPH and S1P are the best-studied bioactive SLs, and they exert opposite effects in many systems, with Cer and SPH usually inhibiting proliferation and promoting apoptosis, and S1P stimulating differentiation and suppressing apoptosis (56;62;63). Therefore, this so called "sphingolipid rheostat" can direct a cell towards either an apoptotic or a survival program (Fig. 8). It is well established that Cer signaling has been intimately involved in the regulation of cell growth, differentiation, senescence and apoptosis (51). Furthermore, Cer has several intracellular targets that mediate its apoptotic action, including the protein phosphatases, cathepsin and protein kinase. By contrast, specific intracellular targets of S1P have remained elusive. Moreover, subsequent release of S1P through membrane transporters might contribute to inside out protection against apoptosis through the stimulation of S1P receptors, the so called Edg-receptor family. Indeed, exogenous S1P has been shown to regulate the expression of pro apoptotic and anti apoptotic proteins (64). Thus, S1P can be seen as a tumor-promoting lipid involved in the regulation of proliferation. Therefore, S1P may be regarded as a biomarker for cancer (64).

Furthermore, beside the role as "cancer lipid", S1P regulates the induction of inflammation and atherosclerosis through the activation of specific G-protein-coupled receptors on the cells of the immune, cardiovascular and nervous system (65-67).
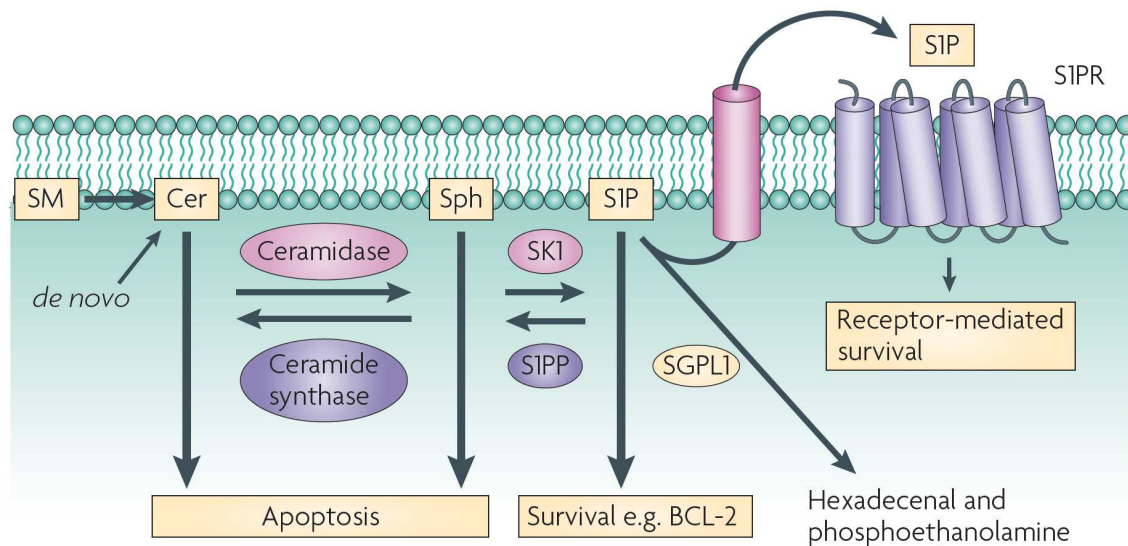
Fig. 8. The sphingolipid rheostat. Adapted from Pyne et al. (<u>64</u>)

More recent studies have broadened the attention to additional bioactive SLs such as Cer1P, GluCer and SPC. Cer1P has been implicated in playing roles in inflammation, proliferation and vesicular trafficking. The formation of arachidonic acid (AA) via the activation of phospholipase A$_2$ (PLA2) is the initial rate-limiting step in eicosanoid biosynthesis. Cer1P mediates the activation of PLA2 and therefore the release of AA in response to interleukin-β (<u>68</u>). Furthermore, Cer1P appears to act in a similar fashion to S1P. Thus, Cer1P has anti-apoptotic functions via the inhibition of protein phosphatase 1, which has been attributed to Cer induced apoptosis (<u>50</u>). Thus, both ceramide kinase and SK are emerging as key determinants of the balance between cell death and survival. GluCer has shown to be involved in post-Golgi trafficking and in drug resistance (<u>50;69</u>).

Interestingly, SPC seems to have cell type specific functions. In some cell types, SPC elicit similar cellular responses to those of S1P but in other cells these two lipids have opposite effects (<u>70</u>).

1.3.2.3 *Sphingolipids in disease*

Within the past decade, real progress has been made in our understanding of how SLs contribute to disease processes, which is leading to novel therapeutic approaches based on interventions in SL homeostasis.

Since Cer, S1P and Cer1P are involved in cell death and survival, these lipids might be involved in the growth of cancer cells. These findings have led to the

realization that manipulating apoptosis via the inhibition or activation of distinct enzymes within the SL pathway (Fig. 5) could be a novel way of approaching cancer therapy. A number of studies have shown that Cer can have anti-carcinogenic activity. Direct administration of Cer analoga decreased tumor activity and therefore induced apoptosis in cancer cells ([70]). In addition, anticarcinogenic effects have been observed upon increasing Cer levels by slowing its conversion to GluCer via GluCer-synthase, or to SPH via ceramidases ([18;70]). Thus, a number of chemotherapeutic agents appear to be related to their ability to activate Cer-induced apoptosis. In contrast to Cer, S1P is a contributing factor in carcinogenesis ([17;64]). Further, human SK1 is upregulated in many cancers. SK1 upregulation often correlates with higher clinical grade and chemotherapy resistance, whereas inhibition of SK activity increases apoptosis and autophagy in cancer cells. Additional studies implicate SK1 in adhesion and migration of cancer cells, properties associated with metastatic potential ([71]). These findings demonstrate that SK1 functions as an oncogene ([71]) and therefore, SK became a target in cancer therapy.

Beside their role in cancer, emerging data support a function for SLs in metabolic diseases including obesity, diabetes, atherosclerosis and metabolic syndrome ([17]). Overnutrition increases plasma non-esterified fatty acids (NEFAs). As a consequence, increased palmitate concentrations induce de novo SL biosynthesis via action of SPTLC. Especially, aberrant Cer biosynthesis and therefore alterations in key Cer-mediated signaling pathways are associated to obesity and insulin resistance which causes type 2 diabetis ([17]). Moreover, the inflammatory factor (TNFα) has been shown to affect SL synthesis by routes that include SK ([55]). Recent data implicate S1P and Cer1P in inflammation. S1P is associated to inflammation via cyclooxygenase (COX-2) upregulation and subsequent production of prostaglandin E_2 (PGE_2). A particularly interesting series of studies demonstrated that a related SL metabolite, Cer1P, participates in regulating the AA cascade via activation of cytosolic phospholipase A_2 ($cPLA_2$), the major enzyme for pro-inflammatory AA production in cells ([17;55]). Thus, aberrant production of SLs might also promote inflammation.

Although roles for SLs in mediating apoptosis, cell proliferation and inflammation are increasingly well defined, other SL actions cannot be excluded from consideration in mediating metabolic disease pathology. In fact, recent data implicate SLs in other cell processes that will probably prove relevant to metabolic disease.

These functions include autophagy, an alternative route for cell death, atherosclerosis and mitochondrial function that is required for energy production. Further work is needed to elucidate these functions, mechanisms and contribution to the pathogenesis of metabolic syndrome (17;18).

SL content in various tissues undergoes dramatic alterations in several diseases. A lot of research in this area is rapidly developing with assistance of novel technologies, including lipid MS. This technology is just beginning to provide more information in the field of "sphingolipidomics".

1.3.2.4   Mass spectrometric analysis of sphingolipid species

During the last decade liquid chromatography coupled to MS/MS has become a powerful tool for SL analysis (12-15;72-78). However, either these methods do not cover a broad spectrum of SL metabolites or they show disadvantages like laborious sample preparation, time consuming LC-separation, high sample volumes or insufficient data validation. Furthermore these methods lack co-elution of internal standards and analytes. RP-chromatography in contrast to NP-chromatography, which offers polar head group specific separation, shows chain length-dependent separation of species (13;73;75;77). Especially for lipid analysis, coelution of lipid species and internal standards within a lipid class is of major importance, since many lipid species only differ by their chain length or saturation degree. Hence, commonly used RP-C18 columns (12-15;72;73;77) may lead to limited reproducibility and in mis-quantification.

Although analysis of the "sphingolipidome" by shotgun approaches has been recently demonstrated for yeast (79), an analysis of a more complex SL pattern in mammalian systems may be hampered, especially for minor metabolites, by signal suppressing matrix effects or lack of sensitivity (13;73;74). To understand regulatory and metabolic mechanisms involved in cellular SL homeostasis, specific, accurate and sensitive methods are necessary. Furthermore, "sphingolipidomic" studies in huge clinical trials require high sample throughput.

1.3.3 Bile acids

1.3.3.1 Structure and biosynthesis

Bile acids (BAs), together with cholesterol, phospholipids and bilirubin, comprise the principal constituents of bile (80). BAs were first isolated from bile early in the 19th century, and the field of bile acid chemistry preceded the development of classical biochemistry. Bile acids are amphipathic molecules with a steroid backbone that are synthesized from cholesterol exclusively in parenchymal cells (hepatocytes) of the liver and are subsequently stored in the gall bladder (81). The great number of BAs and bile alcohols with a surprising complexity in structure (Fig. 9) occurring in nature can be explained by the evolution of multiple biochemical pathways that serve to convert cholesterol, a poorly water soluble membrane lipid, into conjugated BAs or bile alcohols (82). BAs and alcohols are characterized by a highly water-soluble, amphipathic, membranolytic structure (Fig. 9). Beside their role as "cholesterol-solubilizer", BAs are involved in nascent bile formation and intestinal absorption of lipids and lipid-soluble molecules. Various transport proteins have been identified in the liver, which are tightly regulated by nuclear receptors such as the bile acid nuclear receptor Farnesoid X Receptor (FXR) and the Liver X Receptor (LXR) (83). Currently, BAs are also increasingly recognized as signaling molecules in a wide range of fields, such as energy homeostasis and metabolism of glucose and lipids. Bile acid-mediated activation of FXR is a major underlying pathway for these effects (80).
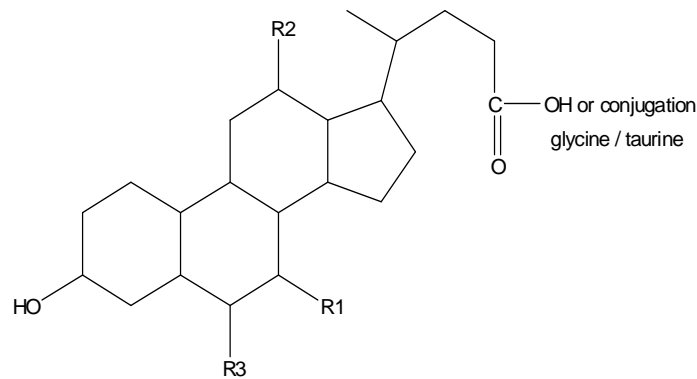
Bile acid species	R1	R2	R3
Cholic acid (CA)	OH	OH	H
Chenodeoxycholic acid (CDCA)	OH	H	H
Deoxycholic acid (DCA)	H	OH	H
Hyodeoxycholic acid (HDCA)	H	H	OH
Lithocholic acid (LCA)	H	H	H
Ursodeoxycholic acid (UDCA)	OH	H	H

Fig. 9. Structure and nomenclature of BAs.

BA synthesis is the primary pathway for cholesterol catabolism. Approximately 500 mg of cholesterol is converted into BAs each day in the adult human liver (80). BA biosynthesis involves modification of the ring structure of cholesterol, oxidation and shortening of the side chain, and finally conjugation of BAs to amino acids (84) (Fig. 10). The major primary BAs are CA and CDCA (85).
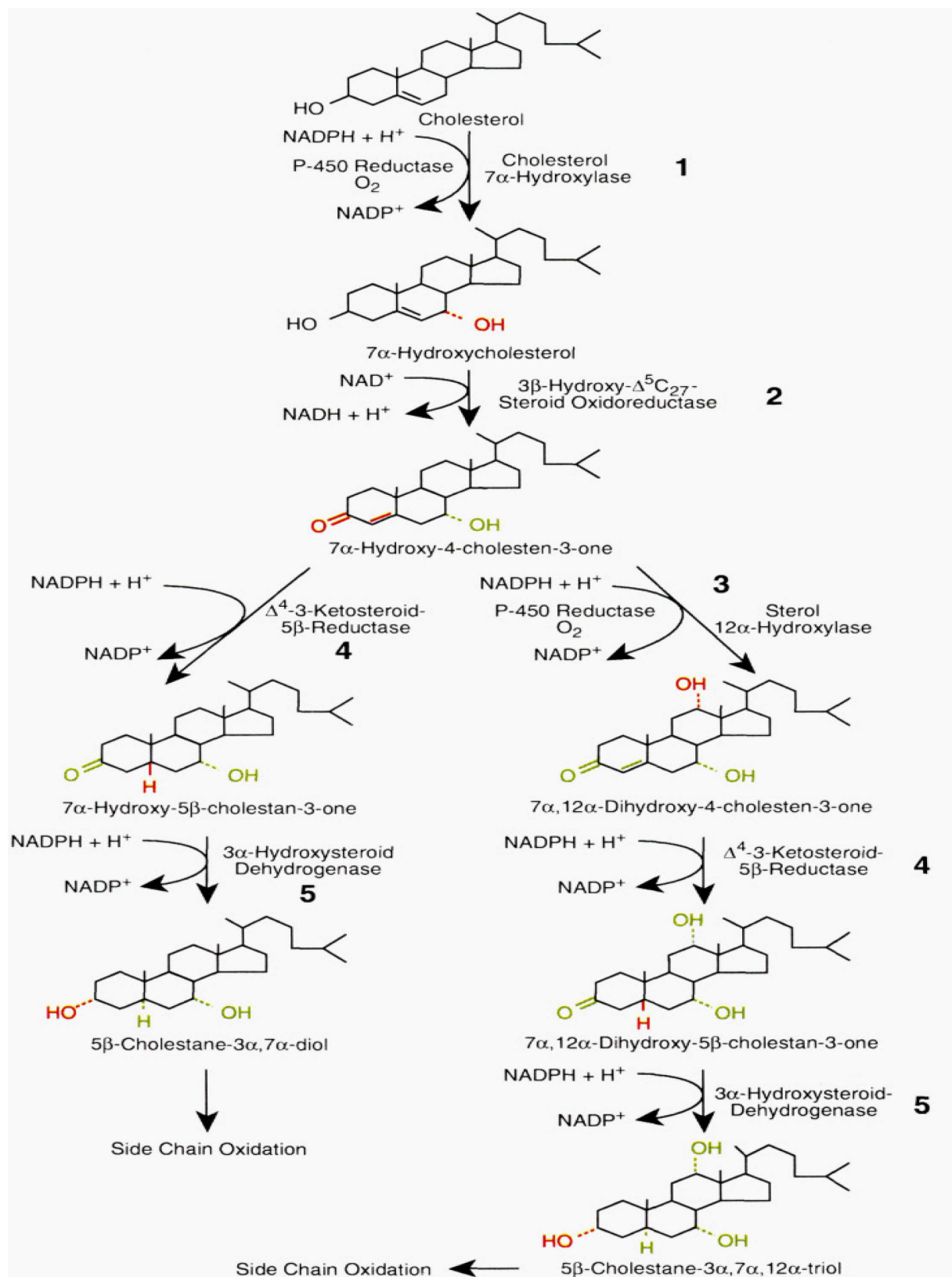
Fig 10. Biosynthesis of bile acids. Reactions are numbered in bold type. The modifications introduced by an individual enzyme are indicated in red on the product of the reaction. Cumulative changes to the ring structures are indicated in green.

Adapted from Russell et al. ([85]).

The steps leading to the formation of these molecules can be divided into two categories: those that modify the cyclopentanoperhydrophenanthrene ring or nucleus (Fig. 10) or those that oxidize and shorten the 8 carbon atom side chain of the sterol (not shown). The first step in modification of the ring structure (reaction 1, Fig 10) involves the introduction of a hydroxyl group at the position C-7 of cholesterol. This reaction is catalyzed by a unique cytochrome P-450 enzyme, cholesterol 7α-hydroxylase, and utilizes molecular oxygen, NADPH, and a protein cofactor, cytochrome P-450 reductase. In the second step of the BA pathway, 7α-hydroxycholesterol is acted upon by a microsomal 3β-hydroxy-C27- steroid oxidoreductase (reaction 2, Fig. 10). This reaction utilizes NAD$^+$ as a cofactor. The 7α-hydroxy-4-cholesten-3-one product of 30-hydroxy-C27-steroid oxidoreductase can take one of two paths in BA biosynthesis (Fig. 10). If this intermediate is acted upon by the second microsomal cytochrome P-450 enzyme of the pathway, sterol 12α-hydroxylase (reaction 3, Fig. 10), then the resulting product is ultimately converted into CA. 7α-hydroxy-4-cholesten-3-one can alternatively serve as a substrate for a soluble 3-oxosteroid-5β-reductase (reaction 4, Fig. 10) to yield a sterol intermediate that is ultimately converted into CDCA. The products of the 3-oxosteroid-5β-reductase reactions are the substrates for a soluble 3α-hydroxysteroid-dehydrogenase enzyme (reaction 5, Fig. 10). The products of the 3α-hydroxysteroid-dehydrogenase reaction next undergo oxidation and shortening of the side chain (85). Newly synthesized free BAs will be extensively conjugated (98%) into glycine- and taurine-conjugates.

In the intestinal lumen, especially in the colon, gut flora deconjugates, oxidizes and dehydroxylates the primary BAs produced in the liver to generate secondary BAs. Once transported back to the liver, these secondary BAs can be further processed to form tertiary BAs, which represent only a marginal BA species under normal conditions. These synthesis and metabolic pathways allow the generation of more than 18 different BA species, which ensures the perfect solubilization and absorption of a broad range of lipophilic molecules in the intestine and a multitude of signaling activities in the body (80).

1.3.3.2 *Enterohepatic circulation*

To ensure the presence of adequate concentrations of these biologically active compounds at the sites of their actions, i.e. liver, biliary tract, and intestine,

BAs are maintained within the enterohepatic circulation by the combined actions of transporter systems in the liver and intestine (81). The primary transporter responsible for canalicular bile salt secretion is the bile salt export pump (BSEP). This membrane transporter belongs to the ATP-binding cassette (ABC) superfamily of proteins and therefore BSEP plays a critical role in the physiologic maintenance of the enterohepatic circulation of bile acids (86).

The key components of the enterohepatic circulation are the synthesis of primary BAs and efficient intestinal absorption. The synthesis of primary BAs replaces the small amount of BAs not absorbed by the intestine. Intestinal absorption results in a recycling pool of BAs, permitting each BA to serve its function multiple times. Both the synthesis (input) of primary bile acids and intestinal absorption are highly regulated (82).

1.3.3.3 *Roles of nuclear hormone receptors*

BAs and oxysterols derived from cholesterol are signaling molecules that regulate cholesterol homeostasis in mammals. Many nuclear receptors play pivotal roles in the regulation of BA and cholesterol metabolism (87). BAs activate the farnesoid X receptor (FXR) to inhibit transcription for cholesterol 7-hydroxylase, and stimulate excretion and transport of BAs. Therefore, FXR is a BA sensor that protects the liver from accumulation of toxic bile acids and xenobiotics. Oxysterols activate the liver X receptors (LXR) to induce cholesterol 7-hydroxylase and ATP-binding cassette transporters and thus promote reverse cholesterol transport from the peripheral tissues to the liver for degradation to BAs. Therefore, FXR and LXR play critical roles in coordinated control of BA, cholesterol, and triglyceride metabolism to maintain lipid homeostasis. Nuclear receptors and BA/oxysterol-regulated genes are potential targets for developing drug therapies for lowering serum cholesterol and triglycerides and treating cardiovascular and liver diseases (87).

1.3.3.4 *Bile acids in diseases*

BAs are highly biologically active compounds and are therefore involved in several diseases. Some of the most common disease associations to BAs and possible drug targets are described in the following.

BA pathochemistry occurs in inborn errors of BA biosynthesis and conjugation. As around 14 enzymes are involved in the conversion of cholesterol to BAs (85), inborn errors of BA biosynthesis are not uncommon (88). Because of lack of feedback regulation by the end product of BA biosynthesis, there may be striking increase in the formation of intermediates. These intermediates accumulate in the hepatocytes inducing necrosis and or apoptosis (88).

The essential physiologic function of BSEP in hepatobiliary bile salt secretion is apparent in several forms of cholestasis where BSEP gene mutations have been identified. A common result of these various gene mutations is the reduction or the total loss of expression of the BSEP protein on the canalicular membrane (86). Cholestasis results in intra-hepatic and systemic accumulation of substances normally secreted into bile (81). Particularly, accumulations of detergent BAs in millimolar amounts may lead to liver cell damage, inflammation, and eventually organ failure (81). Treatment options are very limited and, apart from liver transplantation for some of the inherited forms of cholestasis, mainly aimed at reduction of symptoms.

BAs have been reported to reduce diet-induced obesity and prevent hyperglycaemia, which suggests that they also have effects on energy homeostasis (89). This metabolic effect is highly dependent on induction of the cAMP-dependent thyroid hormone-activating enzyme type 2 iodothyronine deiodinase (D2), as this effect is lost in D2-knockout mice (80).

In addition to their pleiotropic effect on lipid homeostasis, BAs also affect glucose metabolism and therefore play an important role in dyslipidaemia and type 2 diabetes (90). However, the exact mechanism in mediating the effects of BAs on glucose homeostasis still remains unclear and needs to be further investigated (80).

From what is currently known, it is clear that FXR activation could have some interesting therapeutic applications. Through stimulation of BA conjugation and secretion from hepatocytes into the bile to enhance bile flow, FXR agonists could protect the liver against the hepatotoxic accumulation of BAs that is seen in cholestatic liver diseases such as primary biliary cirrhosis (91). FXR activation could also be beneficial to reduce levels of liver and serum triglyceride in conditions such as the metabolic syndrome, type 2 diabetes, and obesity (91). Also, the FXR-dependent increases in biliary BAs and phospholipids could restore cholesterol solubility in the bile and thereby prevent gallstone formation (92). In bile, cholesterol

is solubilized in mixed micelles together with bile salts and phospholipids. Under supersaturated conditions, the sterol is solubilized by phospholipids into vesicles, called liquid crystals. As monohydrate crystals enucleate from these cholesterol-enriched vesicles, they aggregate, fuse and eventually precipitate into larger pathogenic crystals which lead to the disease (92).

1.3.3.5   Bile acids analysis by LC-MS/MS

The study of BA functions requires methods which cover the complexity of this structurally diverse group of molecules. A number of methods using LC-MS/MS were developed allowing analysis of free and conjugated BAs without derivatization (93-104). Nevertheless, most methods show disadvantages with time consuming extraction procedures (93;96;105), long analysis times (94-96;102-106) or lack of baseline separation of isobaric species (93;96;97;105;106). Direct BA analysis by ESI-MS/MS does not allow identification of isobaric species (107). For routine BA analysis, high sample throughput is of major importance. Hence, it is imperative to develop a LC-MS/MS based method with a run-time below 10 min including baseline separation of isobaric species. This method should be applied for BA routine diagnostics, as well as for the determination of bile acid species in huge clinical trials.

1.4 Scope and Objectives

Biologically active lipids including SPH, S1P, Cer1P, PG, BMP, CL and BAs are involved in a multitude of important cellular functions such as migration, proliferation and apoptosis. Moreover, these lipids are partially ubiquitous lipid messengers, which function as ligands for G-protein-coupled receptors and mediate important physiological processes. Therefore, SLs, polyglycerophospholipids and BAs are known as potential biomarkers for various diseases, including atherosclerosis, obesity, inflammation, diabetes and cancer. To understand the differential role of these lipids in a regulatory network involved in cellular lipid homeostasis it is important to use structure-specific and quantitative methods.

During the last decade liquid chromatography coupled to tandem MS (LC-MS/MS) has become a powerful tool for lipid species analysis. However, existing methods for the analysis of the above mentioned lipids, show disadvantages like laborious sample preparation, time consuming LC-separation, high sample volumes or insufficient validation data. Therefore, high sample throughput may not be accomplished. Furthermore most of these methods lack co-elution of analytes and internal standard, a prerequisite for targeted lipid species analysis.

Major aim of the present work was to develop novel LC-MS/MS methods for the analysis of GLs, SLs and BAs from biological materials. These methods should be characterized by high sample throughput, co-elution of analytes and internal standards, an easy sample preparation and an automated data analysis, to enable biomarker screening in huge clinical trials.

Thus, the first aim of this thesis was to develop LC-MS/MS-methods for the simultaneous quantification of SLs and metabolites. Beside blood plasma SLs should be monitored in other biological matrices, such as cellular homogenates and tissues.

Furthermore the present work aimed at the development of a fast and sensitive LC-MS/MS-method for the quantification of BA species in human plasma samples. This method should be validated according to FDA-guidelines for the application as a diagnostic parameter in the routine laboratory.

Additionally, a method for the simultaneous identification and quantification for CL and metabolites should be developed. This method should be applied for monitoring alterations in the polyglycerophospholipid metabolism in different cell types and tissues. Moreover, since istopic overlap is a major problem, especially for

high molecular weight lipids like CL, this method should comprise, for the first time, correction for the complex isotope overlap of MS/MS experiments.

1.5   References

1. Yetukuri L, Ekroos K, Vidal-Puig A, Oresic M. Informatics and computational strategies for the study of lipids. Mol Biosyst 2008;4:121-7.

2. Han X, Gross RW. Shotgun lipidomics: electrospray ionization mass spectrometric analysis and quantitation of cellular lipidomes directly from crude extracts of biological samples. Mass Spectrom Rev 2005;24:367-412.

3. Blanksby SJ, Mitchell TW. Advances in mass spectrometry for lipidomics. Annu Rev Anal Chem (Palo Alto Calif) 2010;3:433-65.

4. Han X, Gross RW. Electrospray ionization mass spectroscopic analysis of human erythrocyte plasma membrane phospholipids. Proc Natl Acad Sci U S A 1994;91:10635-9.

5. Ivanova PT, Milne SB, Myers DS, Brown HA. Lipidomics: a mass spectrometry based systems level analysis of cellular lipids. Curr Opin Chem Biol 2009;13:526-31.

6. Brugger B, Erben G, Sandhoff R, Wieland FT, Lehmann WD. Quantitative analysis of biological membrane lipids at the low picomole level by nano-electrospray ionization tandem mass spectrometry. Proc Natl Acad Sci U S A 1997;94:2339-44.

7. Hopfgartner G, Varesio E, Tschappat V, Grivet C, Bourgogne E, Leuthold LA. Triple quadrupole linear ion trap mass spectrometer for the analysis of small molecules and macromolecules. J Mass Spectrom 2004;39:845-55.

8. Minkler PE, Hoppel CL. Separation and characterization of cardiolipin molecular species by reverse-phase ion pair high-performance liquid chromatography-mass spectrometry. J Lipid Res 2010;51:856-65.

9. Scherer M, Schmitz G, Liebisch G. High-throughput analysis of sphingosine 1-phosphate, sphinganine 1-phosphate, and lysophosphatidic acid in plasma samples by liquid chromatography-tandem mass spectrometry. Clin Chem 2009;55:1218-22.

10. Scherer M, Leuthauser-Jaschinski K, Ecker J, Schmitz G, Liebisch G. A rapid and quantitative LC-MS/MS method to profile sphingolipids. J Lipid Res 2010;51:2001-11.

11. Scherer M, Gnewuch C, Schmitz G, Liebisch G. Rapid quantification of bile acids and their conjugates in serum by liquid chromatography-tandem mass spectrometry. J Chromatogr B Analyt Technol Biomed Life Sci 2009;877:3920-5.

12. Berdyshev EV, Gorshkova IA, Garcia JG, Natarajan V, Hubbard WC. Quantitative analysis of sphingoid base-1-phosphates as bisacetylated derivatives by liquid chromatography-tandem mass spectrometry. Anal Biochem 2005;339:129-36.

13. Bielawski J, Szulc ZM, Hannun YA, Bielawska A. Simultaneous quantitative analysis of bioactive sphingolipids by high-performance liquid chromatography-tandem mass spectrometry. Methods 2006;39:82-91.

14. Murph M, Tanaka T, Pang J, Felix E, Liu S, Trost R et al. Liquid chromatography mass spectrometry for quantifying plasma lysophospholipids: potential biomarkers for cancer diagnosis. Methods Enzymol 2007;433:1-25.

15. Shaner RL, Allegood JC, Park H, Wang E, Kelly S, Haynes CA et al. Quantitative analysis of sphingolipids for lipidomics using triple quadrupole and quadrupole linear ion trap mass spectrometers. J Lipid Res 2009;50:1692-707.

16. Tyurina YY, Tyurin VA, Kaynar AM, Kapralova VI, Wasserloos KJ, Li J et al. Oxidative lipidomics of hyperoxic acute lung injury: Mass spectrometric characterization of cardiolipin and phosphatidylserine peroxidation. Am J Physiol Lung Cell Mol Physiol 2010.

17. Cowart LA. Sphingolipids: players in the pathology of metabolic disease. Trends Endocrinol Metab 2009;20:34-42.

18. Wymann MP, Schneiter R. Lipid signalling in disease. Nat Rev Mol Cell Biol 2008;9:162-76.

19. Bleijerveld OB, Houweling M, Thomas MJ, Cui Z. Metabolipidomics: profiling metabolism of glycerophospholipid species by stable isotopic precursors and tandem mass spectrometry. Anal Biochem 2006;352:1-14.

20. Vance JE, Vance DE. Phospholipid biosynthesis in mammalian cells. Biochem Cell Biol 2004;82:113-28.

21. KIYASU JY, PIERINGER RA, PAULUS H, KENNEDY EP. The biosynthesis of phosphatidylglycerol. J Biol Chem 1963;238:2293-8.

22. Houtkooper RH, Rodenburg RJ, Thiels C, van LH, Stet F, Poll-The BT et al. Cardiolipin and monolysocardiolipin analysis in fibroblasts, lymphocytes, and tissues using high-performance liquid chromatography-mass spectrometry as a diagnostic test for Barth syndrome. Anal Biochem 2009;387:230-7.

23. Hullin-Matsuda F, Kawasaki K, ton-Vandenbroucke I, Xu Y, Nishijima M, Lagarde M et al. De novo biosynthesis of the late endosome lipid, bis(monoacylglycero)phosphate. J Lipid Res 2007;48:1997-2008.

24. Kolter T, Sandhoff K. Principles of lysosomal membrane digestion: stimulation of sphingolipid degradation by sphingolipid activator proteins and anionic lysosomal lipids. Annu Rev Cell Dev Biol 2005;21:81-103.

25. Meikle PJ, Duplock S, Blacklock D, Whitfield PD, Macintosh G, Hopwood JJ, Fuller M. Effect of lysosomal storage on bis(monoacylglycero)phosphate. Biochem J 2008;411:71-8.

26. Kobayashi T, Beuchat MH, Lindsay M, Frias S, Palmiter RD, Sakuraba H et al. Late endosomal membranes rich in lysobisphosphatidic acid regulate cholesterol transport. Nat Cell Biol 1999;1:113-8.

27. Matsuo H, Chevallier J, Mayran N, Le B, I, Ferguson C, Faure J et al. Role of LBPA and Alix in multivesicular liposome formation and endosome organization. Science 2004;303:531-4.

28. Houtkooper RH, Vaz FM. Cardiolipin, the heart of mitochondrial metabolism. Cell Mol Life Sci 2008;65:2493-506.

29. Fry M, Green DE. Cardiolipin requirement for electron transfer in complex I and III of the mitochondrial respiratory chain. J Biol Chem 1981;256:1874-80.

30. Jiang F, Ryan MT, Schlame M, Zhao M, Gu Z, Klingenberg M et al. Absence of cardiolipin in the crd1 null mutant results in decreased mitochondrial membrane potential and reduced mitochondrial function. J Biol Chem 2000;275:22387-94.

31. Haines TH, Dencher NA. Cardiolipin: a proton trap for oxidative phosphorylation. FEBS Lett 2002;528:35-9.

32. Gonzalvez F, Gottlieb E. Cardiolipin: setting the beat of apoptosis. Apoptosis 2007;12:877-85.

33. Kagan VE, Tyurina YY, Bayir H, Chu CT, Kapralov AA, Vlasova II et al. The "pro-apoptotic genies" get out of mitochondria: oxidative lipidomics and redox activity of cytochrome c/cardiolipin complexes. Chem Biol Interact 2006;163:15-28.

34. Schlame M, Ren M. Barth syndrome, a human disorder of cardiolipin metabolism. FEBS Lett 2006;580:5450-5.

35. Hauff KD, Hatch GM. Cardiolipin metabolism and Barth Syndrome. Prog Lipid Res 2006;45:91-101.

36. Valianpour F, Mitsakos V, Schlemmer D, Towbin JA, Taylor JM, Ekert PG et al. Monolysocardiolipins accumulate in Barth syndrome but do not lead to enhanced apoptosis. J Lipid Res 2005;46:1182-95.

37. Vreken P, Valianpour F, Nijtmans LG, Grivell LA, Plecko B, Wanders RJ, Barth PG. Defective remodeling of cardiolipin and phosphatidylglycerol in Barth syndrome. Biochem Biophys Res Commun 2000;279:378-82.

38. Xu Y, Sutachan JJ, Plesken H, Kelley RI, Schlame M. Characterization of lymphoblast mitochondria from patients with Barth syndrome. Lab Invest 2005;85:823-30.

39. Chicco AJ, Sparagna GC. Role of cardiolipin alterations in mitochondrial dysfunction and disease. Am J Physiol Cell Physiol 2007;292:C33-C44.

40. Fobker M, Voss R, Reinecke H, Crone C, Assmann G, Walter M. Accumulation of cardiolipin and lysocardiolipin in fibroblasts from Tangier disease subjects. FEBS Lett 2001;500:157-62.

41. Loftus SK, Morris JA, Carstea ED, Gu JZ, Cummings C, Brown A et al. Murine model of Niemann-Pick C disease: mutation in a cholesterol homeostasis gene. Science 1997;277:232-5.

42. Pulfer M, Murphy RC. Electrospray mass spectrometry of phospholipids. Mass Spectrom Rev 2003;22:332-64.

43. Han X, Yang J, Cheng H, Yang K, Abendschein DR, Gross RW. Shotgun lipidomics identifies cardiolipin depletion in diabetic myocardium linking altered substrate utilization with mitochondrial dysfunction. Biochemistry 2005;44:16684-94.

44. Han X, Yang K, Yang J, Cheng H, Gross RW. Shotgun lipidomics of cardiolipin molecular species in lipid extracts of biological samples. J Lipid Res 2006;47:864-79.

45. Hsu FF, Turk J. Characterization of cardiolipin from Escherichia coli by electrospray ionization with multiple stage quadrupole ion-trap mass spectrometric analysis of [M - 2H + Na]- ions. J Am Soc Mass Spectrom 2006;17:420-9.

46. Valianpour F, Wanders RJ, Barth PG, Overmars H, van Gennip AH. Quantitative and compositional study of cardiolipin in platelets by electrospray ionization mass spectrometry: application for the identification of Barth syndrome patients. Clin Chem 2002;48:1390-7.

47. Sparagna GC, Johnson CA, McCune SA, Moore RL, Murphy RC. Quantitation of cardiolipin molecular species in spontaneously hypertensive heart failure rats using electrospray ionization mass spectrometry. J Lipid Res 2005;46:1196-204.

48. Ejsing CS, Duchoslav E, Sampaio J, Simons K, Bonner R, Thiele C et al. Automated identification and quantification of glycerophospholipid molecular species by multiple precursor ion scanning. Anal Chem 2006;78:6202-14.

49. Futerman AH, Riezman H. The ins and outs of sphingolipid synthesis. Trends Cell Biol 2005;15:312-8.

50. Lahiri S, Futerman AH. The metabolism and function of sphingolipids and glycosphingolipids. Cell Mol Life Sci 2007;64:2270-84.

51. Bartke N, Hannun YA. Bioactive sphingolipids: metabolism and function. J Lipid Res 2009;50 Suppl:S91-S96.

52. Tani M, Iida H, Ito M. O-glycosylation of mucin-like domain retains the neutral ceramidase on the plasma membranes as a type II integral membrane protein. J Biol Chem 2003;278:10523-30.

53. Pitson SM, D'Andrea RJ, Vandeleur L, Moretti PA, Xia P, Gamble JR et al. Human sphingosine kinase: purification, molecular cloning and characterization of the native and recombinant enzymes. Biochem J 2000;350 Pt 2:429-41.

54. Wattenberg BW, Pitson SM, Raben DM. The sphingosine and diacylglycerol kinase superfamily of signaling kinases: localization as a key to signaling function. J Lipid Res 2006;47:1128-39.

55. Spiegel S, Milstien S. Sphingosine-1-phosphate: an enigmatic signalling lipid. Nat Rev Mol Cell Biol 2003;4:397-407.

56. Taha TA, Mullen TD, Obeid LM. A house divided: ceramide, sphingosine, and sphingosine-1-phosphate in programmed cell death. Biochim Biophys Acta 2006;1758:2027-36.

57. Yatomi Y. Plasma sphingosine 1-phosphate metabolism and analysis. Biochim Biophys Acta 2007.

58. Tani M, Sano T, Ito M, Igarashi Y. Mechanisms of sphingosine and sphingosine 1-phosphate generation in human platelets. J Lipid Res 2005;46:2458-67.

59. Penno A, Reilly MM, Houlden H, Laura M, Rentsch K, Niederkofler V et al. Hereditary sensory neuropathy type 1 is caused by the accumulation of two neurotoxic sphingolipids. J Biol Chem 2010;285:11178-87.

60. Merrill AH, Jr., Stokes TH, Momin A, Park H, Portz BJ, Kelly S et al. Sphingolipidomics: a valuable tool for understanding the roles of sphingolipids in biology and disease. J Lipid Res 2009;50 Suppl:S97-102.

61. Tani M, Ito M, Igarashi Y. Ceramide/sphingosine/sphingosine 1-phosphate metabolism on the cell surface and in the extracellular space. Cell Signal 2007;19:229-37.

62. Futerman AH, Hannun YA. The complex life of simple sphingolipids. EMBO Rep 2004;5:777-82.

63. Maceyka M, Payne SG, Milstien S, Spiegel S. Sphingosine kinase, sphingosine-1-phosphate, and apoptosis. Biochim Biophys Acta 2002;1585:193-201.

64. Pyne NJ, Pyne S. Sphingosine 1-phosphate and cancer. Nat Rev Cancer 2010;10:489-503.

65. Kihara A, Mitsutake S, Mizutani Y, Igarashi Y. Metabolism and biological functions of two phosphorylated sphingolipids, sphingosine 1-phosphate and ceramide 1-phosphate. Prog Lipid Res 2007;46:126-44.

66. Kihara A, Igarashi Y. Production and release of sphingosine 1-phosphate and the phosphorylated form of the immunomodulator FTY720. Biochim Biophys Acta 2008;1781:496-502.

67. Rosen H, Goetzl EJ. Sphingosine 1-phosphate and its receptors: an autocrine and paracrine network. Nat Rev Immunol 2005;5:560-70.

68. Chalfant CE, Spiegel S. Sphingosine 1-phosphate and ceramide 1-phosphate: expanding roles in cell signaling. J Cell Sci 2005;118:4605-12.

69. Radin NS, Shayman JA, Inokuchi J. Metabolic effects of inhibiting glucosylceramide synthesis with PDMP and other substances. Adv Lipid Res 1993;26:183-213.

70. Liliom K, Sun G, Bunemann M, Virag T, Nusser N, Baker DL et al. Sphingosylphosphocholine is a naturally occurring lipid mediator in blood plasma: a possible role in regulating cardiac function via sphingolipid receptors. Biochem J 2001;355:189-97.

71. Fyrst H, Saba JD. An update on sphingosine-1-phosphate and other sphingolipid mediators. Nat Chem Biol 2010;6:489-97.

72. Butter JJ, Koopmans RP, Michel MC. A rapid and validated HPLC method to quantify sphingosine 1-phosphate in human plasma using solid-phase extraction followed by derivatization with fluorescence detection. J Chromatogr B Analyt Technol Biomed Life Sci 2005;824:65-70.

73. Haynes CA, Allegood JC, Park H, Sullards MC. Sphingolipidomics: methods for the comprehensive analysis of sphingolipids. J Chromatogr B Analyt Technol Biomed Life Sci 2009;877:2696-708.

74. Lieser B, Liebisch G, Drobnik W, Schmitz G. Quantification of sphingosine and sphinganine from crude lipid extracts by HPLC electrospray ionization tandem mass spectrometry. J Lipid Res 2003;44:2209-16.

75. Mano N, Oda Y, Yamada K, Asakawa N, Katayama K. Simultaneous quantitative determination method for sphingolipid metabolites by liquid chromatography/ionspray ionization tandem mass spectrometry. Anal Biochem 1997;244:291-300.

76. Markham JE, Jaworski JG. Rapid measurement of sphingolipids from Arabidopsis thaliana by reversed-phase high-performance liquid chromatography coupled to electrospray ionization tandem mass spectrometry. Rapid Commun Mass Spectrom 2007;21:1304-14.

77. Schmidt H, Schmidt R, Geisslinger G. LC-MS/MS-analysis of sphingosine-1-phosphate and related compounds in plasma samples. Prostaglandins Other Lipid Mediat 2006;81:162-70.

78. Yoo HH, Son J, Kim DH. Liquid chromatography-tandem mass spectrometric determination of ceramides and related lipid species in cellular extracts. J Chromatogr B Analyt Technol Biomed Life Sci 2006;843:327-33.

79. Ejsing CS, Sampaio JL, Surendranath V, Duchoslav E, Ekroos K, Klemm RW et al. Global analysis of the yeast lipidome by quantitative shotgun mass spectrometry. Proc Natl Acad Sci U S A 2009;106:2136-41.

80. Thomas C, Pellicciari R, Pruzanski M, Auwerx J, Schoonjans K. Targeting bile-acid signalling for metabolic diseases. Nat Rev Drug Discov 2008;7:678-93.

81. Lefebvre P, Cariou B, Lien F, Kuipers F, Staels B. Role of bile acids and bile acid receptors in metabolic regulation. Physiol Rev 2009;89:147-91.

82. Hofmann AF, Hagey LR. Bile acids: chemistry, pathochemistry, biology, pathobiology, and therapeutics. Cell Mol Life Sci 2008;65:2461-83.

83. Gadaleta RM, van Mil SW, Oldenburg B, Siersema PD, Klomp LW, van Erpecum KJ. Bile acids and their nuclear receptor FXR: Relevance for hepatobiliary and gastrointestinal disease. Biochim Biophys Acta 2010;1801:683-92.

84. Russell DW. The enzymes, regulation, and genetics of bile acid synthesis. Annu Rev Biochem 2003;72:137-74.

85. Russell DW, Setchell KD. Bile acid biosynthesis. Biochemistry 1992;31:4737-49.

86. Lam P, Soroka CJ, Boyer JL. The bile salt export pump: clinical and experimental aspects of genetic and acquired cholestatic liver disease. Semin Liver Dis 2010;30:125-33.

87. Chiang JY. Bile acid regulation of gene expression: roles of nuclear hormone receptors. Endocr Rev 2002;23:443-63.

88. Heubi JE, Setchell KD, Bove KE. Inborn errors of bile acid metabolism. Semin Liver Dis 2007;27:282-94.

89. Ikemoto S, Takahashi M, Tsunoda N, Maruyama K, Itakura H, Ezaki O. High-fat diet-induced hyperglycemia and obesity in mice: differential effects of dietary oils. Metabolism 1996;45:1539-46.

90. Garg A, Grundy SM. Cholestyramine therapy for dyslipidemia in non-insulin-dependent diabetes mellitus. A short-term, double-blind, crossover trial. Ann Intern Med 1994;121:416-22.

91. Fiorucci S, Rizzo G, Donini A, Distrutti E, Santucci L. Targeting farnesoid X receptor for liver and metabolic disorders. Trends Mol Med 2007;13:298-309.

92. Moschetta A, Bookout AL, Mangelsdorf DJ. Prevention of cholesterol gallstone disease by FXR agonists in a mouse model. Nat Med 2004;10:1352-8.

93. Ye L, Liu S, Wang M, Shao Y, Ding M. High-performance liquid chromatography-tandem mass spectrometry for the analysis of bile acid profiles in serum of women with intrahepatic cholestasis of pregnancy. J Chromatogr B Analyt Technol Biomed Life Sci 2007;860:10-7.

94. Tagliacozzi D, Mozzi AF, Casetta B, Bertucci P, Bernardini S, Di IC et al. Quantitative analysis of bile acids in human plasma by liquid chromatography-electrospray tandem mass spectrometry: a simple and rapid one-step method. Clin Chem Lab Med 2003;41:1633-41.

95. Ando M, Kaneko T, Watanabe R, Kikuchi S, Goto T, Iida T et al. High sensitive analysis of rat serum bile acids by liquid chromatography/electrospray ionization tandem mass spectrometry. J Pharm Biomed Anal 2006;40:1179-86.

96. Burkard I, von EA, Rentsch KM. Differentiated quantification of human bile acids in serum by high-performance liquid chromatography-tandem mass spectrometry. J Chromatogr B Analyt Technol Biomed Life Sci 2005;826:147-59.

97. Eckers C, New AP, East PB, Haskins NJ. The use of tandem mass spectrometry for the differentiation of bile acid isomers and for the identification of bile acids in biological extracts. Rapid Commun Mass Spectrom 1990;4:449-53.

98. Ikegawa S, Murao N, Motoyama T, Yanagihara T, Niwa T, Goto J. Separation and detection of bile acid 3-glucuronides in human urine by liquid chromatography/electrospray ionization-mass spectrometry. Biomed Chromatogr 1996;10:313-7.

99. Bootsma AH, Overmars H, van RA, van Lint AE, Wanders RJ, van Gennip AH, Vreken P. Rapid analysis of conjugated bile acids in plasma using electrospray tandem mass spectrometry: application for selective screening of peroxisomal disorders. J Inherit Metab Dis 1999;22:307-10.

100. Johnson DW, ten Brink HJ, Schuit RC, Jakobs C. Rapid and quantitative analysis of unconjugated C(27) bile acids in plasma and blood samples by tandem mass spectrometry. J Lipid Res 2001;42:9-16.

101. Mills KA, Mushtaq I, Johnson AW, Whitfield PD, Clayton PT. A method for the quantitation of conjugated bile acids in dried blood spots using electrospray ionization-mass spectrometry. Pediatr Res 1998;43:361-8.

102. Roda A, Gioacchini AM, Cerre C, Baraldini M. High-performance liquid chromatographic-electrospray mass spectrometric analysis of bile acids in biological fluids. J Chromatogr B Biomed Appl 1995;665:281-94.

103. Sakakura H, Suzuki M, Kimura N, Takeda H, Nagata S, Maeda M. Simultaneous determination of bile acids in rat bile and serum by high-performance liquid chromatography. J Chromatogr 1993;621:123-31.

104. Alnouti Y, Csanaky IL, Klaassen CD. Quantitative-profiling of bile acids and their conjugates in mouse liver, bile, plasma, and urine using LC-MS/MS. J Chromatogr B Analyt Technol Biomed Life Sci 2008;873:209-17.

105. Tessier E, Neirinck L, Zhu Z. High-performance liquid chromatographic mass spectrometric method for the determination of ursodeoxycholic acid and its glycine and taurine conjugates in human plasma. J Chromatogr B Analyt Technol Biomed Life Sci 2003;798:295-302.

106. Bentayeb K, Batlle R, Sanchez C, Nerin C, Domeno C. Determination of bile acids in human serum by on-line restricted access material-ultra high-

performance liquid chromatography-mass spectrometry. J Chromatogr B Analyt Technol Biomed Life Sci 2008;869:1-8.

107. Perwaiz S, Tuchweber B, Mignault D, Gilat T, Yousef IM. Determination of bile acids in biological fluids by liquid chromatography-electrospray tandem mass spectrometry. J Lipid Res 2001;42:114-9.

2 Simultaneous Quantification of Cardiolipin, Bis(monoacylglycero)phosphate and their Precursors by Hydrophilic Interaction LC-MS/MS including Correction of Isotopic Overlap

2.1 Abstract

Cardiolipin (CL) and bis(monoacylglycero)phosphate (BMP) are unique lipid structures with important biological roles for mitochondrial integrity and endolysosomal degradation, respectively. They are synthesized from common precursors, phosphatidylglycerol (PG) and phosphatidic acid (PA). Here we present a rapid method for the simultaneous quantification of BMP, CL, PG, and PA using hydrophilic interaction chromatography coupled with electrospray ionization tandem mass spectrometry (HILIC-MS/MS). HILIC provides co-elution of lipid species and their internal standards required for accurate quantification. Co-elution leads to isotope overlap of lipid species which was successfully corrected. This assay was validated in mouse heart tissue and primary human skin fibroblasts. It shows reproducibility and limits of detection sufficient for biomarker studies contributing into basic research on BMP and CL metabolism.

2.2 Introduction

Due to their unique molecular structures cardiolipin (CL) (1) and bis(monoacylglycero)phosphate (BMP)(2) play important roles in the mitochondrial electron transfer complex assembly and integrity and late endosomal lipid sorting and degradation pathway (3), respectively. They are synthesized from phosphatidylglycerol (PG) which is formed from phosphatidic acid (PA) (4;5). However, biosynthesis of both CL and BMP is not well understood. The biological importance of these lipids is highlighted by their usage as biomarkers. For example, in Barth syndrome, CL concentration is reduced and CL species composition is altered (6;7). BMP is described as marker for lysosomal storage disorders and drug-induced phospholipidosis(2;8). Since the biophysical properties of phospholipid

species also depend on the chain length and number of double bonds it is important to get access to lipid species to fully understand their function.

In the last years electrospray ionization mass spectrometry has emerged as a powerful tool for the qualitative and quantitative analysis of complex phospholipids (9;10). A number of methods were described for CL analysis based either on direct mass spectrometry (MS) (11-13) or liquid chromatography coupled to MS (6;7;14;15). BMP analysis requires chromatography to separate the structural isomer PG (8). However, till now methods for the combined analysis of BMP, CL, PG, and PA species are lacking.

Here we describe a method for the fast, simultaneous, quantification of BMP, CL, PG, and PA species in biological samples. This method applies hydrophilic interaction chromatography (HILIC) coupled to electrospray ionization tandem mass spectrometry including correction of isotope overlap.

2.3 Experimental section

2.3.1 Reagents

Butanol, methanol (HPLC grade), citric acid monohydrate, disodium hydrogenphosphate and formic acid (98-100 %, for analysis) were purchased from Merck (Darmstadt, Germany). Water was obtained from B. Braun (Melsungen, Germany). Ammonium formate (Fluka, Buchs, Switzerland), were of the highest analytical grade available. Synthetic glycerophospholipids including CL $(14:0)_4$, CL $(14:1)_3/15:1$, CL $(15:0)_3/16:1$ CL $(18:1)_4$, PA 14:0/14:0, PA 16:0/16:0, PA 18:1/18:1, PA 18:0/20:4, PG 14:0/14:0, PG 16:0/16:0, PG 18:1/18:1, PG 18:0/20:4, BMP 14:0/14:0, BMP 16:0/16:0, BMP 16:0/17:0 and BMP 18:1/18:1 were purchased from Avanti Polar Lipids, Inc. (Alabaster, AL, USA). Concentrations of lipid standard solution were determined by phosphorous assay (16).

2.3.2 Sample preparation

Aliquots of 50µg protein from fibroblast homogenates and 2.5mg wet weight from mouse heart tissue were used for analysis. 20µL of an internal standard mixture containing 20ng PA 28:0, 10ng PG 28:0, 10ng BMP 14:0/14:0 and 10ng CL $(14:0)_4$

were added prior to lipid extraction. We applied a butanolic extraction procedure described by Baker et al. (17). In brief, 500µl cell homogenate or heart tissue were mixed with 60µL of buffer containing 200mM citric acid and 270mM disodium hydrogenphosphate (pH 4). Extraction was performed with 1mL of 1-butanol and 500µL of water-saturated 1-butanol. The recovered butanol phase was evaporated to dryness under reduced pressure. The residue was re-dissolved in 50µL ethanol.

2.3.3 HILIC-MS/MS

Glycerophopholipid analysis was performed with hydrophilic interaction liquid chromatography-tandem mass spectrometry (HILIC-MS/MS). The LC equipment consisted of a 1200-series binary pump, a 1200-series isocratic pump and a degasser (Agilent, Waldbronn, Germany) connected to an HTC Pal autosampler (CTC Analytics, Zwingen, Switzerland). A hybrid triple quadrupole linear ion trap mass spectrometer API 4000 Q-Trap equipped with a Turbo V source ion spray operating in positive ESI mode was used for detection (Applied Biosystems, Darmstadt, Germany). Positive electrospray ionization was carried out at 5500V and the ion source was maintained at 500℃. Both quadru poles Q1 and Q3 were operated at a mass resolution of 0.5 Da FWHM with 5ms dwell time. The MRM mode was used with the parameters displayed in Table S-1. CL and BMP were analyzed using the DAG and MAG fragment with the lower molecular weight, respectively. The MS program was divided into two periods with an initial monitoring of PG and BMP and an analysis of PA and CL after 1.5min.

Gradient chromatographic separation was performed on a Kintex (Phenomenex, Waldbronn, Germany) hydrophilic-interaction chromatography (HILIC) silica column (50 x 2.1mm), with a 2.6µm particle size equipped with a 0.5µm pre-filter (Upchurch Scientific, Oak Harbor, WA, USA). The injection volume was 3µL and the column was maintained at 50℃. The mobile phase consisted of water containing 0.2% formic acid and 200mM ammonium formate (eluent A) and acetonitrile containing 0.2% formic acid (eluent B). A gradient elution was performed with 100% B for 0.2min, a step to 82% B until 2min, a linear increase to 50% B until 3min, 50% B up to 4min and re-equilibration from 4.1 to 4.5min with 100% B. The flow rate was set to 800µL/min. To minimize contamination of the mass spectrometer, the column flow was directed only from 1.0 to 3.0min into the mass spectrometer using a diverter

valve. Otherwise methanol with a 250µL/min flow rate was delivered into the mass spectrometer.

2.3.4 Calibration

Calibration was achieved by standard addition of naturally occurring glycerophospholipid species (PA 32:0, 36:2, 38:4; BMP 32:0, 36:2; PG 32:0, 36:2, 38:4; CL $(18:1)_4$, $(15:1)_3 16:1$). A six point calibration was performed by adding the indicated amounts of a combined glycerophospholipid standard mixture to matrix samples. Calibration curves were calculated using linear regression analysis (Table S-2). The closest related calibration line was used for quantification of not calibrated species. For BMP and CL differences between symmetric and asymmetric species responses were corrected by a factor 2.

2.3.5 Species identification

Lipid extracts from the primary human skin fibroblasts and mouse heart tissue were used for glycerophopholipid species identification. CL and BMP molecular species were identified using an information dependent acquisition method (IDA), which included a survey scan in the enhanced MS (EMS) followed by an enhanced product ion scan (EPI) on the largest ions in the EMS scan. The EMS scan was performed at a rate of 1000Da/s at a spectral range of 1400-1600 for CL and 700-900 for BMP. The EPI scan was performed at a scan rate of 1000Da/s at a spectral range of *m/z* 400-700 for CL and *m/z* 300-400 for BMP. PA and PG molecular species were identified by neutral loss scans of *m/z* 115 and 189, respectively. Detected molecular species were quantitated by MRM in fibroblast and mouse heart tissue lipid extracts (Table S-3 and 4).

2.3.6 Correction of isotopic overlap

The principle of isotopic overlap in MS/MS experiments were described by Ejsing et al. (18). Isotope pattern for the neutral fragments N (precursor overlap) and the charged fragments F (product overlap) used for analysis were calculated with the software tool implemented in Analyst (Applied Biosystems, Darmstadt, Germany). Previously established Excel Macros for the correction of isotopic overlap of

phosphatidylcholine and sphingomyelin (19) were adapted to correct both precursor and product isotopic overlap using a sequential algorithm starting from low mass species. Isotopic overlap resulting from the following isotope combinations were corrected: $F_{2,4}N_0$ and $F_0N_{2,4}$ as well as the overlap resulting from F_2N_2 (F_2 = charged fragment containing two isotopes).

2.4   Results and discussion

2.4.1   Fragmentation of CL and related lipids

Almost all previously published methods of quantification of CL, PG, BMP, and PA used negative ion mode (6-8;11-15;18;20-22). We tested ionization and fragmentation of these lipid classes in positive ion mode, avoiding positive-negative ion mode switching. In ammonium formate containing solvent, PG, BMP, and CL form both protonated and ammonia adduct ions whereas for PA only ammonia adducts were observed. Both protonated (data not shown) and ammonia adduct ions (Figure S-1) showed the similar fragment patterns. CL forms prominent diacylglycerol (DAG) fragment ions leading to two different product ions for asymmetrical CL species (Figure S-1A). PA exhibits a neutral loss of m/z 115 of the ammonia phosphate head group resulting in a DAG fragment (Figure S-1B) (22). The structural isomers BMP (Figure S-1C) and PG (Figure S-1D) differ in their fragment patterns showing MAG and DAG as major fragment ions, respectively. While the observed neutral loss of m/z 189 is specific to PG (22), PG species also form MAG fragments (8) (Fig. 2B). Thus, a specific determination of BMP requires separation from PG. Finally, we optimized MS/MS parameter for both protonated and ammonia adduct ions and found a higher sensitivity for ammonia adduct ions except for BMP (data not shown; MS-parameter see in Table S-1). Moreover, a higher sensitivity was found for positive compared to negative ion mode analysis (data not shown). Positive ion mode detection of CL has the advantage that only singly charged ions were observed compared to singly and doubly charged ions in negative ion mode (7;12;14;15). The ratio of singly to double charged ions is instrument design dependent and analysis of doubly charged ions requires a higher than unit resolution (15). This means that up to now assays for CL quantification are based on MS but not on MS/MS data (7;12;14;15;23).

2.4.2 Chromatography

Due to the mass spectrometric interferences of PG with BMP analysis and in order to reduce ionization suppressions by matrix compounds, we established an LC separation for CL, PG, BMP, and PA. Since reversed phase chromatography shows chain length dependent separation, co-elution of analytes and internal standards may not be accomplished (6;14). However, co-elution is of major importance for compensation of matrix effects and varying ionization efficiencies, especially during gradient elution. 'Classical' normal-phase chromatography may be hampered by limited reproducibility, insufficient peak shapes and solvent mixtures incompatible for ESI-MS-analysis. Therefore, we developed a LC-separation based on hydrophilic interaction chromatography (HILIC) which provides co-elution of analyte species and internal standards within a given lipid class (Fig. 1). Moreover, we achieved excellent peak shapes, especially for BMP, PG and CL as well as baseline separation for PG and BMP within 4.5 min (including re-equilibration).
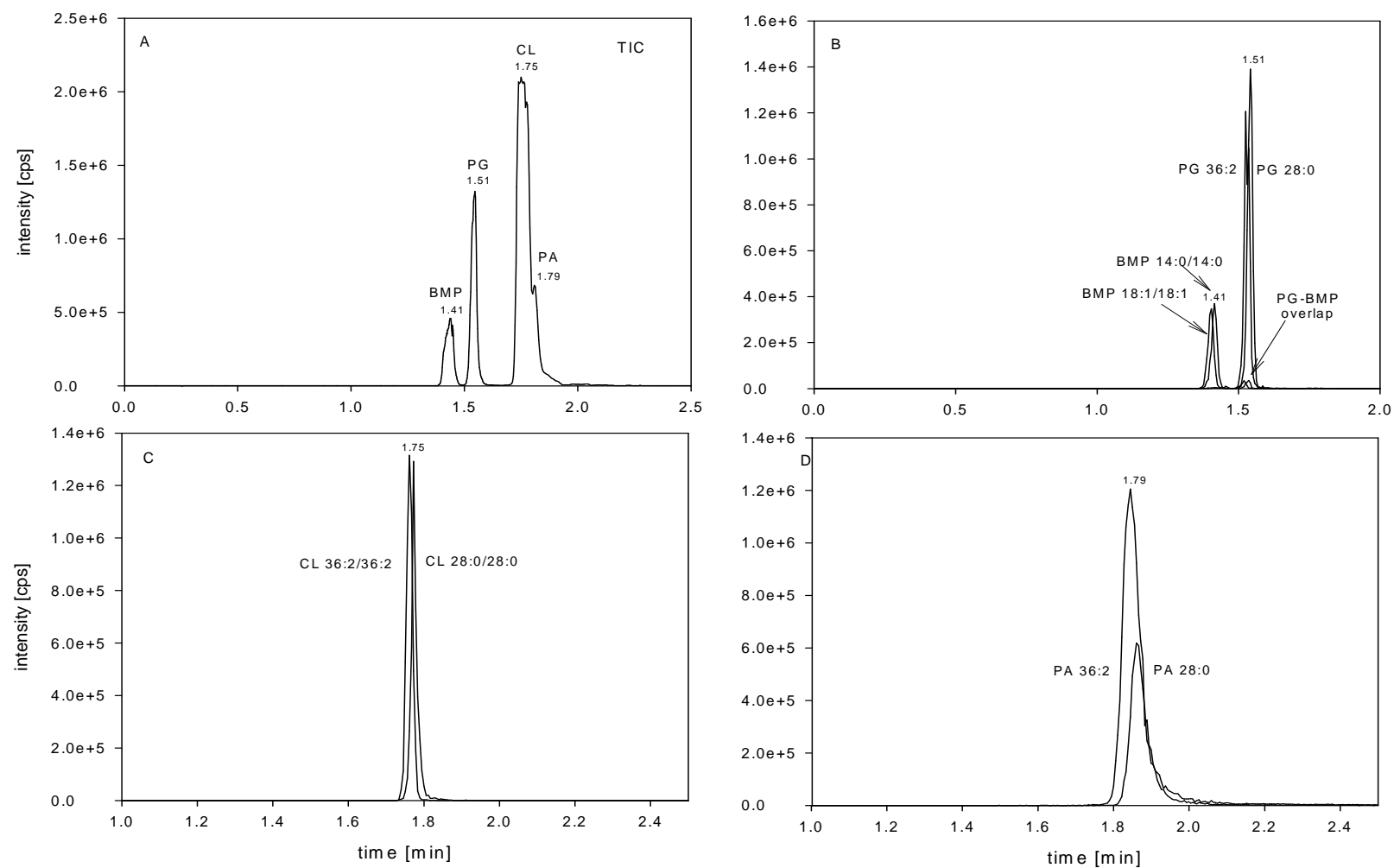
Fig. 1. BMP, PG, CL, PA chromatogram of a mouse heart tissue.

Representative mass chromatograms obtained from a mouse heart tissue lipid extract are displayed.

2.4.3   Correction of isotope overlap

HILIC provides co-elution of lipid species within each lipid class. Consequently, we observed an isotope overlap of species due to a variable number of double bonds. A correction of this overlap is especially important for high molecular weight lipids like CL. Most assays published up to now quantified CL from MS spectra which may be corrected by the isotope pattern of the molecular ion (9). Isotopic overlap in MS/MS experiments is more complex since isotope distributions of charged fragments and neutral fragments have to be considered (18). To illustrate isotopic overlap we acquired a product ion spectrum of monoisotopic CL $(18:1)_4$ which revealed only one signal at m/z 603.5 (Fig. 2A). However, the product ion spectrum of the M+2 isotope of CL $(18:1)_4$ showed signals at m/z 603.5, 604.5 and 605.5, corresponding to $[DAG\ 36:2]^+$, $[DAG\ 36:2 + 1]^+$ and $[DAG\ 36:2 + 2]^+$ fragment ions, respectively (Fig. 2B).

There are two types of isotope overlaps which need to be considered during quantitative analysis. One, termed as precursor-overlap, is due to isotopes in the neutral fragment (N_0) but not in the product ion used for analysis (Fig. 3A), as for example observed for the M+2 isotope of CL 34:2/36:3 with CL 34:2/36:2 analyzed using the same product ion. The second type, termed as product-overlap, is derived from isotopes present in the charged product ion (F_2) used for analysis (Fig. 3B). We calculated isotope profiles for both types of overlaps using Excel Macros for peak area corrections. BMP isotope overlaps were corrected similarly.

In order to validate this approach, precursor- and product-overlaps were determined experimentally. The standard mixtures containing the symmetric species BMP 18:1/18:1 and CL $(14:0)_4$ as well as the asymmetric species BMP 16:0/17:0 and CL $(14:1)_3(15:1)$ were analyzed. Both measured precursor- and product-overlaps resemble the theoretically calculated isotope profiles (Tab. 1). We analyzed mouse heart tissue and cultured human skin fibroblast with and without isotopic correction. Omission of isotopic correction leads not only to mis-quantification but also to misidentification of species. For example, 11 CL species in heart and 7 CL species in fibroblast would have been identified erroneously above detection limit without correction of isotope overlap (Table S-3 and 4). Since PA and PG molecular species are characterized by a specific neutral loss scan of m/z of 115 and 189, respectively, only a product-overlap has to be considered.
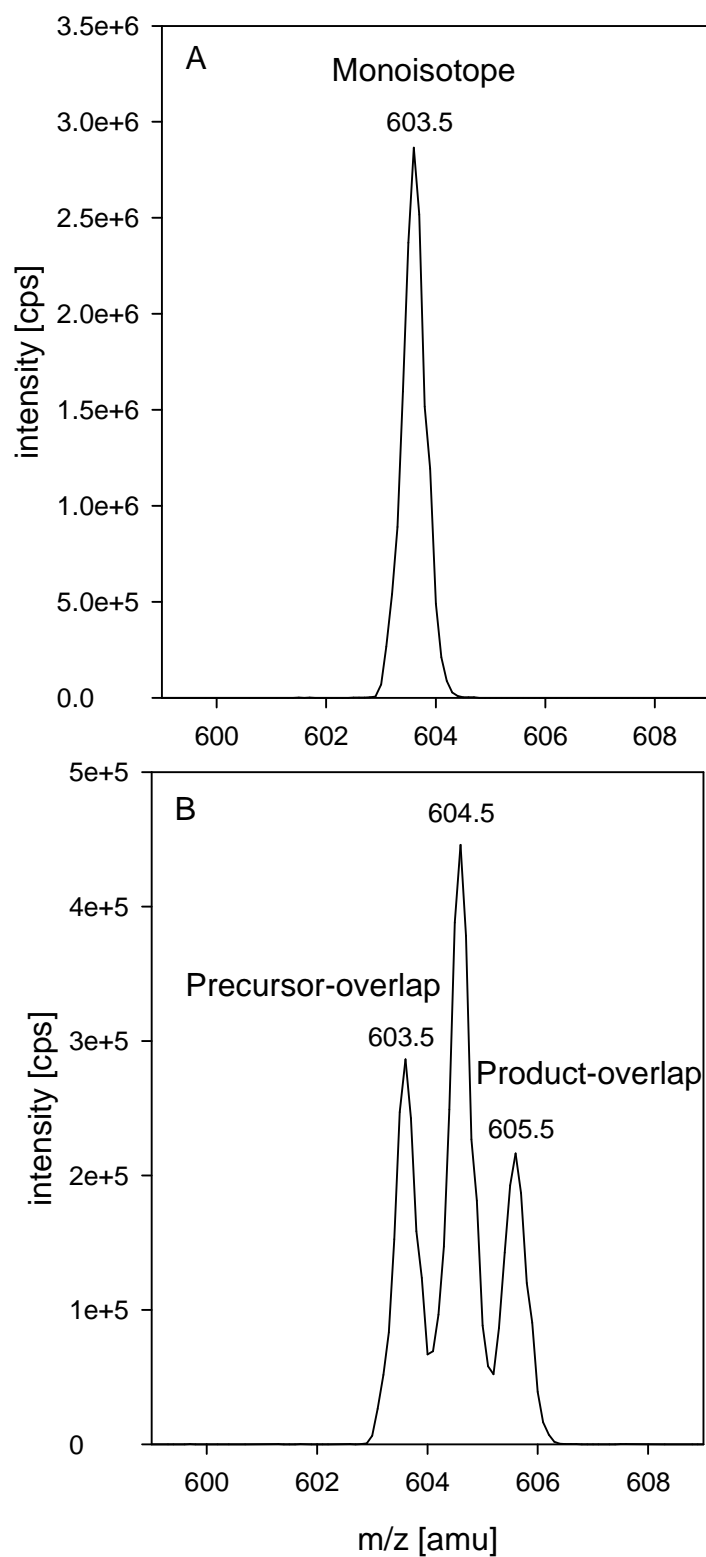
Fig. 2. Product ion spectra of CL (18:1)$_4$.

Product ion spectra of CL (18:1)$_4$ of the monoisotopic [M+NH$_4$]$^+$ (Panel A) and the isotope +2 [M+2+NH$_4$]$^+$ precursors (Panel B) obtained in the positive ionization mode are presented. Panel B shows the signals corresponding to the precursor- and the product-overlaps.

A

mass transition: 1447 ⟶ 575.5

$[N_2-F_0]^+ \longrightarrow [F_0]^+$ CL 34:2/36:3 ⎫
$[N_0-F_0]^+ \longrightarrow [F_0]^+$ CL 34:2/36:2 ⎭ Precursor-overlap

B

mass transition: 1447 ⟶ 577.5

$[N_0-F_2]^+ \longrightarrow [F_2]^+$ CL 34:2/36:3 ⎫
$[N_0-F_0]^+ \longrightarrow [F_0]^+$ CL 34:1/36:3 ⎭ Product-overlap
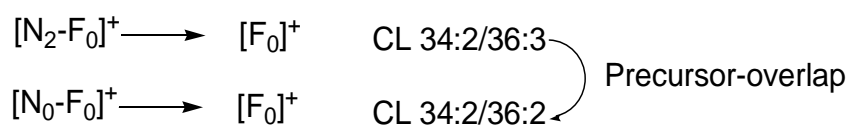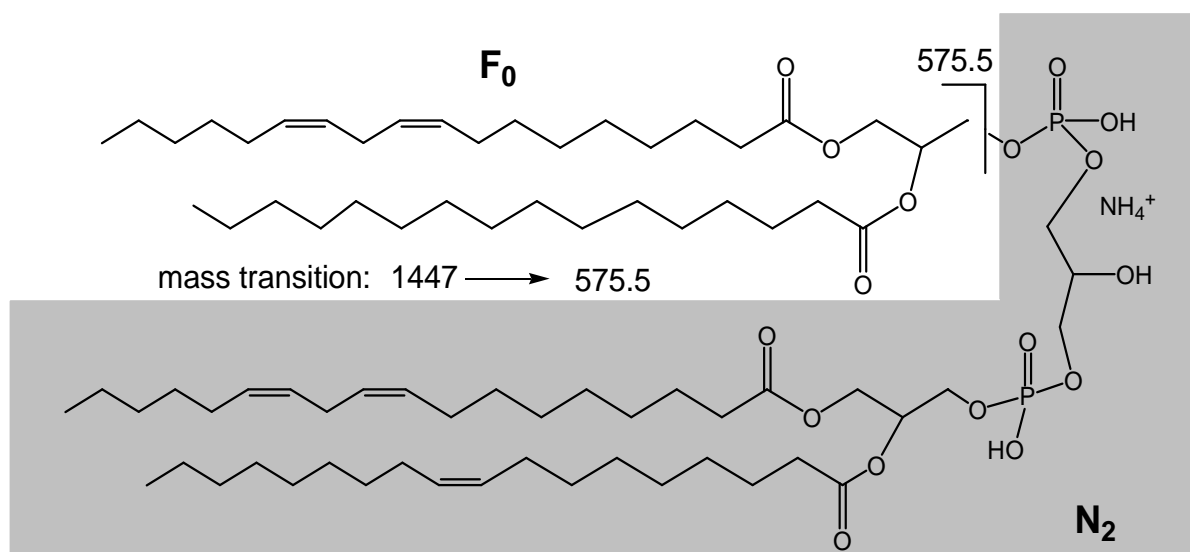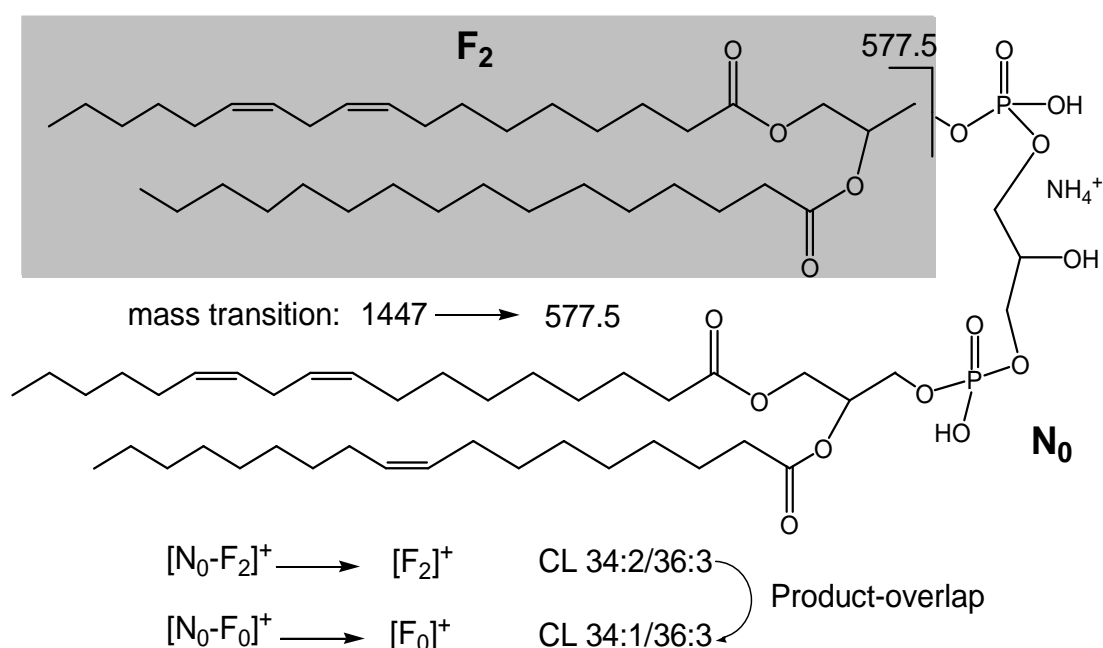
Fig. 3. Structure and isotope distribution in CL 34:2/36:3.

Panel A shows the structure, isotope distribution and the corresponding mass transition for the precursor-overlap.

Panel B shows the structure, isotope distribution and the corresponding mass transition for the product-overlap.

Table 1. Isotope overlap

Analyte	Spiked amount [ng/ml]	Analyte area [cps *10³]	Precursor-overlap [%]		Product-overlap [%]	
			measured	theoretical	measured	theoretical
BMP 16:0/17:0	250	382 ± 1	4.18 ± 0.33	3.91	2.71 ± 0.15	2.82
	500	756 ± 39	4.01 ± 0.17	3.91	2.68 ± 0.05	2.82
BMP 18:1/18:1	250	1020 ± 10	4.55 ± 0.22	4.16	3.17 ± 0.14	3.32
	500	2025 ± 67	4.49 ± 0.11	4.16	3.15 ± 0.07	3.32
CL (14:0)$_4$	250	942 ± 80	10.75 ± 0.98	10.16	7.06 ± 0.53	6.82
	500	1967 ± 35	10.69 ± 0.43	10.16	7.35 ± 0.30	6.82
CL (14:1)$_3$(15:1)	250	23.8 ± 1.6	11.14 ± 1.21	10.59	7.08 ± 0.98	6.80
	500	44.8 ± 2.3	10.36 ± 0.5	10.59	6.80 ± 0.65	6.80

A standard mixture spiked with the indicated concentration of BMP 16:0/17:0, BMP 18:1/18:1, CL (14:0)$_4$, CL (14:1)$_3$(15:1) was analyzed in a triplicate measurement. Precursor-overlap percentages were calculated as the peak areas of the $[N_2F_0]^+ \rightarrow [F_0]^+$ mass transition related to the monoisotopic mass transition. Product-overlap percentages were calculated as the peak areas of the $[N_0F_2]^+ \rightarrow [F_2]^+$ mass transition related to the monoisotopic mass transition.

2.4.4 Quantification

For quantification purposes, the analytical response of glycerophospholipid species may depend on their degree of saturation and their fatty acid chain length (12;15;24). Thus, we established calibration lines by addition of saturated and unsaturated species (Table S-2). The calibration lines were linear in the tested concentration range with correlation coefficients >0.992. Polyunsaturated species showed a lower response compared to more saturated species. It is important to keep in mind that symmetric CL and BMP species show a double response compared to asymmetric species since both moieties of these species generate the same DAG and MAG fragment, respectively. Concentrations of the glycerophospoholipid species were calculated using the closest related calibration slope.

2.4.5 Method validation

Finally, we performed method validation in the samples of cultured primary human skin fibroblasts and mouse heart tissue. Overall precision showed CVs <9%, for the major, and <13%, for the minor species (Tables S-3 and -4). Limits of detection ranged from 1.5fmol for PA up to 119fmol for BMP species (Table S-1). Extraction efficiencies were between 60%, for the apolar CL, and up to 80%, for the polar PA species (Table S-5). The influence of the sample matrix on the signal intensities was similar in fibroblasts lysed in SDS and mouse heart tissues (data not shown). While the presence of the biological matrix showed no effect on BMP and slight signal suppression on CL (10%), PA and PG signals were enhanced up to 40% (Table S-5).

2.5 Conclusion

We developed a novel LC-MS/MS method for the quantification of PA, PG, BMP, and CL species in biological samples. This method shows a number of improvements compared to other existing methods. Moreover, a combined, rapid and sensitive quantification method of these biologically important lipid classes does not exist till now. Quantification of CL from MS/MS data provides information about the

DAG moieties, in contrast to summary composition derived from MS analysis. We could show that HILIC allows co-elution of analytes and internal standards, in our opinion, a prerequisite for quantification. This co-elution necessitates a correction of isotopic overlap of the species which differ in one double bond. Here we applied and validated previously described principles of isotope overlap in MS/MS experiments (18). As shown for CL, these corrections are required for accurate quantification and identification of lipid species.

Finally, it should be mentioned that this method can be easily combined with previously established HILIC-MS/MS methods for lysophosphatidic acid and sphingolipid profiling (25;26), since the same butanolic extracts are used for all assays.

2.6   References

1. Schlame M, Ren M. The role of cardiolipin in the structural organization of mitochondrial membranes. Biochim Biophys Acta 2009;1788:2080-3.

2. Hullin-Matsuda F, Luquain-Costaz C, Bouvier J, ton-Vandenbroucke I. Bis(monoacylglycero)phosphate, a peculiar phospholipid to control the fate of cholesterol: Implications in pathology. Prostaglandins Leukot Essent Fatty Acids 2009;81:313-24.

3. Kolter T, Sandhoff K. Lysosomal degradation of membrane lipids. FEBS Lett 2010;584:1700-12.

4. Houtkooper RH, Vaz FM. Cardiolipin, the heart of mitochondrial metabolism. Cell Mol Life Sci 2008;65:2493-506.

5. Hullin-Matsuda F, Kawasaki K, ton-Vandenbroucke I, Xu Y, Nishijima M, Lagarde M et al. De novo biosynthesis of the late endosome lipid, bis(monoacylglycero)phosphate. J Lipid Res 2007;48:1997-2008.

6. Houtkooper RH, Rodenburg RJ, Thiels C, van LH, Stet F, Poll-The BT et al. Cardiolipin and monolysocardiolipin analysis in fibroblasts, lymphocytes, and tissues using high-performance liquid chromatography-mass spectrometry as a diagnostic test for Barth syndrome. Anal Biochem 2009;387:230-7.

7. Valianpour F, Wanders RJ, Barth PG, Overmars H, van Gennip AH. Quantitative and compositional study of cardiolipin in platelets by electrospray ionization mass spectrometry: application for the identification of Barth syndrome patients. Clin Chem 2002;48:1390-7.

8. Meikle PJ, Duplock S, Blacklock D, Whitfield PD, Macintosh G, Hopwood JJ, Fuller M. Effect of lysosomal storage on bis(monoacylglycero)phosphate. Biochem J 2008;411:71-8.

9. Han X, Gross RW. Shotgun lipidomics: electrospray ionization mass spectrometric analysis and quantitation of cellular lipidomes directly from crude extracts of biological samples. Mass Spectrom Rev 2005;24:367-412.

10. Pulfer M, Murphy RC. Electrospray mass spectrometry of phospholipids. Mass Spectrom Rev 2003;22:332-64.

11. Han X, Yang J, Cheng H, Yang K, Abendschein DR, Gross RW. Shotgun lipidomics identifies cardiolipin depletion in diabetic myocardium linking altered substrate utilization with mitochondrial dysfunction. Biochemistry 2005;44:16684-94.

12. Han X, Yang K, Yang J, Cheng H, Gross RW. Shotgun lipidomics of cardiolipin molecular species in lipid extracts of biological samples. J Lipid Res 2006;47:864-79.

13. Hsu FF, Turk J. Characterization of cardiolipin from Escherichia coli by electrospray ionization with multiple stage quadrupole ion-trap mass spectrometric analysis of [M - 2H + Na]- ions. J Am Soc Mass Spectrom 2006;17:420-9.

14. Minkler PE, Hoppel CL. Separation and characterization of cardiolipin molecular species by reverse-phase ion pair high-performance liquid chromatography-mass spectrometry. J Lipid Res 2010;51:856-65.

15. Sparagna GC, Johnson CA, McCune SA, Moore RL, Murphy RC. Quantitation of cardiolipin molecular species in spontaneously hypertensive heart failure rats using electrospray ionization mass spectrometry. J Lipid Res 2005;46:1196-204.

16. Bartlett EM, Lewis DH. Spectrophotometric determination of phosphate esters in the presence and absence of orthophosphate. Anal Biochem 1970;36:159-67.

17. Baker DL, Desiderio DM, Miller DD, Tolley B, Tigyi GJ. Direct quantitative analysis of lysophosphatidic acid molecular species by stable isotope dilution electrospray ionization liquid chromatography-mass spectrometry. Anal Biochem 2001;292:287-95.

18. Ejsing CS, Duchoslav E, Sampaio J, Simons K, Bonner R, Thiele C et al. Automated identification and quantification of glycerophospholipid molecular species by multiple precursor ion scanning. Anal Chem 2006;78:6202-14.

19. Liebisch G, Lieser B, Rathenberg J, Drobnik W, Schmitz G. High-throughput quantification of phosphatidylcholine and sphingomyelin by electrospray ionization tandem mass spectrometry coupled with isotope correction algorithm. Biochim Biophys Acta 2004;1686:108-17.

20. Brugger B, Erben G, Sandhoff R, Wieland FT, Lehmann WD. Quantitative analysis of biological membrane lipids at the low picomole level by nano-electrospray ionization tandem mass spectrometry. Proc Natl Acad Sci U S A 1997;94:2339-44.

21. Hermansson M, Uphoff A, Kakela R, Somerharju P. Automated quantitative analysis of complex lipidomes by liquid chromatography/mass spectrometry. Anal Chem 2005;77:2166-75.

22. Schwudke D, Oegema J, Burton L, Entchev E, Hannich JT, Ejsing CS et al. Lipid profiling by multiple precursor and neutral loss scanning driven by the data-dependent acquisition. Anal Chem 2006;78:585-95.

23. Ejsing CS, Sampaio JL, Surendranath V, Duchoslav E, Ekroos K, Klemm RW et al. Global analysis of the yeast lipidome by quantitative shotgun mass spectrometry. Proc Natl Acad Sci U S A 2009;106:2136-41.

24. Koivusalo M, Haimi P, Heikinheimo L, Kostiainen R, Somerharju P. Quantitative determination of phospholipid compositions by ESI-MS: effects of acyl chain length, unsaturation, and lipid concentration on instrument response. J Lipid Res 2001;42:663-72.

25. Scherer M, Schmitz G, Liebisch G. High-throughput analysis of sphingosine 1-phosphate, sphinganine 1-phosphate, and lysophosphatidic acid in plasma samples by liquid chromatography-tandem mass spectrometry. Clin Chem 2009;55:1218-22.

26. Scherer M, Leuthauser-Jaschinski K, Ecker J, Schmitz G, Liebisch G. A rapid and quantitative LC-MS/MS method to profile sphingolipids. J Lipid Res 2010;51:2001-11.

2.7 Supporting Information

Table S-1. MS parameter and limit of detection (LOD) of glycerophospholipids studied.

Lipid class	MRM	IS (MRM)	CE [V]	RT [min]	LOD (n=3) [fmol]
PA	$[M+NH_4]^+ \rightarrow DAG$ NL m/z 115	PA 14:0/14:0 (610.5→495.5)	25	1.79	1.5 ± 0.3
PG	$[M+NH_4]^+ \rightarrow DAG$ NL m/z 189	PG 14:0/14:0 (684.5→495.5)	27	1.51	91 ± 14
BMP	$[M+H]^+ \rightarrow MAG$	BMP 14:0/14:0 (667.5→285.3)	37	1.41	119 ± 12
CL	$[M+NH_4]^+ \rightarrow DAG$	CL 28:0/28:0 (1259.0→495.5)	43	1.75	36 ± 2

MRM = multiple reaction monitoring, IS = internal standard, CE = collision energy, RT = retention time. LODs (injected amount) were calculated as a signal to noise ratio of 3.

Table S-2. Calibration data

Analyte	Calibration range [pmol]	Slope (mean ± S.D.)	Correlation coefficient (mean ± S.D.)
PA 16:0/16:0	4.0 – 40	0.0670 ± 0.005	0.992 ± 0.003
PA 18:1/18:1	4.9 – 49	0.0678 ± 0.006	0.995 ± 0.002
PA 18:0/20:4	3.1 – 31	0.036 ± 0.003	0.994 ± 0.002
BMP 16:0/16:0	6.7 – 67	0.033 ± 0.003	0.996 ± 0.002
BMP 18:1/18:1	9.4 - 94	0.025 ± 0.002	0.997 ± 0.004
PG 16:0/16:0	4.3 – 43	0.171 ± 0.015	0.994 ± 0.002
PG 18:1/18:1	3.6 – 36	0.196 ± 0.013	0.998 ± 0.002
PG 18:0/20:4	1.5 – 15	0.119 ± 0.007	0.997 ± 0.004
CL 30:0/31:1	7.6 – 76	0.034 ± 0.002	0.995 ± 0.002
CL 36:2/36:2	5.9 - 59	0.047 ± 0.003	0.994 ± 0.002

Calibration was performed by standard addition to mouse heart tissue homogenates. Each value represents the average of three determinations.

Table S-3. Intra- and Inter-day precisions in mouse heart tissues

Analyte	Conc. [pmol/mg tissue]	Intraday-precision (%) (n=5)	Interday-precision (%) (n=5)
BMP 18:1/18:1	1.29 ± 0.10	7.5	8.7
PG 32:0	0.58 ± 0.04	7.2	12.0
PG 34:1	48.9 ± 2.1	4.2	6.8
PG 36:3	5.42 ± 0.42	7.8	7.7
PG 36:2	10.95 ± 0.66	6.0	9.73
PG 36:1	2.18 ± 0.14	6.4	6.6
PG 38:4	15.19 ± 0.58	3.8	8.7
CL 34:3/36:4	4.54 ± 0.28	6.2	8.9
CL 34:3/36:3	2.86 ± 0.23	8.0	7.3
CL 34:2/36:3	4.94 ± 0.38	7.7	4.9
CL 36:4/36:5	19.90 ± 1.15	5.8	11.1
CL 36:4/36:4	92.74 ± 3.63	3.9	5.0
CL 36:4/36:3	81.40 ± 2.4	3.0	8.8
CL 36:3/36:3	31.73 ± 2.64	8.3	10.4
CL 36:4/36:1	4.63 ± 0.30	6.5	8.6
CL 36:3/36:2	10.08 ± 1.04	10.35	11.6
CL 36:2/36:2	3.07 ± 0.32	10.3	11.8
CL 36:4/38:6	10.42 ± 0.98	9.4	9.2
CL 36:4/38:5	22.42 ± 1.29	5.8	9.0
CL 36:3/38:6	3.27 ± 0.28	8.5	7.5
CL 36:4/38:4	13.73 ± 1.16	8.5	11.3
CL 36:3/38:5	4.48 ± 0.29	6.5	8.3
CL 36:2/38:6	0.54 ± 0.06	10.9	6.6
CL 36:3/38:4	10.90 ± 0.8	6.9	12.1
CL 36:3/38:3	14.3 ± 1.3	9.0	6.8
CL 36:4/40:8	104.5 ± 6.0	5.8	7.1
CL 36:5/40:7	1.04 ± 0.13	13.0	12.6
CL 36:3/40:9	1.82 ± 0.11	6.0	7.1
CL 36:4/40:7	25.47 ± 1.25	4.9	10.5
CL 36:3/40:8	19.18 ± 1.84	9.6	12.4
CL 36:4/40:6	4.01 ± 0.41	10.0	11.8
CL 36:3/40:7	6.35 ± 0.38	5.9	8.5
CL 36:3/40:6	1.38 ± 0.14	10.3	13.7

The displayed values are mean concentrations from mouse heart tissue lipid extracts and the coefficient of variation (CV) of 5 samples analyzed in series for intraday-precision and on 5 different days for interday-precision. Tissue homogenate corresponding to 2.5mg wet weight were used for quantification.

Table S-4. Intra- and Inter-day precisions in primary human skin fibroblasts

Analyte	Conc. [pmol/mg cellular protein]	Intraday-precision (%) (n=5)	Interday-precision (%) (n=5)
PA 32:0	17.77 ± 1.24	7.0	9.5
PA 34:1	41.88 ± 3.56	8.5	8.1
PA 36:2	13.53 ± 0.74	5.5	6.7
PA 36:1	13.20 ± 1.37	10.3	12.3
PA 38:4	15.64 ± 1.93	12.4	11.4
BMP 16:1/18:1	43.02 ± 3.42	8.0	8.8
BMP 16:0/18:1	36.43 ± 2.28	6.3	7.9
BMP 18:2/18:2	13.89 ± 2.28	8.3	9.7
BMP 18:2/18:1	165.90 ± 15.99	9.6	10.6
BMP 18:1/18:1	388.77 ± 22.25	5.7	7.9
BMP 18:1/18:0	84.66 ± 5.35	7.5	8.1
BMP 18:1/20:4	168.12 ± 9.81	5.8	10.7
BMP 18:1/20:3	146.39 ± 14.56	9.9	8.4
BMP 18:1/20:2	70.49 ± 6.20	8.8	8.6
BMP 18:0/22:6	64.35 ± 8.22	12.8	11.3
BMP 18:1/22:5	294.03 ± 11.66	7.2	8.6
PG 34:1	18.18 ± 1.42	7.8	6.1
PG 36:3	2.54 ± 0.19	7.5	11.2
PG 36:2	4.77 ± 0.44	9.3	8.5
PG 36:1	16.53 ± 1.77	10.7	12.7
CL 34:3/34:3	40.27 ± 3.73	9.3	9.4
CL 34:2/34:2	53.63 ±4.37	8.1	6.3
CL 34:3/36:4	46.75 ± 2.32	5.0	8.0
CL 34:2/36:3	120.72 ± 9.60	8.0	11.8
CL 36:4/36:4	33.81 ± 2.58	7.6	8.9
CL 36:4/36:3	138.80 ± 6.09	4.4	3.3
CL 36:3/36:3	168.62 ± 19.42	11.5	13.1
CL 36:4/36:2	28.81 ± 2.39	8.3	11.9
CL 36:4/36:1	12.9 ± 0.83	6.4	9.8
CL 36:3/36:2	117.21 ± 8.77	7.5	4.3
CL 36:2/36:2	88.72 ± 6.53	7.4	8.6
CL 36:4/38:5	22.56 ± 2.07	9.2	11.5
CL 36:4/38:4	17.45 ± 1.98	11.4	7.9
CL 36:3/38:5	37.78 ± 2.98	7.9	8.7
CL 36:3/38:4	14.6 ± 1.97	13.5	12.9
CL 36:3/38:3	14.47 ± 1.58	10.9	6.5

The displayed values are mean concentrations from primary human skin fibroblasts lipid extracts and the coefficient of variation (CV) of 5 samples analyzed in series for intraday-precision and on 5 different days for interday-precision. Cell homogenate corresponding to 50µg protein were used for quantification.

Table S-5. Recovery and matrix effects

Analyte	Spiked amount [pmol]	Recovery (S.D.) (n=4)	Matrix effect (n=4)
PA 16:0/16:0	3.1	74 ± 8	133 ± 9
PA 18:1/18:1	2.9	79 ± 9	142 ± 5
PA 18:0/20:4	2.8	78 ± 8	140 ± 10
BMP 16:0/16:0	6.7	62 ± 6	108 ± 9
BMP 18:1/18:1	6.5	71 ± 7	109 ± 4
PG 16:0/16:0	1.4	61 ± 2	128 ± 7
PG 18:1/18:1	1.3	70 ± 6	134 ± 4
PG 18:0/20:4	1.3	67 ± 8	141 ± 6
CL 30:2/31:1	7.6	64 ± 3	88 ± 6
CL 36:2/36:2	6.9	65 ± 8	91± 4

Recovery and matrix effects were determined in mouse heart tissue homogenates corresponding to 2.5mg of wet weight. Recovery was calculated as percent of standards spiked before and after extraction. Matrix effects are calculated as the percentage of signal spiked after extraction (corrected by endogenous sphingolipid concentrations) related to a pure standard mixture. Each value represents the average of three determinations ± standard deviation.
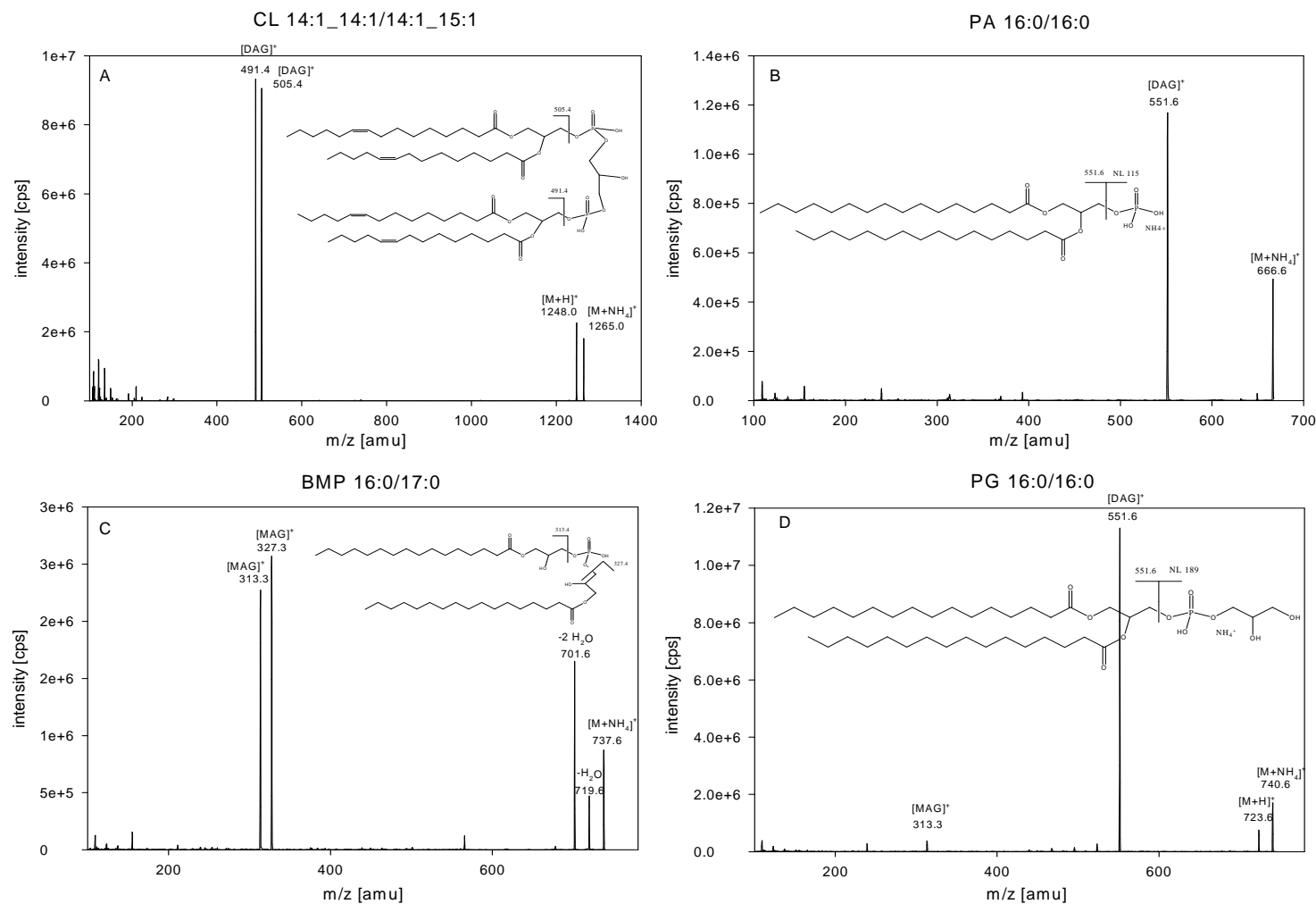
Figure S-1. Product ion spectrum and proposed fragmentation of CL (14:0)$_4$ (Panel A), PA 16:0/16:0 (Panel B), BMP 16:0/17:0 (Panel C) and PG 16:0/16:0 (Panel D) in positive ionization mode. Collision energy was ramped from 5 to 130V.

3   High throughput analysis of sphingosine-1-phosphate, sphinganine-1-phosphate and lysophosphatidic acid in plasma samples by LC-MS/MS

3.1   Abstract

Lysophosphatidic acid (LPA) and sphingosine-1-phosphate (S1P) are ubiquitous lipid messengers found in the blood and most cell types. Both lysophospholipids are ligands of G-protein-coupled receptors and mediate important physiological processes. Moreover, lysophospholipids are potential biomarkers for various diseases including atherosclerosis and cancer. Because existing methodologies are of limited value for a systematic evaluation of S1P and LPA in clinical studies, we developed a fast and simple quantitation method using liquid chromatography tandem mass spectrometry (LC-MS/MS). Sphingoid-base-1-phosphates and LPA species were quantified using fragments of m/z 79 and 153 in negative ion mode, respectively. The internal standards LPA 17:0 and [$^{13}C_2D_2$]-S1P were added prior to butanol extraction. Application of hydrophilic interaction chromatography (HILIC) allowed co-elution of analytes and internal standards with a short analysis time of 2.5min. Comparison of butanol extraction with a frequently used extraction method based on strong acidification of human plasma revealed an artificial formation of LPA from lysophosphatidylcholine. Validation according to FDA guidelines showed an overall imprecision < 12% CV and a limit of detection < 6nmol/L for all lysophospholipid species. S1P and Sphinganine-1-phosphate (SA1P) concentrations in EDTA plasma were found to be stable for 24h at room temperature, whereas LPA concentrations increased substantially. Our validated LC-MS/MS methodology for the quantification of LPA, S1P and SA1P is characterized by simple sample preparation and short analysis time, therefore providing a valuable tool for diagnostic evaluation of these lysophospholipids as biomarkers.

3.2 Introduction

Lysophospholipids in particular lysophosphatidic acid (LPA) and sphingosine-1-phosphate (S1P), are bioactive lipids which elicit a wide range of cellular responses including cell survival, differentiation and migration (1-5). Blood concentrations of S1P and LPA are derived either from cellular release (S1P by platelets and red blood cells (5)) or enzymatic conversion of plasma lipids (lysophosphatidylcholine conversion to LPA by autotaxin (2;4)). Both LPA and S1P act on specific G-protein-coupled receptors on cells of the immune, cardiovascular and nervous systems and thereby regulate the induction of inflammation, atherosclerosis and cancer (1-5). Based on their signaling functions and role in different diseases, LPA and S1P may gain clinical importance as biomarkers. However, so far, the quantitative analysis of LPA and S1P as diagnostic parameters in daily routine or large clinical studies is hindered by laborious and time-consuming methods.

A commonly applied technique for the determination of S1P and LPA is liquid chromatography coupled to tandem mass spectrometry (LC-MS/MS) (6-13). Several methods lack co-elution of internal standard (IS) and analyte, necessary to compensate potential matrix effects or varying ionization efficiency, due to mobile phase gradients (7;10;11;14). Furthermore, laborious sample preparation (8;15), high sample volume (8;11-13), time-consuming derivatization procedures (15), and a lack of sufficient validation (8-11) exclude these methods from routine analysis. Up to now only one methodology for a combined LPA and S1P determination exists (11). Here, we report a simple and rapid LC-MS/MS method for the quantification of S1P, sphinganine-1-phosphate (SA1P) and LPA species.

3.3 Materials and Methods

3.3.1 LC-MS/MS analysis

All analyses described here were performed on a hybrid triple quadrupole linear ion trap mass spectrometer API 4000 Q-Trap (Applied Biosystems, Darmstadt, Germany). The LC equipment consisted of a binary and isocratic pump (Agilent 1200 series, Waldbronn, Germany) connected to an HTC Pal autosampler (CTC Analytics,

Zwingen, Switzerland). Chromatographic separation was performed on a 50 x 2.1mm (i.d.), 3µm particle size HILIC silica column (Waters Atlantis) equipped with a 10 x 2.1mm guard column containing the same material. The column oven temperature was set to 50°C. The mobile phase consisted of wate r containing 0.2% formic acid and 50mmol/L ammonium formate (eluent A) and acetonitrile containing 0.2% formic acid (eluent B). A gradient elution was performed with 5% A for 0.7min, a linear increase to 25% A until 1.5min, followed by 50% A until 1.7min and re-equilibration from 1.7 to 2.5min with 5% A. A flow rate of 500µL/min was used except from 0 to 0.5min and 1.7 to 2.5min, the flow rate was increased to 700µL/min. To minimize the potential contamination of the mass spectrometer, the column flow was directed only from 1.3 to 2.1min into the mass spectrometer using a divert valve. Otherwise methanol with a flow rate of 250µL/min was delivered into the mass spectrometer. The Turbo Ion Spray source was operated in the negative ionization mode using the following settings: Ion spray voltage = -4500V, ion source heater temperature = 300°C, source gas 1 = 40psi, source gas 2 = 35psi a nd curtain gas = 20psi. LPA species revealed fragments resulting from the head group (*m/z* 79, *m/z* 153) and fatty acid moiety (*m/z* 255 for LPA 16:0) (Suppl.-Fig. 1A). To cover all LPA species and due to increased specificity, *m/z* 153 was chosen as product ion for LPA quantification. Product ion spectra of S1P and SA1P showed only one intense fragment of *m/z* 79 (Suppl.-Fig. 1B), which was then used for analysis (see Suppl.-Tab. 1). The collision energy optimum for LPA species and sphingoid base-1-phosphates was 30eV and 58eV, respectively.

3.3.2 Species identification

In order to obtain the naturally occurring lysophospholipid species, we analyzed plasma lipid extracts using a precursor ion scan of 79 and 153 *m/z* revealing the following main species: S1P and SA1P containing a dihydroxy-C18:1 base; LPA 16:0, LPA 18:0, LPA 18:1, LPA 18:2 and LPA 20:4. This pattern is in good accordance with the literature (7;9;11;16). Quantification was achieved by standard addition of S1P, SA1P, LPA 16:0, LPA 18:0, LPA 18:1, LPA 18:2 and LPA 20:4 to human plasma samples, at five different concentrations (Tab. 1).

3.3.3 Sample preparation

Lysophospholipids such as LPA and S1P show a poor recovery using organic solvents like chloroform at neutral pH. Therefore, in a first step, we used a modified extraction procedure according to Bligh & Dyer with 6mol/L HCl (8;12). Although both LPA and S1P showed a high recovery (85-95%), this extraction method was poorly reproducible for plasma samples. Because lysophosphatidylcholine (LPC) might be degraded to LPA under highly acidic conditions (11), we added non-naturally occurring LPC 19:0 to plasma samples. Acidic chloroform extraction of spiked plasma converted about 2% of LPC 19:0 to LPA 19:0 (Suppl.-Tab. 2). This artificial formation of LPA from LPC required the presence of plasma, since acidic extraction of LPC 19:0 without plasma did not result in LPA 19:0 formation (data not shown). For a LPC plasma concentration of 250µmol/L (17), strong acidic extraction could potentially cause a ~7-fold increase of LPA. To circumvent these problems, we used a butanolic extraction reported by Baker et al. (16) and did not observe any LPC-LPA conversion (data not shown). In brief, 75µL EDTA-plasma were mixed with 20ng each of LPA 17:0 and stable isotope labeled [$^{13}C_2D_2$]-S1P (Toronto Research, North York, ON, Canada) and 400µL buffer, containing 30mmol/L citric acid and 40mmol/L disodium hydrogenphosphate (pH 4.0). Extraction was performed with 1mL of 1-butanol and 500µL of water saturated 1-butanol. The recovered butanol phase was evaporated to dryness under reduced pressure. The residue was re-dissolved in 200µL ethanol and 10µL were injected.

3.4 Results and Discussion

3.4.1 Chromatography

Most of the reported LC-MS/MS methods for LPA and S1P analysis use reversed phase chromatography (6;7;10-12;15;17) resulting in a separation of analytes and internal standards. In contrast, we established a separation based on hydrophilic interaction chromatography (HILIC) characterized by co-elution of analytes with their respective internal standards (Fig. 1). The retention times of LPA and S1P were 1.74min and 1.84min, respectively. Due to co-elution, SA1P and S1P as well as LPA species exhibited an isotope overlap. In order to avoid an

overestimation of species concentrations, peak areas were corrected according to the principles described previously ([18]) (Suppl.-Tab. 3).

3.4.2 Validation

Our established LC-MS/MS method was validated according to FDA Guidelines for Bioanalytical Methods ([19]). First, we evaluated a potential suppression of the analyte response due to matrix effects. Because no analyte free EDTA-plasma was available, an internal standard mixture was analyzed with or without plasma extract (C_{spiked} 0.5, 1, 2µmol/L). The presence of plasma extract caused a mean signal reduction (± SD) of 25.0 ± 1.8% and 2.5 ± 1.4% for $[^{13}C_2D_2]$-S1P and LPA 17:0, respectively. Moreover, co-elution of analytes and internal standards may result in suppression of the MS response for multi-component analytes. Although we found signal suppression by analyte co-elution, the ratios of internal standard to analyte did not change significantly (Suppl.-Tab. 4).

3.4.3 Quantification

Calibration by standard addition to plasma samples showed linearity and accuracy of the analytes in the spiked concentration range (Tab. 1). For accurate quantification considering the different responses of species, e.g. only 30% response to LPA 20:4 compared to other LPA (Tab. 1), multiple calibration lines were used. Furthermore, we tested the influence of the plasma lipid content on the response for the analytes by varying the cholesterol concentrations as a surrogate marker. The slopes of the calibration lines showed no notable differences at cholesterol concentrations of 2.97, 4.52 and 7.49mmol/L, respectively (Suppl.-Tab. 5).

Table 1. Standard addition of S1P, SA1P and LPA species to human plasma samples[a]

Analyte	Concentration added, µmol/L	Concentration measured (n=5), µmol/L[b]	Recovery of added analyte, (n=5), %[b]	Linear regression equation (n=5)
S1P	0	0.470 (0.061)		$y=1.08x + 0.44$µmol/L ($r^2=0.997$)
	0.352	0.773 (0.056)	109.8 (6)	
	0.703	1.174 (0.177)	109.3 (12.9)	
	1.407	1.829 (0.105)	96.6 (8.4)	
	2.111	2.485 (0.188)	96.1 (8.9)	
	3.518	3.999 (0.034)	99.8 (1.4)	
SA1P	0	0.286 (0.049)		$y=0.301x + 0.088$µmol/L ($r^2=0.999$)
	0.175	0.439 (0.127)	88.3 (6.7)	
	0.350	0.651 (0.110)	97.4 (12.1)	
	0.700	1.022 (0.146)	105.8 (13.9)	
	1.05	1.313 (0.091)	98.1 (8)	
	1.75	2.039 (0.075)	100.2 (1.7)	
LPA 16:0	0	0.051 (0.005)		$y=2.13x + 0.053$µmol/L ($r^2=0.999$)
	0.162	0.199 (0.023)	91.7 (14.7)	
	0.325	0.366 (0.057)	102.7 (12.4)	
	0.65	0.704 (0.061)	100.6 (9)	
	0.97	1.028 (0.045)	100.6 (4.8)	
	1.62	1.658 (0.023)	99.1 (1.3)	
LPA 18:0	0	0.011 (0.001)		$y=1.90x + 0.020$µmol/L ($r^2=0.997$)
	0.0304	0.036 (0.003)	89.6 (6.7)	
	0.0607	0.070 (0.008)	98.3 (14.4)	
	0.1214	0.131 (0.008)	99.4 (6.3)	
	0.18	0.151 (0.009)	97.6 (2.3)	
	0.30	0.314 (0.0002)	99.7 (0.5)	
LPA 18:1	0.0000	0.048 (0.006)		$y=1.93x + 0.10$µmol/L ($r^2=0.998$)
	0.0917	0.132 (0.007)	92.6 (10.9)	
	0.1834	0.232 (0.027)	100.2 (13.9)	
	0.3670	0.412 (0.027)	99 (6.8)	
	0.55	0.595 (0.017)	99.3 (3.3)	
	0.92	0.964 (0.017)	99.9 (1.53)	
LPA 18:2	0	0.379 (0.031)		$y=1.99x + 0.70$µmol/L ($r^2=0.999$)
	0.308	0.676 (0.063)	96.4 (14.9)	
	0.616	0.984 (0.092)	100.3 (16.1)	
	1.232	1.604 (0.070)	99.5 (5.1)	
	1.85	2.229 (0.052)	100.1 (2.2)	
	3.08	3.448 (0.017)	100.1 (0.8)	
LPA 20:4	0	0.316 (0.026)		$y=1.99x + 0.70$µmol/L ($r^2=0.998$)
	0.291	0.584 (0.032)	92.1 (9.1)	
	0.582	0.880 (0.106)	96.9 (14.3)	
	1.164	1.511 (0.073)	102.7 (4.8)	
	1.75	2.065 (0.110)	100.2 (6.9)	
	2.91	3.200 (0.104)	99 (2.8)	

Stock solutions of lipid species were prepared in methanol from authentic standards (Avanti Polar Lipids). To ensure the accuracy of calibrator concentrations, we performed a phosphate determination [Bartlett and Lewis (13)]. Lysophospholipid standards were added to EDTA-containing plasma samples prior to extraction from a combined methanolic stock solution with the following concentrations (in g/mL): 1.0 (S1P), 0.5 (SA1P), 0.5 (LPA 16:0), 0.1 (LPA 18:0), 0.3 (LPA 18:1), 1.0 (LPA 18:2), and 1.0 (LPA 20:4). For each analyte, calibration curves were calculated by least-squares fitting of the concentration against the peak area ratio of the analyte to the internal standard. The data shown were calculated from 5 independent samples. The recovery of the added analytes was calculated by means of a separate 6-point calibration.

Data are presented as the mean (SD).

3.4.4 Precision

The intra-day imprecisions were below 9% and the inter-day coefficients of variation (CVs) were below 11% (Suppl.-Tab. 6). The limit of detection, defined as a signal-to-noise ratio of 3, were found to be ~6nmol/L for S1P and SA1P and <2nmol/L for LPA (Suppl.-Tab. 1).
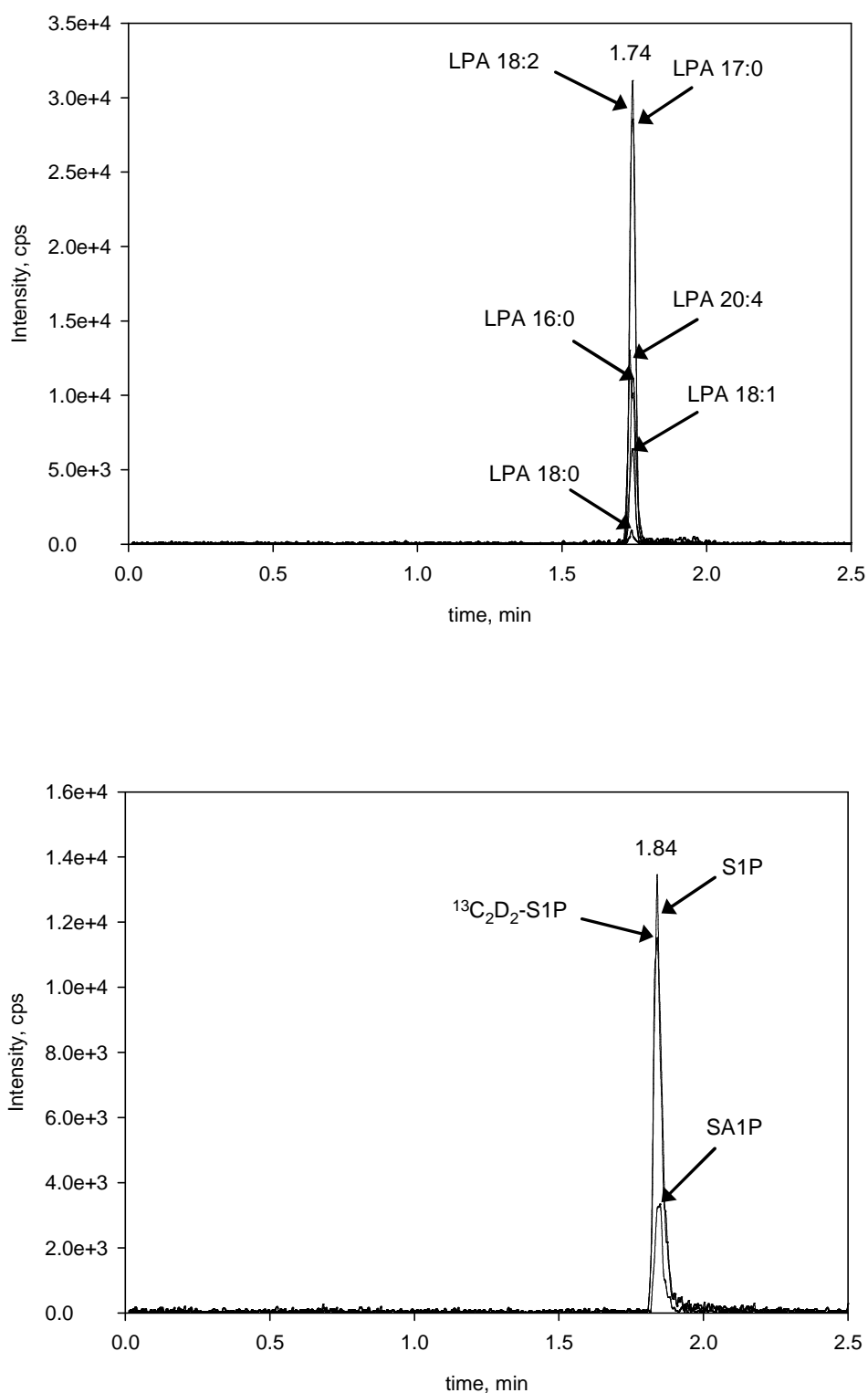
Fig.1. Chromatograms of sphingoid base-1-phosphates and LPA analysis.

Chromatograms show a human plasma sample (75µL), spiked with 20ng each $[^{13}C_2D_2]$-S1P and LPA 17:0 as internal standards. Upper chromatogram displays LPA 16:0, 18:0, 18:1, 18:2, 20:4 and 17:0; lower chromatogram displays S1P, SA1P and $[^{13}C_2D_2]$-S1P.

3.4.5 Sample stability

To investigate sample stability, EDTA-plasma samples were stored immediately at -80℃ or frozen after 1, 4, 8 and 24 h incubation at room temperature. For immediately stored samples, we did not observe any concentration changes compared to freshly analyzed plasma samples (data not shown). S1P and SA1P were stable in EDTA-plasma and serum up to 24 hours at room temperature. In contrast, LPA concentrations increased up to 8-fold when samples were stored at room temperature for 24h (Suppl.-Tab. 7). This increase is most likely due to LPA conversion from LPC by the autotaxin an lyso-phospholipase D (2). In whole blood samples, sphingoid base-1-phosphates showed a rapid increase at room temperature (Suppl.-Tab. 9). Consequently, in order to achieve reliable results, immediate plasma separation and storage at -80℃ is of paramount importance.

3.4.6 S1P and LPA level in human EDTA-plasma

Finally, we determined LPA, S1P and SA1P in freshly drawn EDTA-plasma samples from healthy human volunteers (n=10, Suppl.-Tab. 10). The mean concentrations for S1P and SA1P were 0.59 and 0.19µmol/L, respectively. Total mean LPA concentrations were 0.7µmol/L with the two dominating species LPA 20:4 (~55%) and LPA 18:2 (~25%) contributing 80% to the overall measured LPA concentrations. These values are in good agreement within previously reported concentrations (7;11;12;14-16). In contrast, total LPA concentrations determined after highly acidic extraction were much higher (~5µmol/L) most likely resulting from LPC degradation (8).

3.5 Conclusion

Compared to existing LC-MS-based reports (6;7;11;12;15;16), our novel method shows major advantages in terms of small sample volumes, easy sample preparation and short run times of 2.5min (Suppl.-Tab. 11). Most importantly, HILIC allows co-elution of analytes and internal standards, a prerequisite for accurate compensation of potential matrix effects and varying ionization efficiencies. In

summary, the simultaneous determination of S1P, SA1P and LPA described here may be a useful analytic tool for the clinical chemistry laboratory.

3.6 References

1. Rosen H, Goetzl EJ. Sphingosine 1-phosphate and its receptors: an autocrine and paracrine network. Nat Rev Immunol 2005;5:560-70.

2. van Meeteren LA, Moolenaar WH. Regulation and biological activities of the autotaxin-LPA axis. Prog Lipid Res 2007;46:145-60.

3. Meyer zu HD, Jakobs KH. Lysophospholipid receptors: signalling, pharmacology and regulation by lysophospholipid metabolism. Biochim Biophys Acta 2007;1768:923-40.

4. Lin DA, Boyce JA. Lysophospholipids as mediators of immunity. Adv Immunol 2006;89:141-67.

5. Kihara A, Igarashi Y. Production and release of sphingosine 1-phosphate and the phosphorylated form of the immunomodulator FTY720. Biochim Biophys Acta 2008;1781:496-502.

6. Bielawski J, Szulc ZM, Hannun YA, Bielawska A. Simultaneous quantitative analysis of bioactive sphingolipids by high-performance liquid chromatography-tandem mass spectrometry. Methods 2006;39:82-91.

7. Schmidt H, Schmidt R, Geisslinger G. LC-MS/MS-analysis of sphingosine-1-phosphate and related compounds in plasma samples. Prostaglandins Other Lipid Mediat 2006;81:162-70.

8. Yoon HR, Kim H, Cho SH. Quantitative analysis of acyl-lysophosphatidic acid in plasma using negative ionization tandem mass spectrometry. J Chromatogr B Analyt Technol Biomed Life Sci 2003;788:85-92.

9. Meleh M, Pozlep B, Mlakar A, Meden-Vrtovec H, Zupancic-Kralj L. Determination of serum lysophosphatidic acid as a potential biomarker for ovarian cancer. J Chromatogr B Analyt Technol Biomed Life Sci 2007;858:287-91.

10. Merrill AH, Jr., Sullards MC, Allegood JC, Kelly S, Wang E. Sphingolipidomics: high-throughput, structure-specific, and quantitative analysis of sphingolipids by liquid chromatography tandem mass spectrometry. Methods 2005;36:207-24.

11. Murph M, Tanaka T, Pang J, Felix E, Liu S, Trost R et al. Liquid chromatography mass spectrometry for quantifying plasma lysophospholipids: potential biomarkers for cancer diagnosis. Methods Enzymol 2007;433:1-25.

12. Shan L, Jaffe K, Li S, Davis L. Quantitative determination of lysophosphatidic acid by LC/ESI/MS/MS employing a reversed phase HPLC column. J Chromatogr B Analyt Technol Biomed Life Sci 2008.

13. Bartlett EM, Lewis DH. Spectrophotometric determination of phosphate esters in the presence and absence of orthophosphate. Anal Biochem 1970;36:159-67.

14. Butter JJ, Koopmans RP, Michel MC. A rapid and validated HPLC method to quantify sphingosine 1-phosphate in human plasma using solid-phase extraction followed by derivatization with fluorescence detection. J Chromatogr B Analyt Technol Biomed Life Sci 2005;824:65-70.

15. Berdyshev EV, Gorshkova IA, Garcia JG, Natarajan V, Hubbard WC. Quantitative analysis of sphingoid base-1-phosphates as bisacetylated derivatives by liquid chromatography-tandem mass spectrometry. Anal Biochem 2005;339:129-36.

16. Baker DL, Desiderio DM, Miller DD, Tolley B, Tigyi GJ. Direct quantitative analysis of lysophosphatidic acid molecular species by stable isotope dilution electrospray ionization liquid chromatography-mass spectrometry. Anal Biochem 2001;292:287-95.

17. Liebisch G, Drobnik W, Lieser B, Schmitz G. High-throughput quantification of lysophosphatidylcholine by electrospray ionization tandem mass spectrometry. Clin Chem 2002;48:2217-24.

18. Liebisch G, Lieser B, Rathenberg J, Drobnik W, Schmitz G. High-throughput quantification of phosphatidylcholine and sphingomyelin by electrospray ionization tandem mass spectrometry coupled with isotope correction algorithm. Biochim Biophys Acta 2004;1686:108-17.

19. U.S.Department of Health and Human Services Food and Drug Administration. Guidance for Industry
Bioanalytical Method Validation. 2001.
Ref Type: Generic

3.7 Data Supplement

Suppl.-Table 1. Summary of precursor/product ion *m/z's* for MRM detection.

Analyte	mass transition [*m/z*]	collision energy [eV]	limit of detection [nmol/L]
S1P	378.2 → 79	58	6
SA1P	380.2 → 79	58	4.95
$^{13}C_2D_2$-S1P	382.2 → 79	58	-
LPA 16:0	409.2 → 153	30	0.37
LPA 18:0	437.3 → 153	30	0.31
LPA 18:1	435.3 → 153	30	0.55
LPA 18:2	433.3 → 153	30	1.7
LPA 20:4	457.2 → 153	30	1.26
LPA 17:0	423.3 → 153	30	-

Suppl.-Table 2. LPC degradation to LPA generation during strong acidic extraction.

Spiked LPC 19:0 [µmol/L]	LPA 19:0 generation [µmol/L]	LPA generation [% of LPC]
2.48	0.042 (0.041-0.044)	1.7
4.96	0.11 (0.10-0.14)	2.2
9.92	0.206 (1.89-2.2)	2.1

The indicated concentration of LPC 19:0 were added to plasma. LPA was extracted by a modified Bligh and Dyer protocol in the presence of 6mol/L HCl. The displayed values are median and range of a triplicate measurement.

Suppl.-Table 3. 75µL human EDTA-plasma was spiked with increasing amounts of LPA 18:2 and S1P.

LPA 18:2 spiked [ng]	Ratio LPA 18:2/IS	Uncorrected ratio LPA18:1/IS	Corrected ratio LPA 18:1/IS
0	1.624 (1.552-1.691)	0.384 (0.375-0.427)	0.355 (0.348-0.382)
20	2.451 (2.443-2.695)	0.402 (0.377-0.439)	0.356 (0.331-0.381)
60	4.67 (4.537-4.771)	0.482 (0.488-0.516)	0.353 (0.335-0.369)
100	6.459 (6.396-6.810)	0.552 (0.518-0.555)	0.366 (0.348-0.400)

S1P spiked [ng]	Ratio S1P/IS	Uncorrected ratio SA1P/IS	Corrected ratio SA1P/IS
0	0.803 (0.796-0.852)	0.257 (0.235-0.258)	0.224 (0.209-0.237)
20	1.578 (1.555-1.723)	0.248 (0.244-0.290)	0.222 (0.2-0.237)
60	2.956 (2.953-3.106)	0.3 (0.27-0.302)	0.216 (0.201-0.236)
100	4.225 (4.052-4.332)	0.343 (0.315-0.351)	0.227 (0.213-0.258)

Values represent peak area ratios of LPA 18:2 and 18:1 to LPA 17:0 as well as S1P and SA1P to $^{13}C_2D_2$-S1P, respectively. The LPA 18:1 and SA1P peak area ratios were shown before and after isotope correction. The displayed values are median and range of a triplicate measurement.

Suppl.-Table 4. 75µl EDTA-plasma were spiked either with the indicated amount of LPA 16:0, 18:0, 18:2, 20:4 or S1P.

	spiked [ng]	peak area [cps]	% peak area of unspiked	ratio analyte/IS	% ratio analyte/IS of unspiked
LPA 18:1	0	7245 (6611-7492)	100 (91-103)	0.343 (0.315-0.351)	100 (92-102)
	20	6452 (6275-6812)	89 (87-94)	0.309 (0.296-0.337)	90 (86-98)
	60	6204 (6030-6650)	85.6 (83-92)	0.302 (0.289-0.315)	88 (84-92)
	100	6914 (6440-7251)	95.4 (89-100)	0.320 (0.309-0.345)	93 (90-100)
SA1P	0	1351 (1324-1512)	100 (98-112)	0.157 (0.15-0.173)	100 (96-110)
	20	1160 (1143-1323)	86 (85-98)	0.147 (0.133-0.149)	94 (85-95)
	60	1148 (1007-1205)	85 (75-89)	0.166 (0.152-0.177)	106 (97-113)
	100	1047 (987-1103)	76 (73-82)	0.141 (0.139-0.162)	90 (89-103)

The peak areas, and ratios analyte to internal standard as well as their percentage related to the unspiked sample were calculated for LPA 18:1 and SA1P, respectively. The displayed values are median and range of a triplicate measurement.

Suppl.-Table 5. Influence of plasma cholesterol on the slopes of the calibration lines

Plasma cholesterol [mmol/L]	S1P	LPA 16:0	LPA 18:0	LPA 18:1	LPA 20:4
2.97	1.05	2.20	2.55	2.52	0.66
4.52	0.93	2.26	2.58	2.75	0.66
7.49	1.07	2.15	2.41	2.66	0.65

Calibration lines were generated by standard addition of S1P, LPA 16:0, LPA 18:0, LPA 18:1 and LPA 20:4. Regression line coefficients were all above 0.99 and the displayed values show the slope of the regression lines generated by linear regression.

Suppl.-Table 6. Intra- and inter-day-imprecisions.

	S1P	SA1P	LPA 16:0	LPA18:0	LPA 18:1	LPA18:2	LPA20:4	Total LPA
				Intra-day				
Plasma 1 [µmol/L]	0.49	0.12	0.043	0.0085	0.055	0.17	0.37	0.65
CV [%]	4.42	3.69	3.78	6.19	2.99	7.18	6.43	3.19
Plasma 2 [µmol/L]	0.76	0.34	0.044	0.0086	0.052	0.30	0.43	0.89
CV [%]	3.66	7.50	4.89	7.60	7.09	5.64	8.88	5.63
Plasma 3 [µmol/L]	1.62	0.07	0.24	0.024	0.18	0.79	1.43	2.67
CV [%]	6.06	5.07	6.69	8.65	7.42	5.63	7.58	6.04
				Inter-day				
Plasma 4 [µmol/L]	0.44	0.080	0.042	0.008	0.051	0.20	0.33	1.29
CV [%]	8.20	8.47	9.80	8.58	7.04	3.93	5.42	10.58
Plasma 5 [µmol/L]	0.70	0.11	0.045	0.009	0.052	0.26	0.39	0.70
CV [%]	9.68	7.56	10.55	8.34	7.72	6.51	5.54	5.00
Plasma 6 [µmol/L]	0.67	0.14	0.10	0.012	0.08	0.40	0.67	0.71
CV [%]	7.84	7.79	9.64	8.0	9.40	11.46	10.06	5.66

The displayed values are mean plasma concentrations in µmol/L and the coefficient of variation (CV) of 6 sample aliquots at 3 concentrations analyzed in series for intra-day and on 6 different days for inter-day imprecision.

Suppl.-Table 7. Plasma sample stability.

Conditions	S1P	SA1P	LPA 16:0	LPA 18:0	LPA 18:1	LPA 18:2	LPA 20:4	Total LPA
1h RT	111	102	138	122	138	145	135	138
4h RT	100	92	295	216	239	302	262	273
8h RT	112	87	521	400	462	503	424	456
24h RT	102	90	1087	777	856	821	756	801

Separated plasma samples were stored at room temperature (RT) for the time indicated. The displayed values are percent (mean of two different plasma samples) related to plasma stored at -80℃ u ntil analysis.

Suppl.-Table 8. Serum sample stability.

Conditions	S1P	SA1P	LPA 16:0	LPA 18:0	LPA 18:1	LPA 18:2	LPA 20:4	Total LPA
1h RT	94	92	118	119	121	130	99	103
4h RT	94	112	287	237	248	288	128	148
8h RT	95	104	520	345	436	526	158	206
24h RT	96	101	2004	1237	1301	1485	298	477

Separated serum samples were stored at room temperature (RT) for the time indicated. The displayed values are percent (mean of two different serum samples) related to serum stored at -80℃ unt il analysis.

Suppl.-Table 9. Whole blood sample stability.

Conditions	S1P	SA1P	LPA 16:0	LPA 18:0	LPA 18:1	LPA 18:2	LPA 20:4	Total LPA
1h RT	317	150	206	165	206	328	188	223
4h RT	718	302	379	258	364	632	343	414
8h RT	763	350	498	328	462	885	466	558
24h RT	845	410	737	495	669	1112	718	803

EDTA whole blood samples were stored at room temperature (RT) for the time indicated until separation of plasma. The displayed values are percent (mean of two different plasma samples) related to plasma stored at -80℃ until analysis.

Suppl.-Table 10. Concentrations of sphingoid base phosphates and LPA in EDTA-plasma separated immediately upon drawing.

Analyte	Plasma [µmol/L]
S1P	0.59 ± 0.15
SA1P	0.19 ± 0.07
LPA 16:0	0.058 ± 0.008
LPA 18:0	0.010 ± 0.0012
LPA 18:1	0.061 ± 0.05
LPA 18:2	0.18 ± 0.05
LPA 20:4	0.39 ± 0.09
Total LPA	0.699 ± 0.20

The displayed values are means ± SD of 10 healthy volunteers.

Suppl.-Table 11. Comparison of present method to previously published mass spectrometric methods for lysophospholipid quantification.

Authors	LC type	Analysis time [min]	Plasma volume [μL]	IS S1P/SA1P	Co-elution S1P/IS	IS LPA	Co-elution LPA species/IS
Baker et al.	Normal-phase	>10	450	-	-	LPA !8:0 d_{35}	yes
Berdyshev et al.	Reversed-phase C8	10	100	C17-S1P	no	-	-
Murph et al.	Reversed-phase C5	7.5	500	LPA 17:0	no	LPA 17:0	no
Schmidt et al.	Reversed-phase C18	14.5	n.d.	C17-S1P	no	-	-
Shan et al.	Reversed-phase C18	5	500	-		LPA 16:0 ($^{13}C_{16}$)	only LPA 16:0
Scherer et al.	**HILIC**	**2.5**	**75**	**$^{13}C_2D_2$-S1P**	**yes**	**LPA 17:0**	**yes**
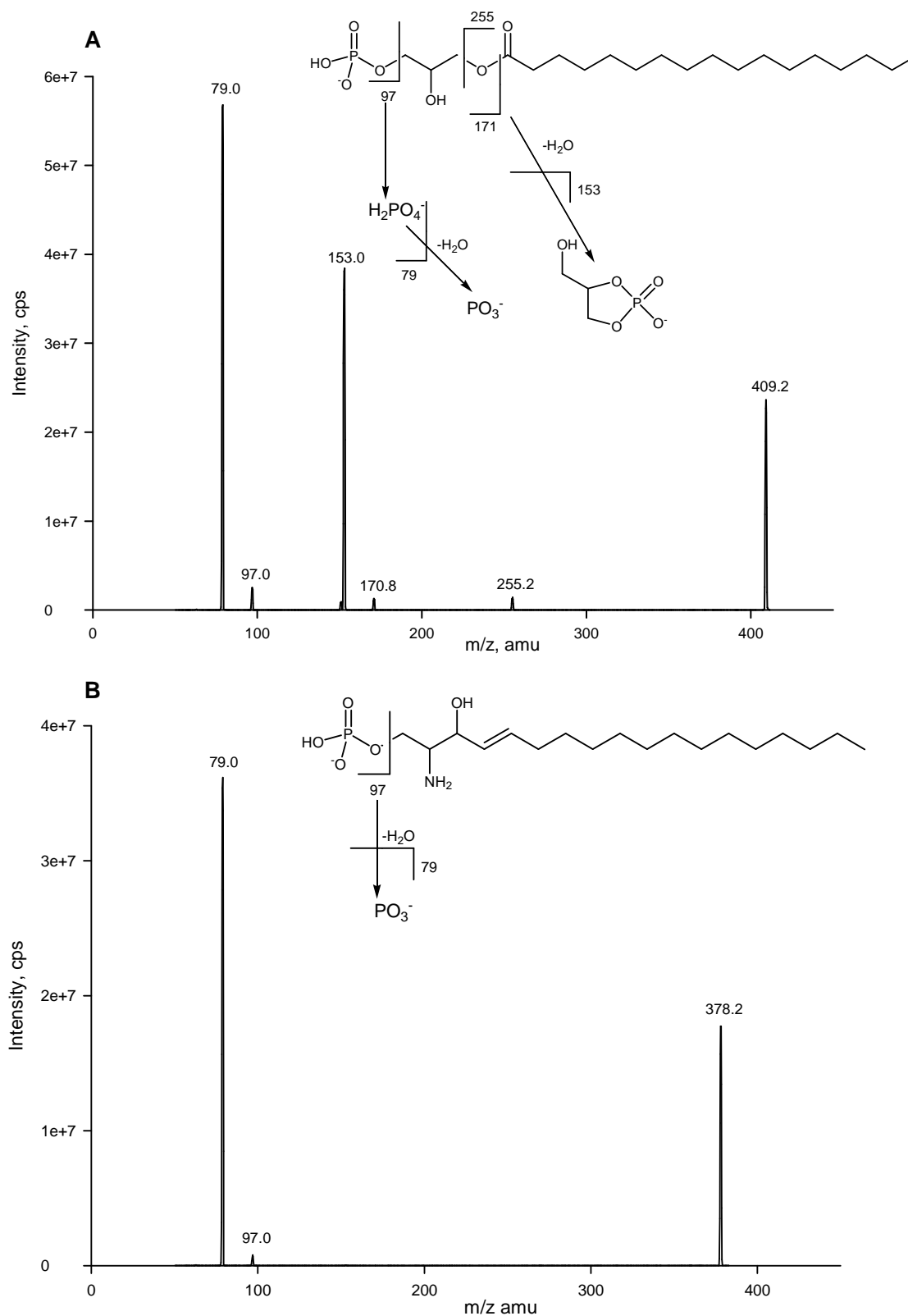
Suppl.-Fig. 1. Product ion spectra and suggested fragmentation scheme of authentic LPA 16:0 (Panel A) and S1P (Panel B) using negative ESI mode.

4   A rapid and quantitative LC-MS/MS method to profile sphingolipids

4.1   Abstract

Sphingolipids comprise a highly diverse and complex class of molecules that serve not only as structural components of membranes but also as signaling molecules. To understand the differential role of sphingolipids in a regulatory network it is important to use specific and quantitative methods.

We developed a novel LC-MS/MS method for the rapid, simultaneous quantification of sphingolipid metabolites including sphingosine, sphinganine, phyto-sphingosine, di- and trimethyl-sphingosine, sphingosylphosphorylcholine, hexosylceramide, lactosylceramide, ceramide-1-phosphate and dihydroceramide-1-phosphate. Appropriate internal standards were added prior to lipid extraction. In contrast to most published methods based on reversed phase chromatography, we used hydrophilic interaction liquid chromatography (HILIC) and achieved good peak shapes, a short analysis time of 4.5 min and most important co-elution of analytes and their respective internal standards. In order to avoid an overestimation of species concentrations, peak areas were corrected regarding isotopic overlap where necessary. Quantification was achieved by standard addition of naturally occurring sphingolipid species to the sample matrix. The method showed excellent precision, accuracy, detection limits and robustness. As an example, sphingolipid species were quantified in fibroblasts treated with myriocin or sphingosine-kinase-inhibitor.

In summary this method represents a valuable tool to evaluate the role of sphingolipids in the regulation of cell functions.

4.2 Introduction

Sphingolipids comprise a highly diverse and complex class of molecules that serve not only as structural components of cellular membranes but also as bioactive compounds with crucial biological functions (1). Some metabolites, including ceramide, sphingosine and sphingosine-1-phosphate have been shown to be involved in different cell functions such as proliferation, differentiation, growth arrest and apoptosis (2). Especially the counter-regulatory functions of ceramide and sphingosine-1-phosphate, resembling the sphingolipid rheostat, indicate that not only a single metabolite concentration, but rather the relative levels of these lipids are important to determine the cell fate (2-5). Sphingolipids are associated to several diseases such as cancer, obesity and atherosclerosis (1;2;6-9). Structural diversity and inter-conversion of these sphingolipid metabolites represent technical challenges. Nevertheless, to understand the differential role of sphingolipids in a regulatory network, it is imperative to use specific and quantitative methods.

During the last decade liquid chromatography coupled to tandem-mass spectrometry (LC-MS/MS) has become a powerful tool for sphingolipid analysis (10-21). However, either these methods do not cover a broad spectrum of sphingolipid metabolites or they show disadvantages like laborious sample preparation, time consuming LC-separation or separation of analytes and internal standards.

Therefore, we applied, as previously described for lysophosphatidic acid and sphingoid base phosphates, hydrophilic interaction chromatography (HILIC) coupled to mass spectrometry (18) to achieve co-elution of sphingolipid species and their internal standards. We present a fast and simple LC-MS/MS-method for the quantification of hexosylceramide (HexCer), lactosylceramide (LacCer), sphingosine (SPH), sphinganine (SPA), phyto-sphingosine (PhytoSPH), di- and trimethyl-sphingosine (Di-; TrimetSPH), sphingosylphosphorylcholine (SPC), ceramide-1-phosphate (Cer1P) and dihydroceramide-1-phosphate (dhCer1P). This method was validated and applied to fibroblasts treated with myriocin and a sphingosine-kinase inhibitor, respectively.

4.3 Material and Methods

4.3.1 Chemicals and solutions

Butanol, methanol (HPLC grade) and formic acid (98-100 %, for analysis) were purchased from Merck (Darmstadt, Germany). Water was obtained from B. Braun (Melsungen, Germany). Ammonium formate (Fluka, Buchs, Switzerland), citric acid monohydrate, disodium hydrogenphosphate (Merck, Darmstadt, Germany) were of the highest analytical grade available. Sphingosine-1-phosphate (d18:1); C17-sphingosine (d17:1); sphingosine (d18:1); sphinganine (d18:0); C17-sphingosylphosphorylcholine (d17:1); N,N-dimethyl- sphingosine (d18:1); N,N,N-trimethyl-sphingosine (d18:1); phyto-sphingosine (t18:0); sphingosylphosphorylcholine (d18:1); C12:0-glucosylceramide; C16:0-glucosylceramide; C24:1-galactosylceramide; C12:0-lactosylceramide; C16:0-lactosylceramide; C24:0-lactosylceramide; C12:0-Cer-1-phosphate; C16:0-Cer-1-phosphate and C24:0-Cer-1-phosphate were purchased from Avanti Polar Lipids (Alabaster, AL, USA) with purities higher than 99 %. $^{13}C_2D_2$-sphingosine-1-phosphate (d18:1) was purchased from Toronto Research Chemicals (Toronto, Canada). Stock-solutions of individual sphingolipid compounds at a concentration of 1 mg/mL were prepared in methanol and stored at -20°C. Working s olutions of the desired concentrations were prepared by dilution in methanol. Myriocin and sphingosine-kinase-inhibitor [2-(p-Hydroxyanilino)-4-(p-chlorphenyl) thiazole] were purchased from Calbiochem (San Diego, USA).

Table 1. MS parameter and LOD of sphingolipids studied

Sphingolipid	[M+H]$^+$ m/z	MRM	IS (MRM)	CE [V]	RT [min]	LOD [fmol] on column
SPH	300.3	300.3→282.2	C17 SPH (286.3→268.2)	17	1.04	7.3
		300.3→252.2	C17 SPH (286.3→238.2)	25	1.04	7.7
SPA	302.3	302.3→284.2	C17 SPH (286.3→268.2)	21	1.04	6.1
		302.3→254.2	C17 SPH (286.3→238.2)	29	1.04	8.84
PhytoSPH	318.4	318.4→282.2	C17 SPH (286.3→268.2)	23	1.06	24.2
DimetSPH	328.4	328.4→280.3	C17 SPH (286.3→268.2)	29	1.02	0.2
TrimetSPH	342.4	342.4→60.1	C17 SPH (286.3→268.2)	49	1.05	0.1
SPC	465.3	465.3→184	C17 SPC (451.3→184)	31	1.75	4.9
HexCer	var.	M+H$^+$→264.3	C12 GluCer (644.5→264.3)	55	0.80	0.6
LacCer	var.	M+H$^+$→264.3	C12 LacCer (806.6→264.3)	65	0.94	2.7
Cer1P	var.	M+H$^+$→264.3	C12 Cer1P (562.4→264.3)	39	1.29	6.3
dhCer1P	var.	Neutral loss 98	C12 Cer1P (562.4→262.3)	29	1.29	53.6

4.3.2 Cell culture

Primary human skin fibroblasts were cultured as described previously (22) in Dulbecco´s modified Eagle´s medium supplemented with L-glutamine and 10% fetal calf serum in a humidified 5% CO_2 atmosphere at 37℃. For lipid analysis, cells were seeded into 6-well plates and grown to confluence. Cells were rinsed two times with ice-cold phosphate buffer saline (PBS) and either lysed in 0.2% sodium dodecyl sulfate (SDS) in water or scraped in PBS. Subsequently samples were subjected to centrifugation at 240 g for 7 min and the resulting pellet was homogenized in distilled water by sonication. Fibroblasts treated with myriocin or sphingosine kinase inhibitor (Calbiochem) as indicated in Figure 4 were lysed in 0.2% SDS. Aliquots of the cell homogenates were taken for protein determination. Protein concentrations were measured using bicinchoninic acid as described previously (23).

4.3.3 Sample preparation

Unless otherwise indicated aliquots of 100 µg protein from the fibroblast homogenates were used for sphingolipid analysis. 20 µL of an internal standard mixture containing 20 ng SPH d17:1, 2 ng SPC d17:1, 20 ng GluCer 12:0, 20 ng LacCer 12:0 and 20 ng Cer1P 12:0 were added prior to lipid extraction. We applied a butanolic extraction procedure described by Baker et al. (24). In brief, 500 µl cell homogenate corresponding to 100 µg of cellular protein were mixed with 60 µL of a buffer containing 200 mM citric acid and 270 mM disodium hydrogenphosphate (pH 4). Extraction was performed with 1 mL of 1-butanol and 500 µL of water-saturated 1-butanol. The recovered butanol phase was evaporated to dryness under reduced pressure. The residue was redissolved in 200 µL ethanol.

4.3.4 Sphingolipid analysis by LC-MS/MS

Sphingolipid analysis was performed by liquid chromatography-tandem mass spectrometry (LC-MS/MS). The HPLC equipment consisted of a 1200 series binary pump (G1312B), a 1200 series isocratic pump (G1310A) and a degasser (G1379B) (Agilent, Waldbronn, Germany) connected to an HTC Pal autosampler (CTC Analytics, Zwingen, CH). A hybrid triple quadrupole linear ion trap mass spectrometer API 4000 Q-Trap equipped with a Turbo V source ion spray operating in positive ESI

mode was used for detection (Applied Biosystems, Darmstadt, Germany). High purity nitrogen was produced by a nitrogen generator NGM 22-LC/MS (cmc Instruments, Eschborn, Germany).

Gradient chromatographic separation was performed on an Interchim (Montlucan, France) hydrophilic-interaction chromatography (HILIC) silica column (50 x 2.1 mm), with a 1.8 µm particle size equipped with a 0.5 µm pre-filter (Upchurch Scientific, Oak Harbor, WA, USA). The injection volume was 2 µL and the column was maintained at 50°C. The mobile phase consisted of water containing 0.2% formic acid and 200 mM ammonium formate (eluent A) and acetonitrile containing 0.2% formic acid (eluent B). Gradient elution was performed with 100% B for 0.1 min, a step to 90% B until 0.11 min, a linear increase to 50% B until 2.5 min, 50% B until 3.5 min and re-equilibration from 3.51 to 4.5 min with 100% B. The flow rate was set to 800 µL/min. To minimize contamination of the mass spectrometer, the column flow was directed only from 1.0 to 3.0 min into the mass spectrometer using a diverter valve. Otherwise methanol with a flow rate of 250 µL/min was delivered into the mass spectrometer.

The Turbo Ion Spray source was operated in the positive ionization mode using the following settings: Ion spray voltage = 5500V, ion source heater temperature = 400°C, source gas 1 = 40psi, source gas 2 = 35psi and curtain gas setting = 20psi. Analytes were monitored in the multiple reaction monitoring (MRM) mode, mass transitions and MS parameters are shown in Table 1. Quadrupoles Q_1 and Q_3 were working at unit resolution.

4.3.5 Calibration and quantification

Calibration was achieved by standard addition of naturally occurring sphingolipid species (S1P, GluCer 16:0, GalCer 24:1, LacCer 16:0 and 24:0, Cer1P 16:0 and 24:0, SPH, SPA, SPC, DimetSPH, TrimetSPH, PhytoSPH). A 6 point calibration was performed by adding the indicated amounts (0–300 pmol) of a combined sphingolipid standard mixture to matrix samples. Calibration curves were calculated by linear regression without weighting.

Data analysis was performed with Analyst Software 1.4.2. (Applied Biosystems, Darmstadt, Germany). The data were exported to Excel spreadsheets and further processed by self programmed Excel macros which sort the results, calculate the analyte/internal standard peak area ratios, generate calibration lines

and calculate sample concentrations. Where necessary isotopic overlap of the species was corrected based on theoretical isotope distribution according to principles described previously (25). Analytes and their corresponding internal standards are shown in Table 1.

4.3.6 Analysis of sphingosine-1-phosphate, ceramide and sphingomyelin

Sphingosine-1-phosphate (S1P) was analyzed by LC-MS/MS as described previously (18). Ceramide and sphingomyelin species were analyzed by flow injection analysis ESI-MS/MS (25;26).

4.4 Results

4.4.1 Sphingolipid fragmentation

To analyze various sphingolipid classes we applied ESI in the positive ion mode and acquired product ion spectra. The fragmentation patterns obtained were in accordance to previous studies for SPH, SPA, Cer1P and glycosylated ceramide species (Tab. 1) (12;16;19;21;27;28). Glycosylated ceramides displayed $[M+H]^+$ ions as well as $[M+H-H_2O]^+$ ions generated by in-source fragmentation (data not shown). Since $[M+H]^+$ ions exhibited much higher intensities we did not use $[M+H-H_2O]^+$ for further analysis of glycosylated ceramides. As expected, sphingosylphosphorylcholine showed only one intense fragment ion at *m/z* 184 due to the loss of the phosphocholine head group (29). DimetSPH showed beside fragments resulting from a loss of one water molecule (*m/z* 310) or one water molecule and a formaldehyde molecule (*m/z* 280), and an ion at *m/z* 110, possibly a conjugated iminium ion (Fig. 1 A). TrimetSPH showed only one intense fragment representing a trimethylammonium-ion at *m/z* 60 (Fig. 1 B). In contrast to Cer1P species showing a sphingoid base fragment, dihydro-Cer-1P displayed a neutral loss of phosphoric acid in positive ion mode (Fig. 1 C). Collision induced dissociation of PhytoSPH showed two prominent fragment ions, resulting from the loss of one and two water molecules (Fig. 1 D).
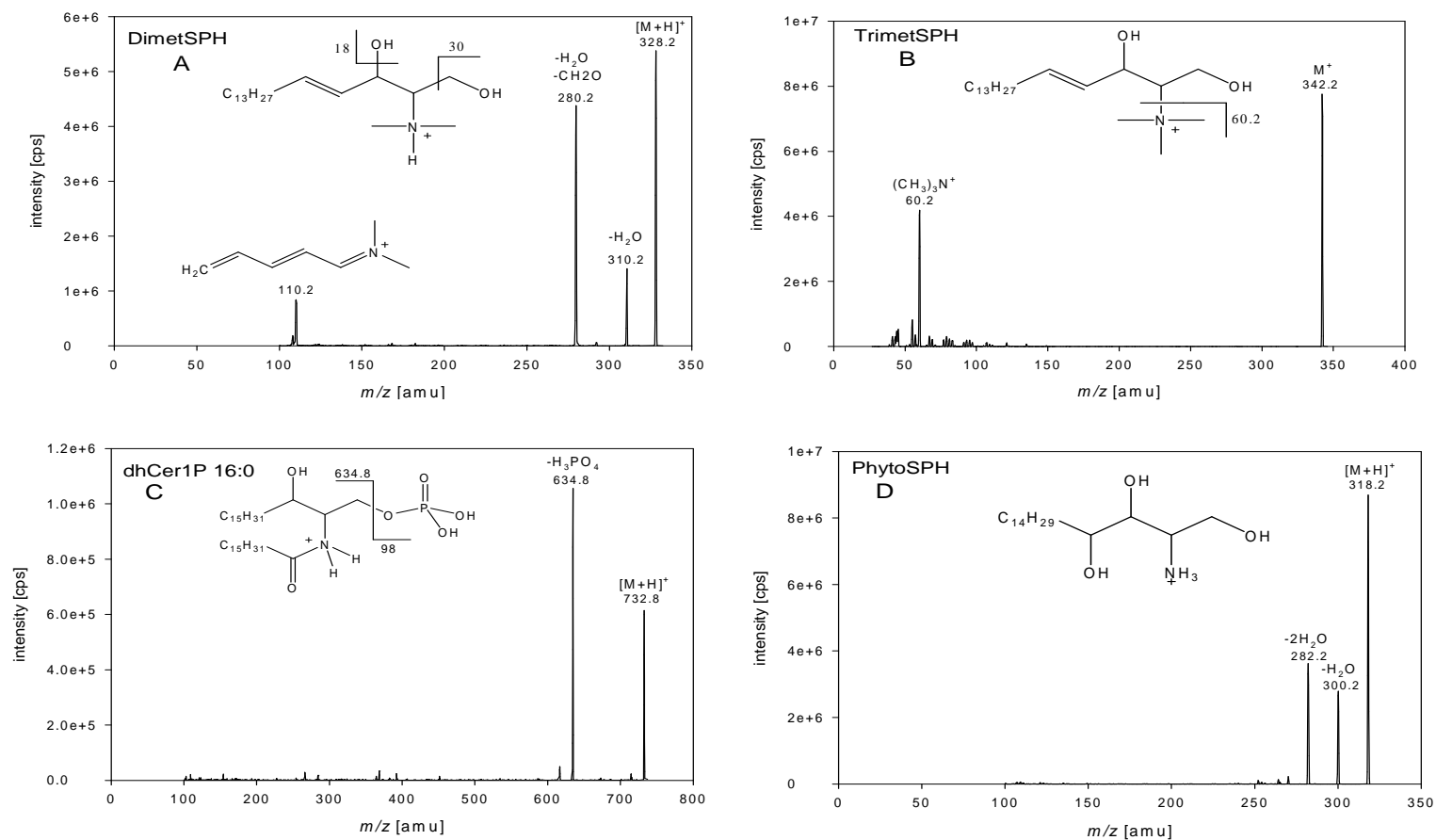
Fig.1. Product ion spectrum and proposed fragmentation of DimetSPH (A), TrimetSPH (B), dhCer1P (C), and PhytoSPH (D) in positive ion mode

4.4.2 Hydrophilic interaction chromatography (HILIC) of sphingolipids

Due to the relatively low level of the selected sphingolipids in crude lipid extracts, a direct analysis using "shotgun approaches" may be hampered by signal suppression caused by other matrix components (12;19;27). Therefore, we decided to establish an HPLC separation of sphingolipids with a short analysis time and coelution of analyte and internal standard. The latter is of major importance to compensate for matrix effects and varying ionization efficiencies, especially during gradient elution. Since reversed phase chromatography shows chain length dependent separation, coelution of analytes and internal standards may not be accomplished (13;16;19;27). 'Classical' normal phase chromatography offers polar head group specific separation, but may be impaired by limited reproducibility and insufficient peak shapes. Moreover, the use of apolar solvents may not provide optimal ionization conditions for ESI. Hence, we established an LC separation based on hydrophilic interaction chromatography (HILIC) which shows lipid head group selectivity along with the use of polar solvents. Using a sub-2-micron particle size we achieved baseline separation for all sphingolipid classes within 2 min and 4.5 min total run time including re-equilibration (Fig. 2 and 3). Gradient elution was performed with a mixture of acetonitrile and water including 0.2% formic acid and 200 mM ammonium formate. Addition of formic acid improved the ionization efficiency, an optimum was found at 0.2%. For optimum performance and reproducibility it is recommended to use at least a concentration of 10 mmol/L ammonium formate in the mobile phase. Therefore, 200 mmol/L buffer and 0.2% formic acid were added to mobile phase A and 0.2% formic acid to mobile phase B.

Since numerous MS transitions are required to cover the naturally occurring sphingolipid species and their internal standards, we split the MS program into 4 periods: 0 – 0.75 min (HexCer); 0.75 – 0.89 (LacCer); 0.89 – 1.5 (sphingosine and related compounds); 1.5 – 4.5 (SPC) (Fig. 2).
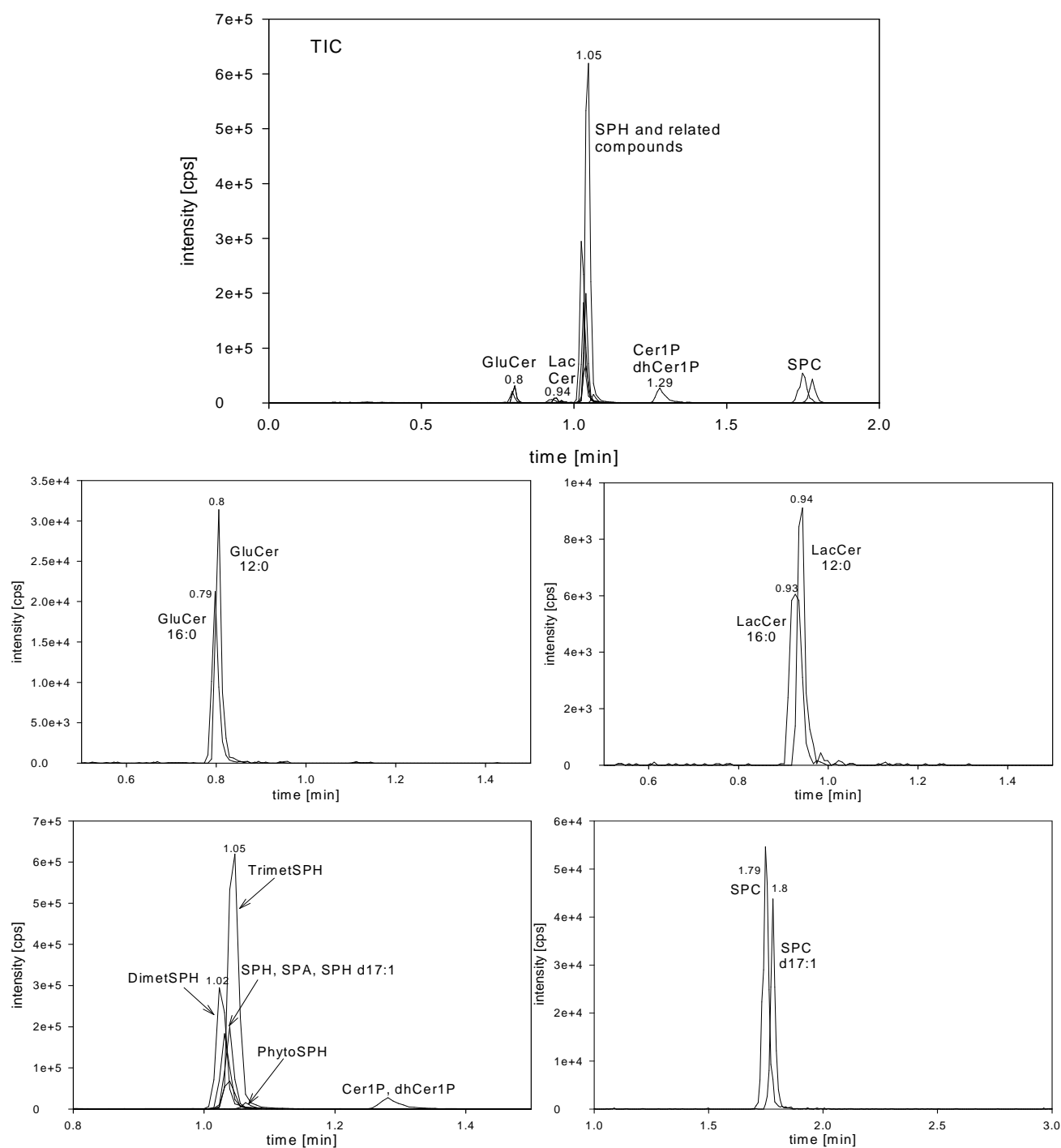
Fig. 2. Chromatogram of a sphingolipid standard mixture. Displayed are MS/MS transitions representative of distinct sphingolipid classes and their respective internal standards.
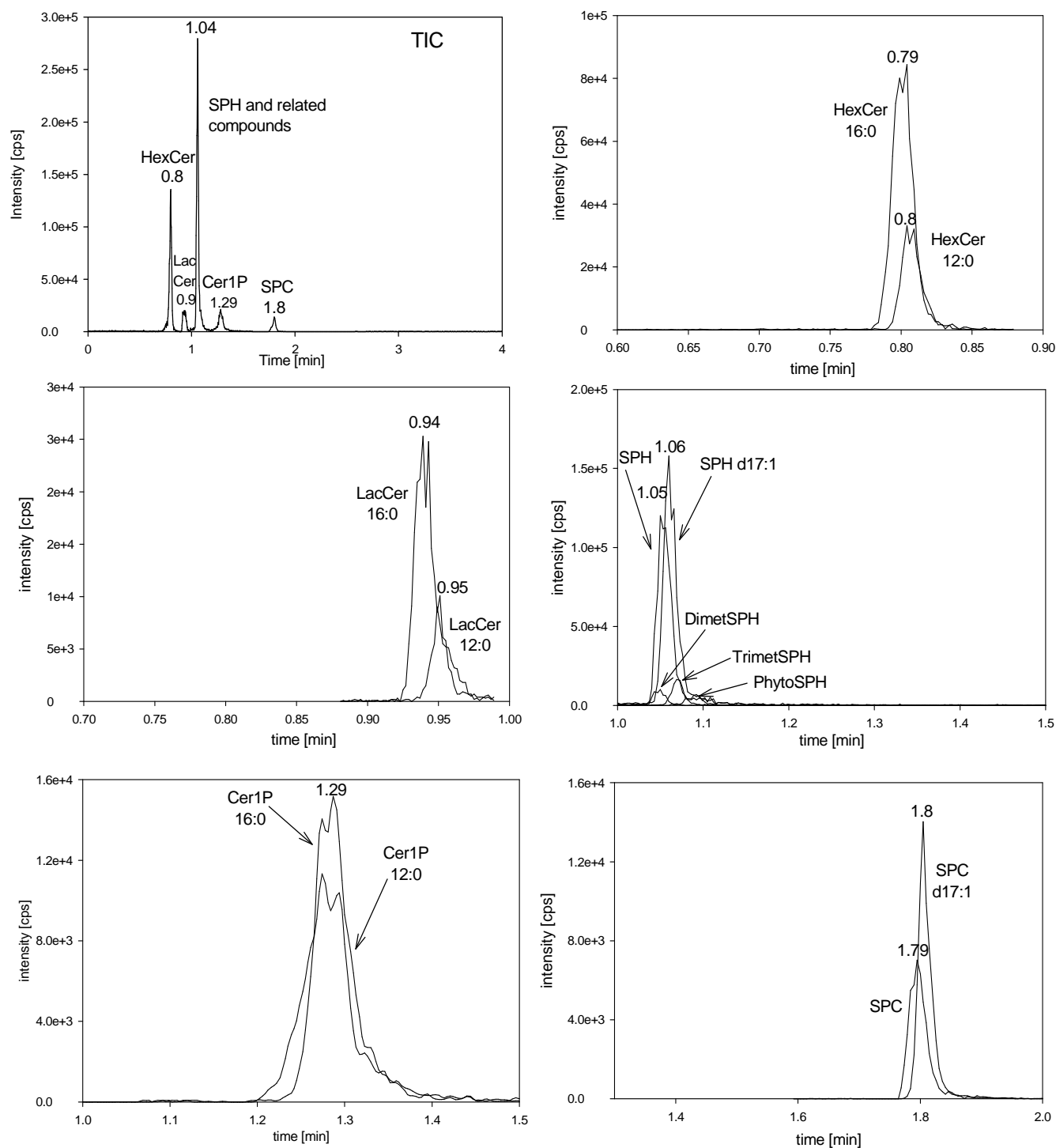
Fig. 3. Chromatogram of a fibroblast sample. Displayed is a representative mass chromatogram obtained from a human skin fibroblast lipid extract.

4.4.3 Extraction efficiency and matrix effects

To analyze polar sphingolipids from one lipid extract, we tested a butanolic extraction as previously described for sphingosine-1-phosphate analysis (18). The extraction efficiency was determined in fibroblast homogenate by adding a sphingolipid standard mixture before and after extraction (Tab. 2). Mean recoveries were between 60-70% and did not vary with concentration of standard added.

We assessed matrix effects by analyzing a standard mixture in methanol and also spiked into fibroblast lipid extracts (Tab.2). Addition of fibroblast cell extract did either not influence or slightly increase the signals up to 20%.

Table 2. Recovery and matrix effects

Analyte	Spiked amount [pmol]	Recovery (S.D.) (n=4)	Matrix effect (n=4)
GluCer 16:0	50	66 ± 3	107 ± 4
	250	62 ± 3	100 ± 5
GalCer 24:1	50	62 ± 3	108 ± 5
	250	60 ± 2	101 ± 4
LacCer 16:0	50	59 ± 2	116 ± 3
	250	62 ± 3	117 ± 4
LacCer 24:0	50	60 ± 2	113 ± 3
	250	61 ± 3	103 ± 5
Cer1P 16:0	30	68 ± 4	100 ± 4
	150	64 ± 3	106 ± 5
Cer1P 24:0	30	64 ± 3	105 ± 4
	150	62 ± 6	112 ± 5
dhCer1P 16:0	10	64 ± 7	106 ± 10
	50	61 ± 2	106 ± 8
dhCer1P 24:0	10	67 ± 5	109 ± 6
	50	62 ± 7	105 ± 3
SPH	60	72 ± 4	100 ± 5
	300	72 ± 3	111 ± 3
SPA	30	68 ± 3	100 ± 5
	150	66 ± 3	104 ± 4
PhytoSPH	10	69 ± 7	103 ± 6
	50	70 ± 2	105 ± 4
DimetSPH	6	69 ± 3	120 ± 6
	30	63 ± 5	108 ± 7
TrimetSPH	6	71 ± 2	100 ± 3
	30	64 ± 5	113 ± 7
SPC	20	67 ± 8	106 ± 2
	100	70 ± 7	101 ± 4

Values represent the percent recovery of standards spiked before and after extraction to examine extraction efficiencies. Matrix effects are calculated from fibroblast lipid extracts corresponding to 50 µg of cellular protein spiked after extraction (corrected by endogenous sphingolipid concentrations) in percent of the same sphingolipid standard mixture used as spike. Each value represents the average of four determinations ± standard deviation

4.4.4 Quantification of sphingolipid species

In order to compensate for variations in sample preparation and ionization efficiency, a set of non naturally occurring sphingolipids, GluCer 12:0, LacCer 12:0, SPH d17:1, Cer1P 12:0 and SPC d17:1 was added as internal standards (IS) prior to extraction. The ratio between analyte and IS was used for quantification as indicated in Table 1. We generated calibration lines by addition of different concentrations of naturally occurring sphingolipids to human skin fibroblasts (Tab. 3). For glycosylated

ceramide species, a possible chain length dependency was addressed by generating 2 independent calibration lines with a short chain (16:0) and a long chain fatty acid (24:0). The obtained standard curves were linear in the tested calibration range. Additional evidence for the specificity of the method is derived from the fact that both mass transitions used for SPH and SPA analysis (Tab. 1) revealed similar results (data not shown).

Due to coelution, monounsaturated species exhibit an overlap of the M+2 isotope peak with the corresponding saturated species. To correct this overlap, we applied an previously described algorithm based on calculated isotope distributions (25). To test this procedure we added increasing amounts of GluCer 24:1 (*m/z* 810.7) to fibroblast homogenate and calculated analyte to IS ratios of GluCer 24:0 (*m/z* 812.7) with and without isotope correction. While GluCer 24:0 to IS ratio increased almost 2-fold upon addition of 200 pmol GluCer 24:1 without correction, no significant increase was detected after correction of isotope overlap (Tab. 4).

Table 3. Calibration data of different sphingolipids.

Sphingolipid	Calibration range [pmol]	Slope (mean ± S.D.)	Correlation coefficient (mean ± S.D.)
GluCer 16:0	25 – 250	59.3 ± 5.6	0.997 ± 0.003
GalCer 24:1	25 – 250	56.1 ± 3.5	0.998 ± 0.001
LacCer 16:0	25 – 250	123.6 ± 7.8	0.996 ± 0.002
LacCer 24:0	25 – 250	107.0 ± 6.0	0.994 ± 0.002
Cer1P 16:0	15 – 150	153.5 ± 8.2	0.997 ± 0.002
Cer1P 24:0	15 – 150	134.1 ± 6.2	0.994 ± 0.001
SPH	30 – 300	25.0 ± 1.3	0.996 ± 0.002
SPA	15 – 150	18.6 ± 2.4	0.998 ± 0.001
PhytoSPH	10 – 100	9.1 ± 0.5	0.996 ± 0.002
DimetSPH	0.3 – 3	70.6 ± 4.5	0.999 ± 0.001
TrimetSPH	0.3 – 3	68.7 ± 7.1	0.996 ± 0.004
SPC	10 – 100	41.0 ± 3.2	0.996 ± 0.003

Calibration lines were generated by plotting the ratios of the areas analyte to IS against the spiked concentrations (pmol). Each value represents the average of four determinations ± SD

Table 4. Correction of isotope overlap.

GluCer 24:1 spiked [pmol]	Ratio GluCer 24:1/IS	Uncorrected ratio GluCer 24:0/IS	Corrected ratio GluCer 24:0/IS
0	2.86 ± 0.16	1.32 ± 0.12	1.18 ± 0.08
25	4.41 ± 0.24	1.53 ± 0.11	1.28 ± 0.07
50	5.99 ± 0.39	1.71 ± 0.16	1.35 ± 0.07
100	8.43 ± 0.44	1.84 ± 0.16	1.30 ± 0.08
150	10.58 ± 0.52	2.06 ± 0.23	1.36 ± 0.12
200	16.66 ± 0.99	2.47 ± 0.26	1.33 ± 0.15

Fibroblast homogenates (100 µg cellular protein) were spiked with increasing amounts of GluCer 24:1. Values represent peak area ratios of GluCer 24:1 and 24:0 to GluCer 12:0. The GluCer 24:0 peak area ratios are shown before and after isotope correction. The displayed values are mean of three independent samples.

4.4.5 Assay characteristics

Assay accuracy was calculated using three spiked fibroblast lipid extracts at different concentrations, covering the entire calibration range. Accuracy was found between 90 and 110% (Tab. 5).

Precision was determined in 3 fibroblast samples, containing 25, 50 and 100 µg of cellular protein (Tab. 5). Coefficients of variation (CVs) were below 10% for most species for both intraday and interday precision (Tab. 5).

Since no analyte free matrix was available, we calculated the limit of detection (LOD) defined as a signal-to-noise-ratio of three. While for most of the analyzed sphingolipid classes, less than 10 fmol are sufficient for quantification, PhytoSPH and dhCer-1P displayed a LOD up to 50 fmol on column (Tab. 1).

Table 5. Intraday and interday precisions and accuracy.

Sphingolipid species	Protein [μg]	Intraday- [pmol±S.D.]	CV [%]	Interday- [pmol±S.D.]	CV[%]	spiked [pmol]	Accuracy [%]
HexCer 16:0	25 μg	2.6±0.1	4.13	2.2±0.2	7.4	25	110±8
	50 μg	5.1±0.3	5.14	5.0±0.2	3.1	150	109±5
	100 μg	10.1±0.8	7.89	9.3±0.6	7	250	104±5
HexCer 22:0	25 μg	2.5±0.1	5.7	3.0±0.2	5.7		
	50 μg	5.1±0.4	8.7	6.1±0.4	5.5		
	100 μg	10.3±0.4	4.1	10.7±0.6	5.4		
HexCer 24:0	25 μg	7.8±0.4	5.3	8.6±0.4	4.2		
	50 μg	15.3±0.7	4.6	17.6±1.0	5.1		
	100 μg	30.3±1.1	3.7	33.4±0.8	2.4		
HexCer 24:1	25 μg	5.1±0.4	6.9	5.5±0.4	4.3	25	109±7
	50 μg	10.0±0.6	6.1	12.1±0.7	6.2	150	108±5
	100 μg	19.9±0.6	2.9	20.3±0.8	3.9	250	104±2
LacCer 16:0	25 μg	1.1±0.1	9	1.4±0.1	7.3	25	97±4
	50 μg	2.6±0.1	5	2.6±0.2	6.8	150	100±6
	100 μg	4.5±0.6	13	4.2±0.4	8.6	250	99±6
LacCer 22:0	25 μg	0.66±0.08	11.9	0.70±0.08	11.3		
	50 μg	1.4±0.1	8.1	1.5±0.13	9.1		
	100 μg	2.6±0.2	7.3	2.6±0.24	9.4		
LacCer 24:0	25 μg	1.7±0.1	7.8	2.3±0.1	6.1	25	95±5
	50 μg	3.8±0.2	5.9	4.8±0.3	7.2	150	97±5
	100 μg	7.3±0.9	11.8	7.8±0.8	9.9	250	95±5
LacCer 24:1	25 μg	1.2±0.05	4.4	1.5±0.1	6.5		
	50 μg	2.9±0.2	8.5	3.6±0.2	6.7		
	100 μg	5.4±0.7	12	5.7±0.5	9.2		
SPH	25 μg	2.5±0.1	4.3	2.1±0.2	9.7	30	95±5
	50 μg	5.1±0.5	9.4	4.6±0.5	10.9	180	97±6
	100 μg	8.7±0.7	8.3	8.5±0.7	7.9	300	95±5
SPA	25 μg	n.d.				15	104±8
	50 μg	n.d.				90	107±5
	100 μg	0.62±0.08	13.3	0.81±0.06	7.4	150	99±2
PhytoSPH	25 μg	n.d.				10	97±9
	50 μg	n.d.				60	96±9
	100 μg	2.4±0.2	7.5	2.2±0.2	8.6	100	97±5
DimetSPH	25 μg	0.12±0.01	9.3	0.13±0.01	11.2	0.3	108±9
	50 μg	0.27±0.03	9.7	0.24±0.03	9.4	1.8	96±9
	100 μg	0.44±0.03	4.8	0.44±0.03	6.6	3	90±5
TrimetSPH	25 μg	0.12±0.01	9.3	0.11±0.01	11	0.3	93±8
	50 μg	0.22±0.03	11.9	0.23±0.03	11.6	1.8	109±7
	100 μg	0.37±0.03	8.4	0.45±0.04	9.7	3	95±5
SPC	25 μg	n.d.				10	111±8
	50 μg	n.d.				60	107±5
	100 μg	0.58±0.06	11.0	0.64±0.06	9.7	100	109±4
Cer1P 16:0	25 μg	n.d.				15	109±8
	50 μg	1.3±0.09	6.4	1.5±0.1	6.8	90	106±7
	100 μg	3.2±0.02	8.0	3.5±0.3	7.5	150	101±4
Cer1P 24:0	25 μg	n.d.				15	107±8
	50 μg	n.d.				90	110±9
	100 μg	4.9±0.4	8.4	5.5±0.5	9.3	150	103±6
dhCer1P 24:0	25 μg	n.d.				5	92±5
	50 μg	n.d.				30	102±7
	100 μg	6.4±0.5	8.1	5.9±0.5	8.1	50	100±5

The displayed values are mean concentrations in pmol and the coefficient of variation (CV) of human skin fibroblasts lipid extracts corresponding to 25, 50 and 100 μg of cellular protein. A pool of fibroblast homogenates was aliquoted and lipid extracts were analyzed in series for intraday precision (n=6) and on 6 different days for interday-precision (n=6).

Accuracy is displayed as the mean of the assayed concentration (corrected by endogenous sphingolipid concentrations in human skin fibroblasts) in percent of the spiked concentration. Each value represents the average of three determinations ± standard deviation

Table 6. Lipid extracts prepared from fibroblasts either homogenized in water by sonication or lysed in 0.2% SDS.

Fatty acid	HexCer					LacCer					SPH	SPA	PhytoSPH	Cer1P
	16:0	22:0	23:0	24:1	24:0	16:0	22:0	23:0	24:1	24:0				16:0
Water	253±13	129.1±7.0	41.2±3.7	290±16	315±19	42.2±3.3	50.6±7.1	16.1±2.9	1356±13	94.5±2.4	72.8±7.1	15.8±2.1	20.7±0.1	3.7±0.5
0.2%SDS	233±5	119.7±0.4	36.0±1.5	265±4	278±10	46.6±1.1	55.0±6.2	17.8±1.9	136±9	110.5±9.5	84.6±4.4	16.1±1.6	17.4±0.7	4±0.5

The displayed values are mean [nmol/mg cellular protein] ± standard deviation of 3 independent samples.

4.4.6 Preparation of cell culture samples and sample stability

Since a main application of this method is the analysis of cultured cells we tested different methods to harvest the cells. First, a precursor ion scan of *m/z* 264 was applied to check which HexCer, LacCer and Cer1P species are found in primary human skin fibroblasts. For both HexCer and LacCer, we found 16:0, 22:0, 23:0, 24:0 and 24:1 species; for Cer1P only 16:0 was detected. To compare sample preparations, fibroblasts were either scraped in PBS and homogenized in water by sonication or lysed in 0.2 % sodium dodecyl sulfate (SDS). Both sample preparations did not differ in their ionization response since IS signals were similar (data not shown). Cells lysed in water showed about 10% higher HexCer and PhytoSPH levels as well as slightly decreased LacCer 16:0, 22:0, 24:0 and 15% decreased SPH level (Tab. 6). For reproducibility, SDS showed advantages compared to water, which gave higher SDs.

Next we tested the stability of the homogenates. Fibroblast homogenates prepared either in water or SDS were frozen immediately or after 6h at room temperature. Storage at room temperature showed no effect on most sphingolipid levels, except a slight increase of SPH and Cer1P in SDS and PhytoSPH in water (Tab. 7).

Table 7. Sample stability

% change after 6h RT	HexCer	LacCer	SPH	SPA	PhytoSPH	Cer1P
Water	98 ± 1	105 ± 6	100 ± 3	96 ± 5	113 ± 9	98 ± 7
0.2%SDS	101 ±7	96 ± 9	111 ± 2	101± 8	97 ± 5	113 ± 3

Fibroblasts, either homogenized in water by sonication or lysed in 0.2% SDS, were stored immediately at -80℃ or for 6 h at room temperature . The displayed values are percent of the immediately stored fibroblast cell homogenates. The displayed values are the mean ± SD of 3 independent samples.

4.4.7 Analysis of fibroblasts treated with myriocin/sphingosine-kinase inhibitor

To test feasibility of this novel method we treated primary human skin fibroblasts either with myriocin, an inhibitior of serine-palmitoyl transferase (SPT) (30) or sphingosine-kinase inhibitor (SKI) (30-33). To obtain the full range of sphingolipid concentrations we additionally analyzed sphingosine-1-phosphate, sphingomyelin and ceramide species using previously described methods (18;25;26;28).

Myriocin decreased cellular S1P and SPC levels at sub-nanomolar concentrations to 60% and 40% of the untreated control (Fig. 4A). The other analyzed sphingolipid classes showed only minor changes upon treatment with myriocin up to 1 nM (Fig. 4A/B). The most pronounced effects were observed at 5 nM myriocin, with decreased Cer, HexCer, LacCer and free sphingoid bases concentrations and a further decline of S1P and SPC level.

SKI treatment of fibroblasts at nanomolar concentrations decreased S1P and SPC by more than 50% (Fig. 4C). Micromolar concentrations of SKI resulted in S1P below and SPC concentration close to the LOD, and lead to a pronounced increase in the level of the free sphingoid base. Interestingly, increased levels of SPA were paralleled by dihydro-SM (Fig. 4C/D). SKI treatment in the pharmacological range (0.5-5 µM) (34) did not change Cer and SM levels significantly (Fig. 4). Surprisingly, SKI treatment decreased LacCer at low concentrations.

Taken together these data show that drug treatments that affect enzymes involved in sphingolipid metabolism may not only affect the targeted metabolites, but the whole pathway.
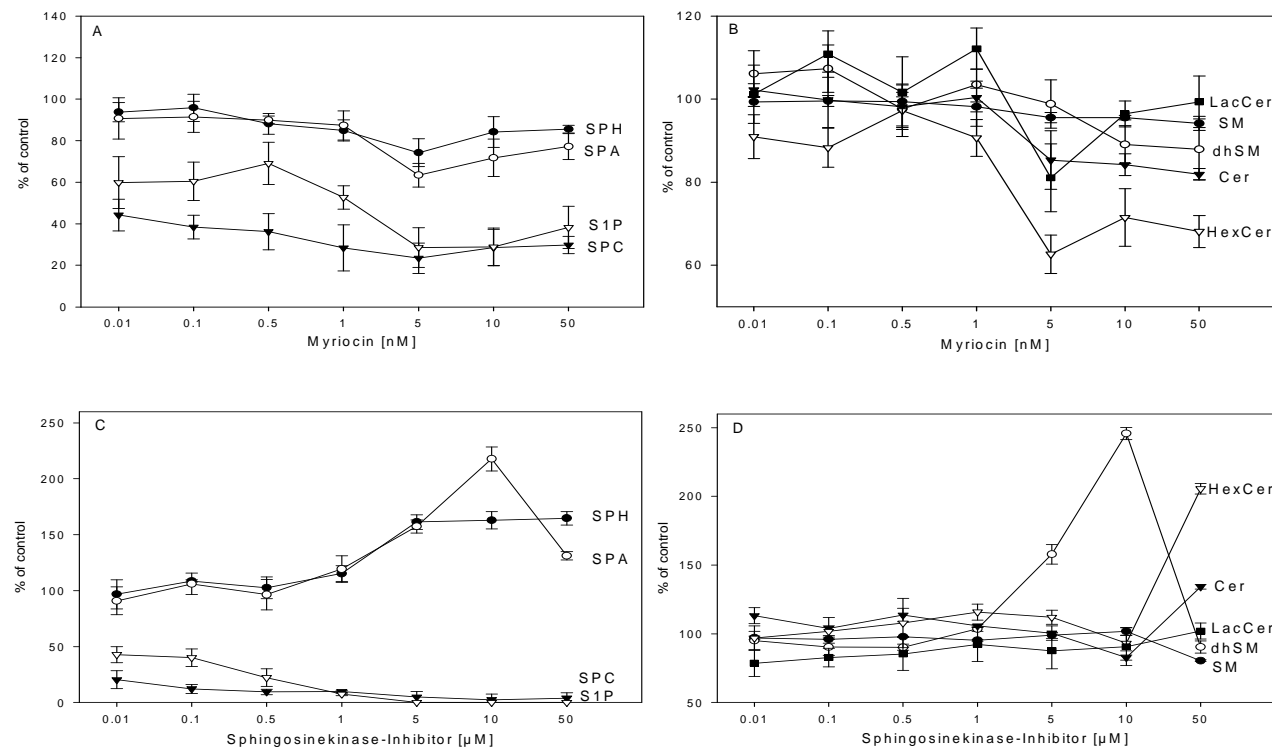
Fig. 4. The effect of myriocin and sphingosine kinase inhibitor on intracellular sphingolipids in primary human skin fibroblasts.

Cells were treated with increasing concentrations of myriocin (A + B) and sphingosine kinase inhibitor (C + D) for 24 hours, respectively. SPH (closed circle), SPA (open circle), SPC (closed triangle), S1P (open triangle), HexCer (open triangle) and LacCer (closed square) were quantified by LC-MS/MS; Cer (closed triangle), SM (closed circle) and dhSM (open circle) were quantified by flow injection analysis (ESI-MS/MS). Values represent the mean ± SD of three independent samples.

4.5 Discussion

Sphingolipid metabolism consists of a dynamic network of molecules including important bioactive signaling molecules (1-9). Therefore, to understand the function of sphingolipids it is necessary to assess a sphingolipid profile instead of one single metabolite.

Although analysis of the "sphingolipidome" by shotgun approaches has been recently demonstrated for yeast (35), an analysis of a more complex sphingolipid pattern in mammalian systems may be hampered, especially for minor metabolites, by signal suppressing matrix effects or lack of sensitivity (12;19;27).

In this study we present a novel LC-MS/MS method to quantify various sphingolipid species from cultured cells. In contrast to most previous methods using reversed-phase chromatography (10;11;15;16;19;21;27), we applied hydrophilic interaction chromatography (HILIC) which allows coelution of analytes and non natural occurring internal standards. This is a key feature of LC-based MS-methods since matrix effects and ionization response may vary during LC-separation especially when gradient methods are used. Consequently, only coelution of analytes with adequate internal standards may compensate for these effects and prevent mis-quantification. Due to the coelution of multiple species an isotopic overlap of species is possible. Therefore, we corrected peak areas according to principles described previously (25) to avoid an overestimation of species.

Further advantages of our method are a short analysis time of 4.5 min per sample and a simple liquid-liquid extraction as sample preparation. Since the presented method uses the same butanolic extraction and LC components as a previously described method for S1P and lysophosphatidic acid analysis (18) it is possible to analyze both sets of analytes from one extract. Consequently, one can achieve with two straightforward liquid-liquid extractions (Bligh and Dyer and butanol) a full coverage of the main sphingolipid metabolites (25;26) as well as glycerophospholipids (22;25;36) and cholesterol/cholesteryl ester (37). Calibration was performed in the sample matrix by addition of naturally occurring species prior to lipid extraction. This allows compensation for potential matrix effects on ionization and extraction efficiency as well as for small retention time differences observed between short chain and very long chain species. Moreover, a full validation was

performed according to FDA guidelines (28). This extensive validation showed excellent precision, accuracy and sensitivity for all analyzed sphingolipid classes.

First applications of this method showed that sample preparation methods may influence sphingolipid levels particularly HexCer and free sphingoid bases. Due to reproducibility and handling reasons we prefer a direct lysis of cultured cells with 0.2% SDS instead of scraping cells. However, immediate freezing of the samples until analysis is advisable. Finally, treatment of fibroblasts with myriocin and SKI demonstrated the importance of methods covering multiple instead of single sphingolipid metabolites. Since treatment affected not only direct metabolites but almost the whole pathway including unexpected concentration changes of some species.

In summary, we could show that LC-MS/MS-based sphingolipid-profiling using HILIC may provide a powerful tool to understand regulatory and metabolic mechanisms involved in cellular sphingolipid homeostasis. Similar as previously shown for glycerophospholipid metabolism (22) this method can be also used for metabolic profiling using stable isotope labeled precursors.

4.6   References

1. Lahiri S, Futerman AH. The metabolism and function of sphingolipids and glycosphingolipids. Cell Mol Life Sci 2007;64:2270-84.

2. Bartke N, Hannun YA. Bioactive sphingolipids: metabolism and function. J Lipid Res 2009;50 Suppl:S91-S96.

3. Spiegel S, Kolesnick R. Sphingosine 1-phosphate as a therapeutic agent. Leukemia 2002;16:1596-602.

4. Spiegel S, Milstien S. Sphingosine-1-phosphate: an enigmatic signalling lipid. Nat Rev Mol Cell Biol 2003;4:397-407.

5. Taha TA, Mullen TD, Obeid LM. A house divided: ceramide, sphingosine, and sphingosine-1-phosphate in programmed cell death. Biochim Biophys Acta 2006;1758:2027-36.

6. Liliom K, Sun G, Bunemann M, Virag T, Nusser N, Baker DL et al. Sphingosylphosphocholine is a naturally occurring lipid mediator in blood plasma: a possible role in regulating cardiac function via sphingolipid receptors. Biochem J 2001;355:189-97.

7. Wymann MP, Schneiter R. Lipid signalling in disease. Nat Rev Mol Cell Biol 2008;9:162-76.

8. Merrill AH, Jr., Stokes TH, Momin A, Park H, Portz BJ, Kelly S et al. Sphingolipidomics: a valuable tool for understanding the roles of sphingolipids in biology and disease. J Lipid Res 2009;50 Suppl:S97-102.

9. Cowart LA. Sphingolipids: players in the pathology of metabolic disease. Trends Endocrinol Metab 2009;20:34-42.

10. Berdyshev EV, Gorshkova IA, Garcia JG, Natarajan V, Hubbard WC. Quantitative analysis of sphingoid base-1-phosphates as bisacetylated derivatives by liquid chromatography-tandem mass spectrometry. Anal Biochem 2005;339:129-36.

11. Butter JJ, Koopmans RP, Michel MC. A rapid and validated HPLC method to quantify sphingosine 1-phosphate in human plasma using solid-phase extraction followed by derivatization with fluorescence detection. J Chromatogr B Analyt Technol Biomed Life Sci 2005;824:65-70.

12. Lieser B, Liebisch G, Drobnik W, Schmitz G. Quantification of sphingosine and sphinganine from crude lipid extracts by HPLC electrospray ionization tandem mass spectrometry. J Lipid Res 2003;44:2209-16.

13. Mano N, Oda Y, Yamada K, Asakawa N, Katayama K. Simultaneous quantitative determination method for sphingolipid metabolites by liquid chromatography/ionspray ionization tandem mass spectrometry. Anal Biochem 1997;244:291-300.

14. Markham JE, Jaworski JG. Rapid measurement of sphingolipids from Arabidopsis thaliana by reversed-phase high-performance liquid chromatography coupled to electrospray ionization tandem mass spectrometry. Rapid Commun Mass Spectrom 2007;21:1304-14.

15. Murph M, Tanaka T, Pang J, Felix E, Liu S, Trost R et al. Liquid chromatography mass spectrometry for quantifying plasma lysophospholipids: potential biomarkers for cancer diagnosis. Methods Enzymol 2007;433:1-25.

16. Schmidt H, Schmidt R, Geisslinger G. LC-MS/MS-analysis of sphingosine-1-phosphate and related compounds in plasma samples. Prostaglandins Other Lipid Mediat 2006;81:162-70.

17. Yoo HH, Son J, Kim DH. Liquid chromatography-tandem mass spectrometric determination of ceramides and related lipid species in cellular extracts. J Chromatogr B Analyt Technol Biomed Life Sci 2006;843:327-33.

18. Scherer M, Schmitz G, Liebisch G. High-throughput analysis of sphingosine 1-phosphate, sphinganine 1-phosphate, and lysophosphatidic acid in plasma samples by liquid chromatography-tandem mass spectrometry. Clin Chem 2009;55:1218-22.

19. Haynes CA, Allegood JC, Park H, Sullards MC. Sphingolipidomics: methods for the comprehensive analysis of sphingolipids. J Chromatogr B Analyt Technol Biomed Life Sci 2009;877:2696-708.

20. Farwanah H, Wirtz J, Kolter T, Raith K, Neubert RH, Sandhoff K. Normal phase liquid chromatography coupled to quadrupole time of flight atmospheric pressure chemical ionization mass spectrometry for separation, detection and mass spectrometric profiling of neutral sphingolipids and cholesterol. J Chromatogr B Analyt Technol Biomed Life Sci 2009;877:2976-82.

21. Shaner RL, Allegood JC, Park H, Wang E, Kelly S, Haynes CA et al. Quantitative analysis of sphingolipids for lipidomics using triple quadrupole and quadrupole linear ion trap mass spectrometers. J Lipid Res 2009;50:1692-707.

22. Binder M, Liebisch G, Langmann T, Schmitz G. Metabolic profiling of glycerophospholipid synthesis in fibroblasts loaded with free cholesterol and modified low density lipoproteins. J Biol Chem 2006;281:21869-77.

23. Smith PK, Krohn RI, Hermanson GT, Mallia AK, Gartner FH, Provenzano MD et al. Measurement of protein using bicinchoninic acid. Anal Biochem 1985;150:76-85.

24. Baker DL, Desiderio DM, Miller DD, Tolley B, Tigyi GJ. Direct quantitative analysis of lysophosphatidic acid molecular species by stable isotope dilution electrospray ionization liquid chromatography-mass spectrometry. Anal Biochem 2001;292:287-95.

25. Liebisch G, Lieser B, Rathenberg J, Drobnik W, Schmitz G. High-throughput quantification of phosphatidylcholine and sphingomyelin by electrospray ionization tandem mass spectrometry coupled with isotope correction algorithm. Biochim Biophys Acta 2004;1686:108-17.

26.   Liebisch G, Drobnik W, Reil M, Trumbach B, Arnecke R, Olgemoller B et al. Quantitative measurement of different ceramide species from crude cellular extracts by electrospray ionization tandem mass spectrometry (ESI-MS/MS). J Lipid Res 1999;40:1539-46.

27.   Bielawski J, Szulc ZM, Hannun YA, Bielawska A. Simultaneous quantitative analysis of bioactive sphingolipids by high-performance liquid chromatography-tandem mass spectrometry. Methods 2006;39:82-91.

28.   U.S.Department of Health and Human Services Food and Drug Administration. Guidance for Industry
Bioanalytical Method Validation. 2001.
Ref Type: Generic

29.   Brugger B, Erben G, Sandhoff R, Wieland FT, Lehmann WD. Quantitative analysis of biological membrane lipids at the low picomole level by nano-electrospray ionization tandem mass spectrometry. Proc Natl Acad Sci U S A 1997;94:2339-44.

30.   Miyake Y, Kozutsumi Y, Nakamura S, Fujita T, Kawasaki T. Serine palmitoyltransferase is the primary target of a sphingosine-like immunosuppressant, ISP-1/myriocin. Biochem Biophys Res Commun 1995;211:396-403.

31.   Glaros EN, Kim WS, Wu BJ, Suarna C, Quinn CM, Rye KA et al. Inhibition of atherosclerosis by the serine palmitoyl transferase inhibitor myriocin is associated with reduced plasma glycosphingolipid concentration. Biochem Pharmacol 2007;73:1340-6.

32.   Hojjati MR, Li Z, Zhou H, Tang S, Huan C, Ooi E et al. Effect of myriocin on plasma sphingolipid metabolism and atherosclerosis in apoE-deficient mice. J Biol Chem 2005;280:10284-9.

33.   Cheon S, Song SB, Jung M, Park Y, Bang JW, Kim TS et al. Sphingosine kinase inhibitor suppresses IL-18-induced interferon-gamma production through inhibition of p38 MAPK activation in human NK cells. Biochem Biophys Res Commun 2008;374:74-8.

34.   French KJ, Upson JJ, Keller SN, Zhuang Y, Yun JK, Smith CD. Antitumor activity of sphingosine kinase inhibitors. J Pharmacol Exp Ther 2006;318:596-603.

35.   Ejsing CS, Sampaio JL, Surendranath V, Duchoslav E, Ekroos K, Klemm RW et al. Global analysis of the yeast lipidome by quantitative shotgun mass spectrometry. Proc Natl Acad Sci U S A 2009;106:2136-41.

36.   Liebisch G, Drobnik W, Lieser B, Schmitz G. High-throughput quantification of lysophosphatidylcholine by electrospray ionization tandem mass spectrometry. Clin Chem 2002;48:2217-24.

37.   Liebisch G, Binder M, Schifferer R, Langmann T, Schulz B, Schmitz G. High throughput quantification of cholesterol and cholesteryl ester by electrospray

ionization tandem mass spectrometry (ESI-MS/MS). Biochim Biophys Acta 2006;1761:121-8.

5   Sphingolipid profiling of human plasma and FPLC-separated lipoprotein fractions by hydrophilic interaction chromatography tandem mass spectrometry

5.1   Abstract

Sphingolipids comprise bioactive molecules which are known to play important roles both as intracellular and extracellular signalling molecules. Here we used a previously developed hydrophilic interaction chromatography tandem mass spectrometry (HILIC-MS/MS) method to profile plasma sphingolipids.

Method validation showed sufficient precision and sensitivity for application in large clinical studies. Sample stability testing demonstrated that immediate plasma separation is important to achieve reliable results. Analysis of plasma from 25 healthy blood donors revealed a comprehensive overview of free sphingoid base, sphingosylphosphorylcholine (SPC), hexosylceramide (HexCer), lactosylceramide (LacCer), and ceramide-1-phosphate (Cer1P) species level. Beside the major sphingoid base sphingosine (d18:1) we found d16:1 and d18:2 species in most of these lipid classes. Interestingly, despite HexCer serves as precursor of LacCer pronounced differences were detected in their species profiles. Additionally, sphingolipids were quantified in lipoprotein fractions prepared by fast performance liquid chromatography (FPLC). HexCer and LacCer showed similar distributions with about 50% in LDL, 40% in HDL and less than 10% in the VLDL fraction. More than 90% of sphingoid base phosphates were found in HDL and albumin containing fractions.

In summary, HILIC-MS/MS provides a comprehensive picture of minor sphingolipid species in plasma and their lipoprotein levels. Comparing profiles from tissues or blood cells, these species profiles may help to address the origin of plasma sphingolipids.

5.2 Introduction

Sphingolipids comprise bioactive molecules (1-7) that influence various cellular functions including growth arrest, apoptosis, proliferation and differentiation. Beside their intracellular signalling functions, sphingolipids act extracellularly by binding to specific receptors. They play important roles in several diseases including cancer, vascular and metabolic diseases (1;5;6;8-10).

A number of publications investigated plasma level of sphingomyelin, ceramide species and sphingosine-1-phosphate as well as their biological function and disease association (3;11-19). Apart from two recent publications (20;21) only limited information is available on the occurrence of minor sphingolipid species in human plasma.

Recently we developed a fast and reliable liquid chromatography-tandem mass spectrometry (LC-MS/MS) method for sphingolipid profiling based on hydrophilic interaction chromatography (HILIC) which allows the simultaneous quantification of sphingoid bases and their methylated products, sphingosylphosphorylcholine (SPC), hexosylceramide (HexCer), lactosylceramide (LacCer) and ceramide-1-phosphate (Cer1P) species (22).

Aim of this study was to provide a detailed sphingolipid pattern of human plasma and lipoprotein fractions. Therefore, we analyzed sphingolipid species of human plasma from healthy blood donors by HILIC-MS/MS (22;23). Additionally, we analyzed the sphingolipid class and species composition of lipoprotein fractions separated by fast performance liquid chromatography (FPLC) (19)

5.3 Material and Methods

5.3.1 Subjects

Blood samples were obtained from healthy normo-lipidemic volunteers. Informed consent and approval of the Hospital Ethics Committee were obtained.

5.3.2 Sample preparation

75 µL human EDTA-plasma were used for sphingolipid analysis. 20 µL of an IS-mixture (20 ng $^{13}C_2D_2$-S1P, 20 ng SPH d17:1, 2 ng SPC d17:1, 20 ng GluCer d18:1/12:0, 20 ng LacCer d18:1/12:0 and 20 ng Cer1P d18:1/12:0) were added prior to lipid extraction. We used a butanolic extraction procedure described by Baker et al. ([24]). In brief, human-EDTA plasma was mixed with 400 µL of a buffer containing 30 mM citric acid and 40 mM disodium hydrogenphosphate (pH 4). Extraction was performed with 1 mL of 1-butanol and 500 µL of water-saturated 1-butanol. The recovered butanol phase was evaporated to dryness under reduced pressure. The residue was redissolved in 50 µL ethanol.

5.3.3 Sphingolipid quantification by LC-MS/MS

Sphingolipid analysis was performed by liquid chromatography-tandem mass spectrometry (LC-MS/MS) as described previously ([22;23]) except following changes: Gradient chromatographic separation was performed on a Interchim (Montlucan, France) hydrophilic-interaction chromatography (HILIC) silica column (50 x 2.1 mm, 2.2 µm particle size) equipped with a 0.5 µm pre-filter (Upchurch Scientific, Oak Harbor, WA, USA). The injection volume was 2 µL for sphingolipid analysis in positive ([22]) and 10 µL for S1P analysis ([23]) in negative ionization mode. The MS/MS parameter used are shown in Tab. 1.

Quantification was achieved by a 6 point standard addition calibration of natural occurring sphingolipid species to plasma (S1P, SA1P, GluCer d18:1/16:0, GalCer d18:1/24:1, LacCer d18:1/16:0, LacCer d18:1/24:0, Cer1P d18:1/16:0, Cer1P d18:1/24:0, SPH d18:1, SPH d18:0, SPH t18:0, SPC d18:1, DimetSPH, TrimetSPH). Because of their co-elution, sphingolipid species may exhibit isotope overlap. To avoid overestimation of these species, their peak areas were corrected based on theoretical isotope distribution according to principles described previously ([25]).

Table 1. MS parameter (IS = internal standard, CE = collision energy) and limit of detection of sphingolipids studied.

Sphingolipid	[M+H]$^+$/[M-H]$^-$ m/z	MRM	IS (MRM)	CE [V]	Retention time [min]	LOD [nmol/L]
SPH d16:1	272.3	272.3→254.2	SPH d17:1 (286.3→268.2)	17	0.95	-
SPH d18:2	298.3	298.3→280.2	SPH d17:1 (286.3→268.2)	17	0.95	-
SPH d18:1	300.3	300.3→282.2	SPH d17:1 (286.3→268.2)	17	0.95	8.8
	300.3	300.3→252.2 *	SPH d17:1 (286.3→238.2)	25	0.95	10.1
SPH d18:0	302.3	302.3→284.2	SPH d17:1 (286.3→268.2)	21	0.95	9.7
SPH d20:1	328.3	328.3→282.2	SPH d17:1 (286.3→268.2)	17	0.95	-
SPH t18:0	318.3	318.3→282.2	SPH d17:1 (286.3→268.2)	23	0.95	16.8
Dimethyl-SPH	328.4	328.4→280.2	SPH d17:1 (286.3→268.2)	29	0.95	0.3
Trimethyl-SPH	342.4	342.4→60.1	SPH d17:1 (286.3→268.2)	49	0.95	0.3
SPC d16:1	437.3	437.3→184	SPC d17:1 (451.3→184)	31	1.70	-
SPC d18:1	463.3	463.3→184	SPC d17:1 (451.3→184)	31	1.70	2.7
SPC d18:2	465.3	465.3→184	SPC d17:1 (451.3→184)	31	1.70	-
HexCer d16:1	var.	M+H$^+$→236.3	GluCer d18:1/12:0 (644.5→264.3)	55	0.68	-
HexCer d18:1	var.	M+H$^+$→264.3	GluCer d18:1/12:0 (644.5→264.3)	55	0.68	3.8
HexCer d18:2	var.	M+H$^+$→262.3	GluCer d18:1/12:0 (644.5→264.3)	55	0.68	-
LacCer d16:1	var.	M+H$^+$→236.3	LacCer d18:1/12:0 (806.6→264.3)	63	0.82	-
LacCer d18:1	var.	M+H$^+$→264.3	LacCer d18:1/12:0 (806.6→264.3)	63	0.82	4.2
LacCer d18:2	var.	M+H$^+$→262.3	LacCer d18:1/12:0 (806.6→264.3)	63	0.82	-
Cer1P d18:1	var.	M+H$^+$→264.3	Cer1P d18:1/12:0 (562.4→264.3)	39	1.07	3.6
S1P d18:1 **	378.1	378.1→79	^{13}C$_2$D$_2$-S1P (382.1→78.9)	-58	1.49	6
S1P d18:0 **	380.1	380.1→79	^{13}C$_2$D$_2$-S1P (382.1→78.9)	-58	1.49	6

* A neutral loss of m/z 48 also used to analyze the sphingoid bases d16:1, d18:2, d18:0, d20:1.

** Analyzed in negative ion mode as described previously [23].

5.3.4   Lipoprotein separation by FPLC

VLDL, LDL and HDL were isolated from healthy blood donors (n=25) as described previously ([19](#)). In brief, a Pharmacia Smart System® FPLC equipped with a Superose 6 PC 3.2/30 column (GE Healthcare Europe GmbH, Munich, Germany) was used with Dulcobecco's PBS containing 1 mM EDTA as a running buffer. After loading of 50 µL plasma into the system, a constant flow of 40 µL/min was applied, and fractionation was started after 18 min with 80 µL per fraction. Fractions 1-20 containing the human plasma lipoproteins were used for further analysis. In order to check lipoprotein fractionation cholesterol and triglyceride levels of each fraction were determined on a Cobas Integra 400 (Roche Diagnostic, Penzberg, Germany) using standard enzymatic, colorimetric methods. Mass spectrometric analysis was performed either from single fractions or pooled lipoprotein fractions (fractions 3 to 6 - VLDL, 7 to 11 - LDL and 12 to 17 – HDL, 18 to 20 - LPDS).

5.3.5   Preparation of lipoproteins by ultracentrifugation

Lipoprotein fractions were isolated from plasma of healthy volunteers by sequential ultracentrifugation as described previously ([26](#)).

5.4   Results

5.4.1   Sphingolipid species of human EDTA-plasma

Here we applied a previously established LC-MS/MS method for sphingolipid profiling based on hydrophilic interaction chromatography (HILIC) for the analysis of human plasma samples ([22](#)). Key feature of this method is co-elution of analytes and internal standards permitting an accurate compensation of matrix effects and varying ionization efficiencies (Fig. 1). To identify naturally occurring sphingolipid species, we screened in an initial step human EDTA-plasma samples (n=15). It is known that plasma sphingolipids contain beside the major base sphingosine d18:1 (mono-unsaturated dihydroxy base with 18 carbon atoms) ([4;27;28](#)) also significant amounts of other sphingoid bases including d16:1 and d18:2 ([29](#)). Therefore, we performed several precursor ion scan experiments using characteristic fragment ions (Tab. 1).

Free sphingoid bases (SPH) d18:1 and d18:0 as well as a variety of hexosylceramides (HexCer), lactosylceramides (LacCer) species and sphingosylphosphorylcholine (SPC) with d16:1, d18:1 and d18:2 backbones were detected (Tab. 2). We did not find methylated sphingoid bases and only ceramide-1-phosphate Cer1P d18:1/16:0.
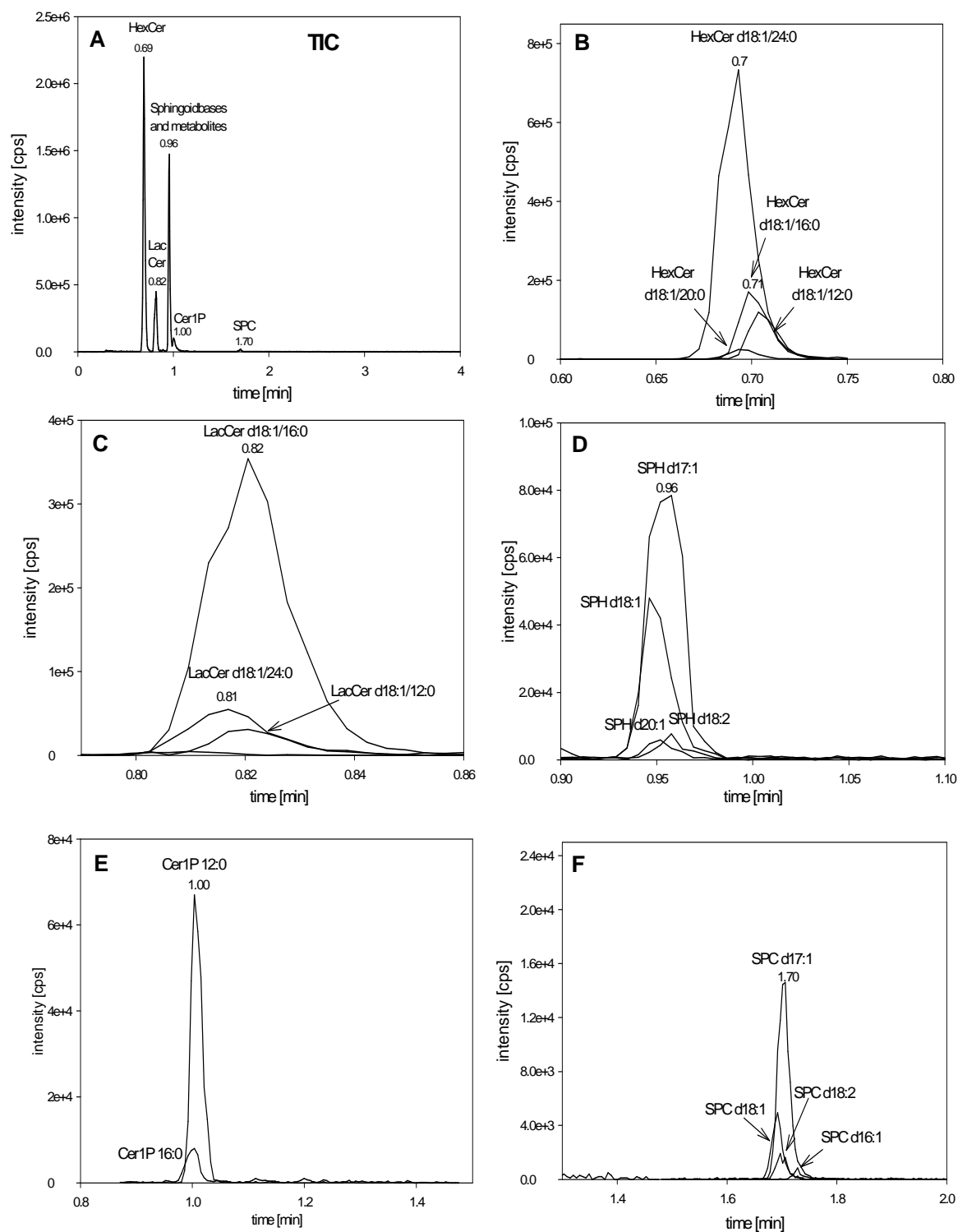
ig. 1. Chromatogram of a representative human EDTA-plasma sample.

Displayed is a representative mass chromatogram obtained from an human EDTA-plasma sphingolipid extract

Table 2. Plasma concentrations of sphingolipids and their distribution on lipoprotein fractions.

Sphingolipid	C [μmol/L] Mean (SD)	VLDL (%)	LDL (%)	HDL (%)	LPDS (%)
SPH d18:1	0.038 (0.013)	-	-	-	-
SPH d18:0	0.012 (0.006)	-	-	-	-
SPH d16:1	n.d.	-	-	-	-
SPH d18:2	n.d.	-	-	-	-
SPH t18:0	n.d.	-	-	-	-
Dimethyl-SPH	n.d.	-	-	-	-
Trimethyl-SPH	n.d.	-	-	-	-
SPC d18:1	0.053 (0.030)	14.2 (0.4)	35.7 (9.9)	45.8 (5.8) *	4.3 (0.68) *
SPC d16:1	0.009 (0.006)	-	-	-	-
SPC d18:2	0.027 (0.017)	-	-	-	-
HexCer Total	6.35 (1.77)	8.0 (4.9)	49.1 (8.3)	42 (8.8)	n.d.
HexCer d16 1	0.22 (0.09)	6.6 (4.8)	50.2 (13.4)	43.3 (13.5)	n.d.
HexCer d18 1	5.56 (1.54)	8.1 (4.8)	49.5 (8.2)	41.5 (8.6)	n.d.
HexCer d18 2	0.57 (0.19)	7.7 (6.5)	45 (8.7)	46.8 (10.3)	n.d.
LacCer Total	2.92 (0.97)	8.2 (5.2)	46.4 (10.2)	44.4 (10)	n.d.
LacCer d16 1	0.13 (0.05)	n.d.	48.7 (11.5)	51.3 (11.5)	n.d.
LacCer d18 1	2.54 (0.84)	9.0 (5.8)	46.9 (10.2)	43.1 (9.9)	n.d.
LacCer d18 2	0.26 (0.10)	5.4 (4.8)	42.3 (11.5)	52.1 (13.1)	n.d.
Cer1P d18:1	0.062 (0.020)	-	-	-	-
S1P d18:1	0.53 (0.09)	1.7 (1)	6.4 (3.8)	90.1 (14.5) *	1.8 (0.1) *
S1P d18:0	0.29 (0.09)	1.8 (3.2)	3.2 (5.7)	90.8 (13.2) *	4.1 (3.8) *

The displayed values are means ± SD of 25 healthy volunteers from freshly drawn EDTA-plasma and their relative distribution on lipoprotein fractions. Lipoprotein fractions were prepared by FPLC separation (following fractions were pooled 3-6 VLDL, 7-11 LDL, 12-17 HDL, 18-20; see Fig. 4). Due to concentrations below or close to the limit of detection, lipoprotein distribution was not calculated for free sphingoid bases, SPC d16:1/d18:2 and Cer1P. For Cer1P only Cer1P d18:1/16:0 was detected above LOD. * HDL fractions contain a significant amount of albumin. n.d. not detected above LOD.

5.4.2 Validation of plasma sphingolipid analysis

To test validity of our analytical setup we performed a number of experiments. EDTA-plasma of 3 donors was analyzed 5 times in a row for intra-assay precision and at 5 different days for inter-assay precision. The coefficients of variation (CV) were below 8% for the major species and below 20% for the minor d16:1 and d18:2 containing HexCer and LacCer species, respectively (data not shown). For quantification a set of non naturally occurring internal standards were added prior to lipid extraction. Calibration lines generated by standard addition showed correlation coefficients >0.99 in the tested calibration range (data not shown). Limits of detection (LODs) were determined in 3 different human plasma samples as a signal to noise ratio of 3 and were found to be <20 nmol/L (Tab.1).

Sample stability was investigated for separated EDTA plasma and whole blood at room temperature. Sphingolipid levels in separated plasma samples did not change significantly up to 24h when stored at room temperature (Tab. 3). Whole blood samples showed an increase of SPH d18:1 and d18:0 levels and a decrease of SPC and Cer1P levels at room temperature (Tab. 4). Consequently, immediate plasma separation is important to achieve reliable results.

Table 3. Stability of plasma samples.

Conditions	HexCer Mean (SD)	LacCer Mean (SD)	SPH Mean (SD)	SPA Mean (SD)	SPC Mean (SD)	Cer1P Mean (SD)
1h RT	103 (5)	110 (9)	96 (10)	91 (4)	93 (12)	104 (8)
4h RT	97 (8)	101 (4)	92 (8)	102 (10)	102 (4)	103 (5)
8h RT	111 (12)	108 (9)	107 (4)	107 (5)	111 (8)	102 (12)
24h RT	108 (8)	113 (19)	97 (9)	101 (11)	102 (2)	112 (9)

EDTA plasma is stored for the indicated time at room temperature (RT). The displayed values are percent of the immediately stored plasma sample. Plasma is stored at -80°C until analysis. The values are mean of two donors.

Table 4. Stability of whole blood samples.

| Conditions	HexCer Mean (SD)	LacCer Mean (SD)	SPH Mean (SD)	SPA Mean (SD)	SPC Mean (SD)	Cer1P Mean (SD)
1h RT	101 (12)	98 (9)	105 (7)	92 (10)	83 (2)	104 (13)
4h RT	106 (6)	104 (4)	136 (6)	112 (3)	61 (4)	88 (4)
8h RT	111 (14)	108 (10)	177 (9)	132 (14)	62 (15)	82 (14)
24h RT	117 (15)	118 (12)	191 (20)	152 (8)	62 (13)	81 (10)

EDTA whole blood is stored at room temperature (RT) and plasma is separated at the time indicated. The displayed values are percent of the immediately stored plasma sample. The values are mean of two donors.

5.4.3 Plasma level of sphingolipid species

We quantified the sphingolipid profile in samples of EDTA-containing plasma and serum, prepared from blood samples freshly drawn from human volunteers (n=25). Sphingolipid concentrations showed no notable differences between plasma and serum samples (data not shown). Mean concentrations of the analyzed sphingolipid classes are shown in Tab.2. The major sphingoid base was d18:1 with 76% of all free bases, 60 % of SPC and almost 90 % of HexCer and LacCer. Additionally, d16:1 and d18:2 bases contribute similarly to HexCer (3.5% and 9.0% of total) and LacCer (4.5% and 8.9% of total), respectively.

In a next step we calculated species profiles of the analyzed glycosylated ceramides. Interestingly, HexCer and LacCer species showed significantly different species pattern (Fig. 2 and 3). Whereas the main HexCer species contained 22:0,

24:1 and 24:0 amide-linked fatty acids, more than 80% of LacCer consisted of LacCer 16:0 and 24:1. Remarkably, the proportion of HexCer d18:1/16:0 was 2-fold higher compared to the proportion of HexCer d16:1/16:0 and HexCer d18:2/16:0.
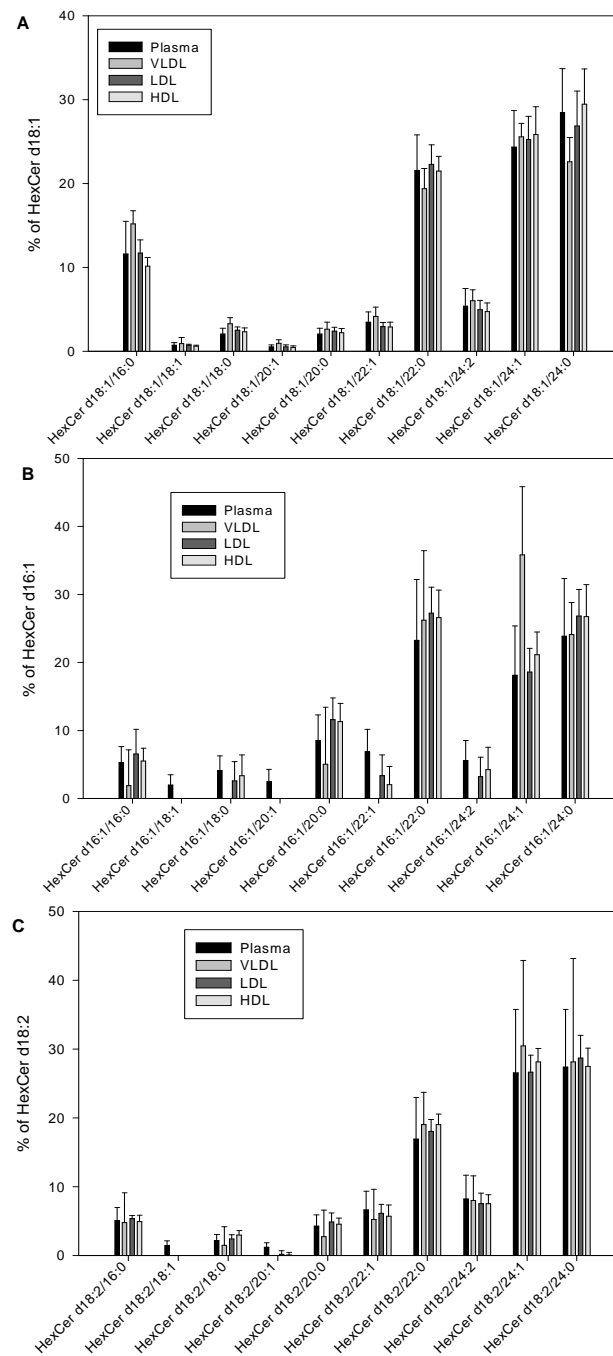
Fig. 2. HexCer species pattern of plasma and lipoprotein classes.

HexCer species were calculated as % mol of the lipid species related to the total HexCer concentration in plasma and lipoprotein fractions, respectively (mean ± SD, n=25 different donors; fractions were pooled as described in Tab. 2). Calculations were made separately for the different sphingoid base backbones.
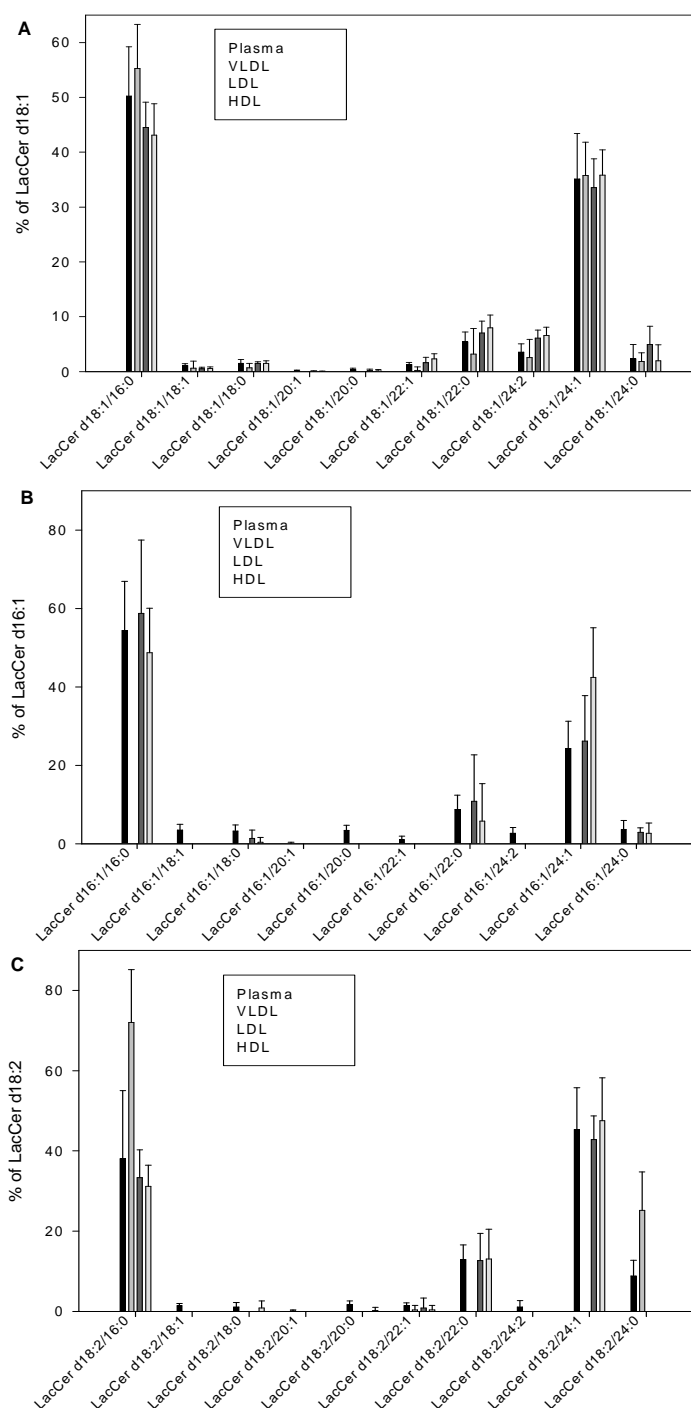
Fig. 3. LacCer species pattern of plasma and lipoprotein classes.

LacCer species were calculated as % mol of the lipid species related to the total LacCer concentration in plasma and lipoprotein fractions, respectively (mean ± SD, n=25 different donors; fractions were pooled as described in Tab. 2). Calculations were made separately for the different sphingoid base backbones.

5.4.4 Sphingolipid distribution on lipoprotein fractions

To gain insight into the sphingolipid composition of lipoproteins we used a previously established FPLC-size exclusion chromatography (19). In a first step, we quantified single FPLC fractions prepared from EDTA plasma by HILIC-MS/MS (22;23). As expected, most of the sphingolipids revealed a distribution representing the three main lipoprotein classes VLDL, LDL and HDL. The majority of both HexCer and LacCer were found in LDL and HDL fractions with similar distribution also for their distinct sphingoid base backbones (Fig. 4A-B). S1P d18:1 and d18:0 were abundantly present in HDL (Fig. 4C). SPC was found in all three lipoprotein fractions VLDL, LDL, HDL with the highest level in HDL. For both sphingoid base phosphates and SPC, a minor fraction also was observed in the lipoprotein deficient serum (LPDS). These distribution profiles are indicative for albumin binding. Since albumin co-elutes with HDL fractions in the used FPLC method (19), HDL and albumin-bound fractions cannot be differentiated for sphingoid base phosphates and SPC.

Similar to our previous study (19) we analyzed pooled VLDL, LDL, HDL, LPDS lipoprotein fractions of 25 healthy blood donors. The distribution of the sphingolipid classes across the main lipoproteins are displayed in Tab. 2. These data confirm the distribution observed in the single fraction analysis (Fig. 4). Additionally, the species profiles of HexCer and LacCer were analyzed in pooled lipoprotein fractions (Fig. 2 and 3). In general, the species profiles of the lipoprotein fractions resemble those of plasma. VLDL shows some striking differences with increased HexCer d16:1/24:1 and LacCer d18:2/16:0 proportions.
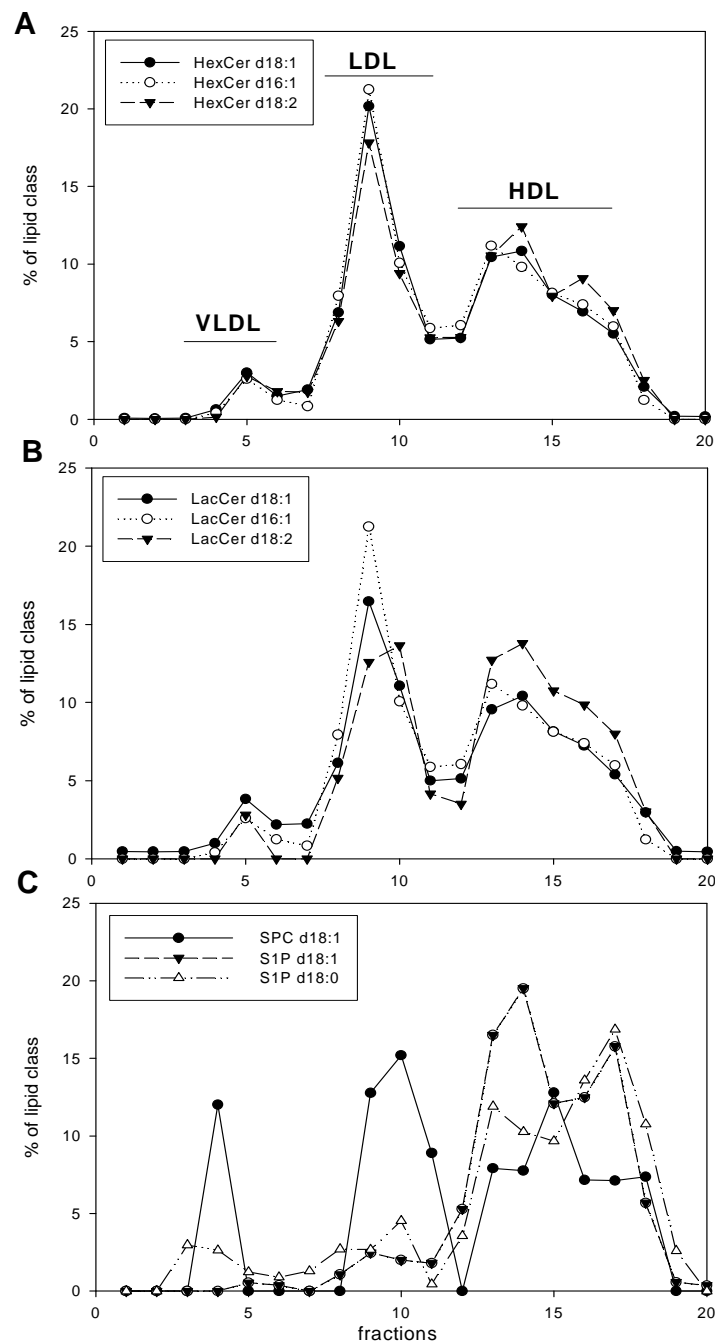
Fig. 4. Sphingolipid profile of FPLC fractions from a human EDTA-plasma sample.

Sphingolipids were quantified by HILIC-MS/MS from FPLC separated fractions in positive and negative ionization mode, respectively. Displayed are percentages of each fraction related to total sphingolipid class concentration: (A) SPC, S1P, SA1P distributions, (B) HexCer d18:1, d16:1 and d18:2 distributions, (C) LacCer d18:1, d16:1 and d18:2 distributions.

5.5 Discussion

Several studies indicated a disease association of plasma sphingolipid species and their potential application as biomarker ([3;11-18](#)). Here we applied and validated a previously reported HILIC-MS/MS method for sphingolipid quantification in cell cultures ([22](#)) for the analysis of plasma. Main advantage of HILIC compared to reversed phase chromatography is co-elution of analytes and internal standards, a prerequisite to compensate for matrix effects and variations in ionization efficiency. Furthermore, the butanol extracts may be used in parallel for the quantification of sphingoid base-phosphates and lysophosphatidic acid (LPA) species, respectively ([23](#)).

Validation showed precision <8% for the major sphingolipids and <20% for the minor sphingolipids sufficient for clinical studies. Although testing of sample stabilities revealed only relevant changes in whole blood samples for free sphingoid bases and SPC, it is generally recommended to separate plasma immediately and to store it at -80℃ until analysis. Particularly, an instant free zing of plasma is mandatory for a combined analysis of sphingoid base-phosphate and LPA ([23](#)).

HILIC-MS/MS was applied to screen and quantify sphingolipid species level of both EDTA-plasma and lipoprotein fractions prepared by FPLC. During the final preparation of this manuscript two other studies using LC-MS/MS were published on plasma lipid species level ([21](#)) and sphingolipid level in plasma/serum and lipoproteins ([20](#)). While Quehenberger et al. ([21](#)) provided data on various sphingoid backbones, Hammad et al. ([20](#)) only analyzed d18:1 and d18:0-based sphingolipid species.

For free sphingoid bases the levels reported were quite heterogeneous: All studies detected SPH d18:0 (Hammad – 4 nM; Quehenberger – 64 nM; this study 12 nM), and SPH d18:1 (Hammad – 6 nM; Quehenberger – 91 nM; this study 38 nM). A biomarker study on fumonisin consumption based on conventional HPLC after fluorescence derivatization quantified sphinganine and sphingosine levels of 6 and 20 nM, respectively.

It is known that the vast majority of HexCer in human plasma is glucosylceramide and only a small fraction of galactosylceramide ([21;30-33](#)). A mean HexCer level of 6.3 µM reported in this study closely matches concentrations of 6.0 µM found by Dawson et al. ([31](#)) (analyzed by TLC followed by GC-MS) and 6.5 µM

by Hammad et al., whereas Quehenberger et al. reported 2.3 µM. LacCer level of 2.9 µM in our study were lower compared to 4.5 µM detected by Dawson et al. (31) and 10.4 µM by Hammad et al.

A Cer1P level of 62 nM measured in this study was dramatically lower than 540 nM determined by Hammad et al. and the species profiles differed considerably (this study detected only 16:0; Hammad: 26:0, 18:0 as major and 16:0 as minor species). For SPC d18:1 Murph et al. reported 20 nM, a similar order of magnitude as 53 nM in this study.

As previously described by Karlsson et al. (29) we found beside the major d18:1 sphingoid backbone significant amounts of d16:1 and d18:2. Interestingly, although GluCer is the precursor of LacCer, HexCer differs completely in its species pattern (Fig. 3 and 4). The pattern described in this study does not correspond to a previous report showing only a minor fraction of C24-fatty acids in HexCer and a significant fraction of C22 and C24 species in LacCer (32). However, major HexCer (except lower Hex 24:1 fraction) and LacCer species found by Hammad et al. and HexCer species in the study by Quehenberger et al. were comparable to our study.

Additionally, we describe the distribution of HexCer, LacCer, SPC and sphingoid base phosphates on lipoprotein fractions separated by a previously established FPLC method (19). As described by Dawson et al. (31), HexCer and LacCer showed a similar distribution on lipoprotein fractions. Compared to this report using ultracentrifugation we found lower proportions in VLDL (8% vs. 13-14%) and LDL (46-49% vs. 59-60%) but higher glycosylated ceramides in the HDL fraction (42-44% vs. 26-28%). The distribution of sphingoid base phosphates measured in this study confirms data by Murata et al. (34) (measured by radioreceptor-binding assay) and Hammad et al. in lipoprotein fractions prepared by ultracentrifugation. Since HDL and albumin overlap in the FPLC separation used (19), we can only report that more than 90% of sphingoid base phosphates reside in these fractions (90% Murata et al.; 95% S1P 18:1 Hammad et al.). Interestingly, LDL carries with 6% a 2-fold higher fraction of S1P 18:1 compared to S1P 18:0 (Tab. 2) which is in contrast to Hammad et al. where 14% of S1P 18:0 was found in the LDL fraction. Taken together a number of discrepancies were observed between studies of sphingolipid species concentration in plasma and lipoproteins. Consequently, further studies and standardization of methods are required to establish reliable sphingolipid level in human plasma.

In summary, HILIC-MS/MS provides a comprehensive overview of minor sphingolipid species in plasma and lipoproteins. These species profiles may help to address the origin of plasma sphingolipids by comparison with tissue or blood cell species pattern (35). Moreover, the presented method may be used for the plasma sphingolipid profiling in large clinical studies to find novel lipid biomarker.

5.6   References

1. Bartke N, Hannun YA. Bioactive sphingolipids: metabolism and function. J Lipid Res 2009;50 Suppl:S91-S96.

2. Chen Y, Liu Y, Sullards MC, Merrill AH, Jr. An Introduction to Sphingolipid Metabolism and Analysis by New Technologies. Neuromolecular Med 2010.

3. Deutschman DH, Carstens JS, Klepper RL, Smith WS, Page MT, Young TR et al. Predicting obstructive coronary artery disease with serum sphingosine-1-phosphate. Am Heart J 2003;146:62-8.

4. Huwiler A, Kolter T, Pfeilschifter J, Sandhoff K. Physiology and pathophysiology of sphingolipid metabolism and signaling. Biochim Biophys Acta 2000;1485:63-99.

5. Kim RH, Takabe K, Milstien S, Spiegel S. Export and functions of sphingosine-1-phosphate. Biochim Biophys Acta 2009;1791:692-6.

6. Lahiri S, Futerman AH. The metabolism and function of sphingolipids and glycosphingolipids. Cell Mol Life Sci 2007;64:2270-84.

7. Taha TA, Mullen TD, Obeid LM. A house divided: ceramide, sphingosine, and sphingosine-1-phosphate in programmed cell death. Biochim Biophys Acta 2006;1758:2027-36.

8. Cowart LA. Sphingolipids: players in the pathology of metabolic disease. Trends Endocrinol Metab 2009;20:34-42.

9. Liliom K, Sun G, Bunemann M, Virag T, Nusser N, Baker DL et al. Sphingosylphosphocholine is a naturally occurring lipid mediator in blood plasma: a possible role in regulating cardiac function via sphingolipid receptors. Biochem J 2001;355:189-97.

10. Wymann MP, Schneiter R. Lipid signalling in disease. Nat Rev Mol Cell Biol 2008;9:162-76.

11. Haus JM, Kashyap SR, Kasumov T, Zhang R, Kelly KR, Defronzo RA, Kirwan JP. Plasma ceramides are elevated in obese subjects with type 2 diabetes and correlate with the severity of insulin resistance. Diabetes 2009;58:337-43.

12. Drobnik W, Liebisch G, Audebert FX, Frohlich D, Gluck T, Vogel P et al. Plasma ceramide and lysophosphatidylcholine inversely correlate with mortality in sepsis patients. J Lipid Res 2003;44:754-61.

13. Ichi I, Nakahara K, Miyashita Y, Hidaka A, Kutsukake S, Inoue K et al. Association of ceramides in human plasma with risk factors of atherosclerosis. Lipids 2006;41:859-63.

14. Jiang XC, Paultre F, Pearson TA, Reed RG, Francis CK, Lin M et al. Plasma sphingomyelin level as a risk factor for coronary artery disease. Arterioscler Thromb Vasc Biol 2000;20:2614-8.

15. Schlitt A, Blankenberg S, Yan D, von GH, Buerke M, Werdan K et al. Further evaluation of plasma sphingomyelin levels as a risk factor for coronary artery disease. Nutr Metab (Lond) 2006;3:5.

16. Dahm F, Nocito A, Bielawska A, Lang KS, Georgiev P, Asmis LM et al. Distribution and dynamic changes of sphingolipids in blood in response to platelet activation. J Thromb Haemost 2006;4:2704-9.

17. Hiukka A, Stahlman M, Pettersson C, Levin M, Adiels M, Teneberg S et al. ApoCIII-enriched LDL in type 2 diabetes displays altered lipid composition, increased susceptibility for sphingomyelinase, and increased binding to biglycan. Diabetes 2009;58:2018-26.

18. Hicks AA, Pramstaller PP, Johansson A, Vitart V, Rudan I, Ugocsai P et al. Genetic determinants of circulating sphingolipid concentrations in European populations. PLoS Genet 2009;5:e1000672.

19. Wiesner P, Leidl K, Boettcher A, Schmitz G, Liebisch G. Lipid profiling of FPLC-separated lipoprotein fractions by electrospray ionization tandem mass spectrometry. J Lipid Res 2009;50:574-85.

20. Hammad SM, Pierce JS, Soodavar F, Smith KJ, Al Gadban MM, Rembiesa B et al. Blood sphingolipidomics in healthy humans: Impact of sample collection methodology. J Lipid Res 2010.

21. Quehenberger O, Armando AM, Brown AH, Milne SB, Myers DS, Merrill AH et al. Lipidomics reveals a remarkable diversity of lipids in human plasma. J Lipid Res 2010.

22. Scherer M, Leuthauser-Jaschinski K, Ecker J, Schmitz G, Liebisch G. A rapid and quantitative LC-MS/MS method to profile sphingolipids. J Lipid Res 2010;51:2001-11.

23. Scherer M, Schmitz G, Liebisch G. High-throughput analysis of sphingosine 1-phosphate, sphinganine 1-phosphate, and lysophosphatidic acid in plasma samples by liquid chromatography-tandem mass spectrometry. Clin Chem 2009;55:1218-22.

24. Baker DL, Desiderio DM, Miller DD, Tolley B, Tigyi GJ. Direct quantitative analysis of lysophosphatidic acid molecular species by stable isotope dilution electrospray ionization liquid chromatography-mass spectrometry. Anal Biochem 2001;292:287-95.

25. Liebisch G, Lieser B, Rathenberg J, Drobnik W, Schmitz G. High-throughput quantification of phosphatidylcholine and sphingomyelin by electrospray ionization tandem mass spectrometry coupled with isotope correction algorithm. Biochim Biophys Acta 2004;1686:108-17.

26. Drobnik W, Borsukova H, Bottcher A, Pfeiffer A, Liebisch G, Schutz GJ et al. Apo AI/ABCA1-dependent and HDL3-mediated lipid efflux from compositionally distinct cholesterol-based microdomains. Traffic 2002;3:268-78.

27. Fujiwaki T, Tasaka M, Yamaguchi S. Quantitative evaluation of sphingomyelin and glucosylceramide using matrix-assisted laser desorption ionization time-of-flight mass spectrometry with sphingosylphosphorylcholine as an internal standard. Practical application to tissues from patients with Niemann-Pick disease types A and C, and Gaucher disease. J Chromatogr B Analyt Technol Biomed Life Sci 2008;870:170-6.

28. Liebisch G, Drobnik W, Reil M, Trumbach B, Arnecke R, Olgemoller B et al. Quantitative measurement of different ceramide species from crude cellular extracts by electrospray ionization tandem mass spectrometry (ESI-MS/MS). J Lipid Res 1999;40:1539-46.

29. Karlsson KA. Sphingolipid long chain bases. Lipids 1970;5:878-91.

30. Clarke JT, Stoltz JM, Mulcahey MR. Neutral glycosphingolipids of serum lipoproteins in Fabry's disease. Biochim Biophys Acta 1976;431:317-25.

31. Dawson G, Kruski AW, Scanu AM. Distribution of glycosphingolipids in the serum lipoproteins of normal human subjects and patients with hypo- and hyperlipidemias. J Lipid Res 1976;17:125-31.

32. Kundu SK, Diego I, Osovitz S, Marcus DM. Glycosphingolipids of human plasma. Arch Biochem Biophys 1985;238:388-400.

33. van den Bergh FA, Tager JM. Localization of neutral glycosphingolipids in human plasma. Biochim Biophys Acta 1976;441:391-402.

34. Murata N, Sato K, Kon J, Tomura H, Okajima F. Quantitative measurement of sphingosine 1-phosphate by radioreceptor-binding assay. Anal Biochem 2000;282:115-20.

35. Leidl K, Liebisch G, Richter D, Schmitz G. Mass spectrometric analysis of lipid species of human circulating blood cells. Biochim Biophys Acta 2008;1781:655-64.

6 Rapid quantification of bile acids and their conjugates in serum by liquid chromatography – tandem mass spectrometry

6.1 Abstract

Beside their role as lipid solubilizers, bile acids (BAs) are increasingly appreciated as signaling factors. As ligands of G-protein coupled receptors and nuclear hormone receptors BAs control their own metabolism and act on lipid and energy metabolism. To study BA function in detail, it is necessary to use methods for their quantification covering the structural diversity of this group.

Here we present a simple, sensitive liquid chromatography-tandem-mass spectrometry (LC-MS/MS) method for the analysis of bile acid profiles in human plasma/serum. Protein precipitation was performed in the presence of stable-isotope labeled internal standards. In contrast to previous LC-MS/MS methods, we used a reversed-phase C18 column with 1.8µm particles and a gradient elution at basic pH. This allows base line separation of eighteen bile acid species (free and conjugated) within 6.5min run time and a high sensitivity in negative ion mode with limits of detection below 10nmol/L. Quantification was achieved by standard addition and calibration lines were linear in the tested range up to 28µmol/L. Validation was performed according to FDA guidelines and overall imprecision was below 11% CV for all species.

The developed LC-MS/MS method for bile acid quantification is characterized by simple sample preparation, baseline separation of isobaric species, a short analysis time and provides a valuable tool for both, routine diagnostics and the evaluation of BAs as diagnostic biomarkers in large clinical studies.

6.2 Introduction

Bile acid (BA) synthesis from cholesterol in liver is the primary pathway of cholesterol catabolism. Thereby cholesterol is modified by oxidation, shortening of the side chain and finally conjugation by glycine and taurine, respectively (1;2). These amphiphatic molecules are essential to solubilize dietary lipids and vitamins to promote their absorption. The most abundant BAs in humans comprise the primary BAs cholic acid (CA) and chenodeoxycholic acid (CDCA) and the secondary BAs deoxycholic acid (DCA), lithocholic acid (LCA) and ursodeoxycholic acid (UDCA) formed by deconjugation and dehydroxylation by intestinal bacteria in the colon. BAs are effectively reabsorbed and transported back to the liver to enter again enterohepatic circulation (1;2).

Beside their well established role in dietary lipid absorption and cholesterol homeostasis, BAs are increasingly recognized as signaling molecules with endocrine functions (1;3;4). BAs are ligands for G-protein-coupled receptors such as TGR5 and modulators of several nuclear hormone receptors, most important farnesoid X receptor (FXR). Through activation of these diverse signaling pathways, BAs can regulate their own metabolism, but also lipid and energy homeostasis. In summary, these signaling functions make BA metabolism an attractive pharmacological target for treatment of vascular and metabolic diseases such as obesity, type 2 diabetes and atherosclerosis (1;3).

The study of BA functions requires methods which cover the complexity of this structurally diverse group of molecules. In the last years a number of methods using liquid chromatography coupled to tandem mass spectrometry (LC-MS/MS) were developed allowing analysis of free and conjugated BAs without derivatization (5-16). Nevertheless, most methods show disadvantages with time consuming extraction procedures (5;8;17), long analysis times (6-8;14-18) or lack of baseline separation of isobaric species (5;8;9;17;18). Direct BA analysis by ESI-MS/MS does not allow identification of isobaric species (19).

Here we present a validated method for the quantification of 18 free and conjugated BAs in plasma (serum) by LC-MS/MS with a short analysis time of 6.5min and baseline separation of isobaric species suitable for high-throughput analysis of patient samples.

6.3   Material and Methods

6.3.1   Chemicals and solutions

Acetonitril, methanol (HPLC grade), ammonium acetate (98%), hydrochloric acid (HCl) and ammonium hydroxide (25%, for analysis) were purchased from VWR Int. GmbH (Darmstadt, Germany). Water was obtained from B. Braun (Melsungen, Germany). Bile acid standards were purchased from Sigma-Aldrich Chemie GmbH (Taufkirchen, Germany), Steraloids Inc. (Newport, USA), Campro Scientific GmbH (Berlin, Germany), Larodan Fine Chemicals AB (Malmö, Sweden) and were at least of 95% purity.

6.3.2   Samples and sample preparation

EDTA-plasma and serum were obtained from healthy volunteers, using standard venipuncture techniques. Samples were immediately centrifuged at 2000 x g for 10min. Plasma and serum were removed and stored at -20℃ until analysis. To investigate sample stability, plasma and serum samples were aliquoted, immediately stored at -20℃ or stored after 1, 4, 8 and 24h at room temperature. The immediately stored samples served as reference point.

The sample preparation procedure was based on a published method ($\underline{6}$) with slight modifications. 100µL EDTA-plasma/serum were spiked with 10µL of IS-mixture (2.4µmol/L D_4-CA, 2.6µmol/L D_4-DCA, 4µmol/L D_4-CDCA, 0.6µmol/L D_4-LCA, 2.6µmol/L D_4-UDCA, 4.6µmol/L D_4-GCA, 14µmol/L D_4-GCDCA). To increase extraction efficiency, 30µL of 1mol/L HCl were added. For protein precipitation, plasma/serum were mixed with 1mL acetonitril, followed by 1min vortex-mixing. After 15min of centrifugation (14000 x g), the supernatant was evaporated to dryness under reduced pressure. The samples were re-dissolved in 100µL methanol/water (1/1; v/v, containing 10mmol/L ammonium acetate and 0.1% ammonium hydroxide). After an additional centrifugation step 5µL of the methanolic supernatant were used for LC-MS/MS-analysis.

6.3.3 LC-MS/MS analysis

BA analysis was performed by liquid chromatography-tandem mass spectrometry (LC-MS/MS). The HPLC equipment consisted of a 1200 series binary pump (G1312B), a 1200 series isocratic pump (G1310A) and a degasser (G1379B) (Agilent, Waldbronn, Germany) connected to an HTC Pal autosampler (CTC Analytics, Zwingen, CH). A hybrid triple quadrupole linear ion trap mass spectrometer API 4000 Q-Trap equipped with a Turbo V source ion spray operating in negative ESI mode was used for detection (Applied Biosystems, Darmstadt, Germany). High purity nitrogen was produced by a nitrogen generator NGM 22-LC/MS (cmc Instruments, Eschborn, Germany).

Gradient chromatographic separation of BAs was performed on a 50 x 2.1 (i.d.) mm Macherey-Nagel NUCLEODUR C18 Gravity HPLC column, packed with 1.8µm particles equipped with a 0.5µm pre-filter (Upchurch Scientific, Oak Harbor, WA, USA). The injection volume was 5µL and the column oven temperature was set to 50°C. Mobile phase A was methanol/water (1/1; v/ v), mobile phase B was 100% methanol, both containing 0.1% ammonium hydroxide (25%) and 10mmol/L ammonium acetate (pH 9). A gradient elution was performed with 100% A for 0.5min, a linear increase to 50% A until 4.5min, followed by 0% A from 4.6 until 5.5min and re-equilibration from 5.6 to 6.5min with 100% A. The flow rate was set to 500µL/min. To minimize contamination of the mass spectrometer, the column flow was directed only from 1.0 to 5.0min into the mass spectrometer using a divert valve. Otherwise methanol with a flow rate of 250µL/min was delivered into the mass spectrometer.

The Turbo Ion Spray source was operated in the negative ion-mode using the following settings: Ion spray voltage = -4500V, ion source heater temperature = 450°C, source gas 1 = 40psi, source gas 2 = 35psi a nd curtain gas setting = 20psi. Analytes were monitored in the multiple reaction monitoring (MRM), mass transitions and MS parameters are shown in Table 1. Quadrupoles Q_1 and Q_3 were working at unit resolution.

6.3.4 Calibration and quantification

Calibration was achieved by addition of BAs to EDTA-plasma (serum). A combined BA standard solution containing the indicated amounts (0.5 – 70.5µmol/L) was placed in a 1.5ml tube and excess solvent was evaporated under reduced

pressure before adding EDTA-plasma/serum. Calibration curves were calculated by linear regression without weighting.

Data analysis was performed with Analyst Software 1.4.2. (Applied Biosystems, Darmstadt, Germany). The data were exported to Excel spreadsheets and further processed by self programmed Excel macros which sort the results, calculate the analyte/internal standard peak area ratios, generate calibration lines and calculate sample concentrations.

6.4   Results

6.4.1   Fragmentation of BAs

First we tested the fragmentation of de-protonated BAs in negative ion mode. Unconjugated BA showed no prominent product ion. Therefore, we used a MS/MS transition without fragmentation and optimized the collision energy to get the highest signal to noise ratio for free BAs in plasma samples (data not shown). For conjugated BAs, fragment ions of the glycine (*m/z* 74) taurine (*m/z* 80) moiety were selected (Table 1). These transitions resemble those used in previous studies (5;6;8;19).

Table 1. MS parameter and limit of detection (LOD) of the BAs studied.

Bile acid	[M-H]⁻ m/z	MRM	IS	CE (V)	RT [min]	LOD [nmol/L]
CA	407.3	407.3→407.3	D_4-CA	-30	2.56	5.79
CDCA	391.3	391.3→391.3	D_4-CDCA	-30	3.51	2.28
DCA	391.3	391.3→391.3	D_4-DCA	-30	3.71	6.52
LCA	375.3	375.3→375.3	D_4-LCA	-30	4.50	9.84
UDCA	391.3	391.3→391.3	D_4-UDCA	-30	1.92	8.82
HDCA	391.3	391.3→391.3	D_4-UDCA	-30	2.15	8.34
GCA	464.3	464.3→464.3	D_4-GCA	-72	2.52	2.46
GCDCA	448.3	448.3→74	D_4-GCDCA	-70	3.44	2.35
GDCA	448.3	448.3→74	D_4-GCDCA	-70	3.65	2.09
GLCA	432.3	432.3→74	D_4-GCDCA	-64	4.41	0.55
GUDCA	448.3	448.3→74	D_4-GCA	-70	1.84	2.82
GHDCA	448.3	448.3→74	D_4-GCA	-70	2.08	1.56
TCA	514.3	514.3→80	D_4-GCA	-116	2.48	4.50
TCDCA	498.3	498.3→80	D_4-GCDCA	-116	3.38	1.75
TDCA	498.3	498.3→80	D_4-GCDCA	-116	3.61	1.64
TLCA	482.3	482.3→80	D_4-LCA	-108	4.35	0.46
TUDCA	498.3	498.3→80	D_4-UDCA	-116	1.83	3.19
THDCA	498.3	498.3→80	D_4-UDCA	-116	2.08	0.37
D_4-CA	411.2	411.2→411.2		-30	2.56	-
D_4-CDCA	395.3	395.3→395.3		-30	3.51	-
D_4-DCA	395.3	395.3→395.3		-30	3.71	-
D_4-LCA	379.3	379.3→379.3		-30	4.49	-
D_4-UDCA	395.3	395.3→395.3		-30	1.92	-
D_4-GCA	468.3	468.3→74		-72	2.52	-
D_4-GCDCA	452.3	452.3→74		-70	3.44	-

IS = internal standard, CE = collision energy, RT = retention time

6.4.2 Analysis of BAs by LC-MS/MS

Because it is impossible to differentiate isobaric BA species by mass spectrometry a separation of isobaric species is necessary. To achieve a fast separation we chose a reversed-phase C18 column with a small particle diameter of 1.8µm. Similar to most previous methods a water–methanol gradient was used for LC separation. Although most studies used acidic mobile phases, we tested the influence of the pH on BA separation. Compared to acidic pH 4 (Fig. 1A), basification of the mobile phase to pH 9 greatly improves resolution of BA species (Fig. 1B).

Finally, we could accomplish baseline separation of isobaric species within 6.5min (standard mixture Fig. 2 A-C and a representative human EDTA-plasma sample Fig. 2 D-F). Since 25 MS transitions are necessary to cover the main natural occurring bile acid species and their respective internal standards, we divided the MS program into 2 periods from 0 to 3min (12 transitions) and from 3 to 6.5min (13 transitions). Using these periods further increased precision and sensitivity (data not

shown). Because we applied only a simple protein precipitation as sample preparation pre- and post-run was diverted into waste to prevent contamination of the mass spectrometer. Despite the use of crude samples, a column lifetime greater than 1000 injections was observed.

0.1% H_2CO_3 (pH 4)
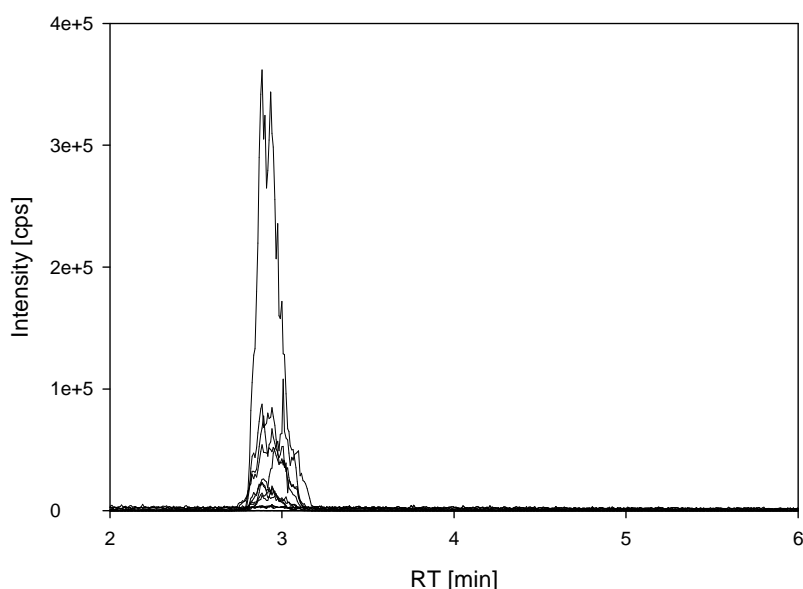
0.1% NH_3 (pH 9)
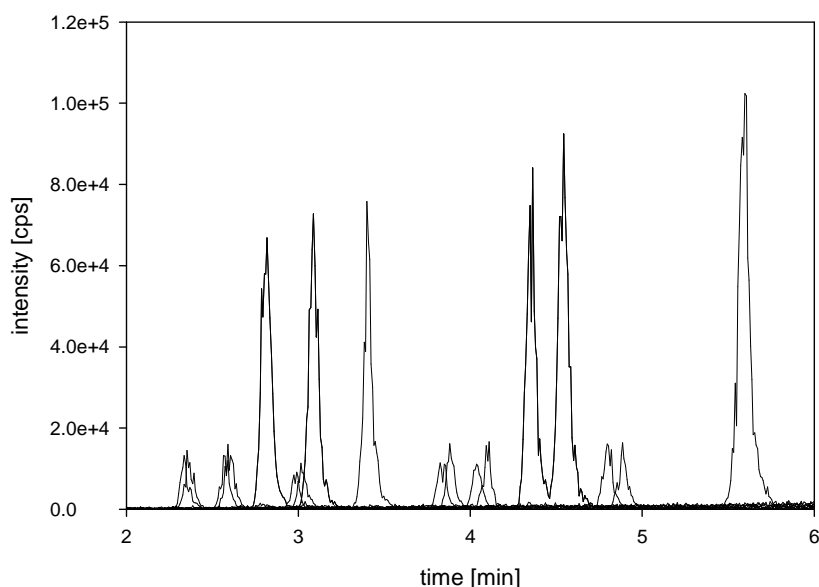
Fig. 2. Effect of mobile phase pH on the separation of BAs. Displayed are mass chromatograms obtained using a bile acid standard mixture and the same linear gradient. The mobile phases consisted of methanol/water (1:1, v/v) (eluent A) and methanol (eluent B) containing 10mM ammonium acetate as well as (A) 0.1% formic acid or (B) 0.1% ammonia (25%).D) unconjugated, (B and E) glycin-conjugated and (C and F) taurin-conjugated BAs.

6.4.3 Matrix effects

Due to the use of crude samples and the fast LC separation we analyzed the influence of the matrix on signal intensities. Because no analyte free EDTA-plasma was available, an internal standard mixture (D_4-CA, D_4-CDCA. D_4-DCA, D_4-LCA, D_4-UDCA, D_4-GCA and D_4-GCDCA) was analyzed with or without plasma extract. The presence of plasma extract caused a mean signal reduction (± S.D.) of 25 ± 6%.

6.4.4 Quantification

In order to compensate for variations in sample preparation and ionization efficiency, a set of stable isotope labeled BAs, D_4-CA, D_4-CDCA. D_4-DCA, D_4-LCA, D_4-UDCA, D_4-GCA and D_4-GCDCA were added as IS prior to extraction. We generated calibration lines by addition of different concentrations of naturally occurring BAs to human EDTA-plasma (Suppl.-Fig. 1.). A five point calibration was performed within the concentration range indicated in Tab 2. For each analyte a calibration line was calculated by least square fitting of concentration against the peak area ratio of analyte to internal standard (Tab. 1.). The obtained standard curves were linear in the tested calibration range (Suppl.-Fig. 1.).

Table 2. Calibration data of the BA species (n=4).

Bile acid	Calibration range up to [µM]	Slope (mean ± S.D.)	Intercept (mean ± S.D.)	Correlation coefficient (mean ± S.D.)
CA	4.4	1.26±0.12	0.258±0.229	0.9983±0.0006
CDCA	8	1.54±0.14	0.430±0.295	0.9951±0.0019
DCA	5.2	2.05±0.11	0.733±0.392	0.9971±0.0032
LCA	0.4	4.74±0.06	0.136±0.149	0.9993±0.0006
UDCA	4.7	2.01±0.14	0.129±0.072	0.9956±0.0048
HDCA	4.7	4.64±0.21	0.861±0.712	0.9962±0.0014
GCA	9.4	1.07±0.02	0.239±0.201	0.9971±0.0015
GCDCA	28.2	0.45±0.05	0.376±0.428	0.9970±0.0004
GDCA	3.3	0.39±0.03	0.186±0.222	0.9964±0.0021
GLCA	0.2	4.73±0.07	0.378±0.470	0.9968±0.0010
GUDCA	0.32	0.48±0.03	0.074±0.060	0.9963±0.0044
GHDCA	0.32	0.79±0.09	0.023±0.025	0.9971±0.0025
TCA	2.8	0.72±0.08	0.016±0.014	0.9972±0.0024
TCDCA	9.2	0.27±0.03	0.019±0.012	0.9960±0.0024
TDCA	0.77	0.36±0.04	0.011±0.012	0.9975±0.0024
TLCA	0.2	4.27±0.14	0.025±0.022	0.9991±0.0015
TUDCA	0.32	0.49±0.05	0.002±0.001	0.9966±0.0018
THDCA	0.32	0.50±0.10	0.001±0.002	0.9967±0.0045

6.4.5 Assay characteristics

Assay accuracy was calculated using three spiked plasma samples in different concentration levels (low, medium, high), covering the entire range of plasma BA levels. We found mean accuracies (± S.D.) between 89 and 111%. Similarly, extraction efficiency was tested by the addition BAs before and after sample preparation. Recoveries were calculated by the ratio of spiked BA area before and after extraction. The mean relative recovery was >80% and no correlation to the spiked amount was observed (Suppl.-Tab. 1.).

Precision of the developed method was determined in 3 unspiked plasma samples, containing low, medium and high bile acid levels. Coefficients of variation (CVs) were <9% for intraday precision and <11% for interday precision (Suppl.-Tab. 2).

The limit of detection (LOD) was determined in three different human plasma samples as a signal-to-noise-ratio of three. LOD was below 10nmol/L for all BA species (Tab. 1).

Stability of human EDTA-plasma was assessed immediately and after storage for 1, 4, 8 and 24h at room temperature. Immediately frozen samples did not differ in

BA levels compared with samples stored for 1, 4, 8 and 24h at room temperature (data not shown).
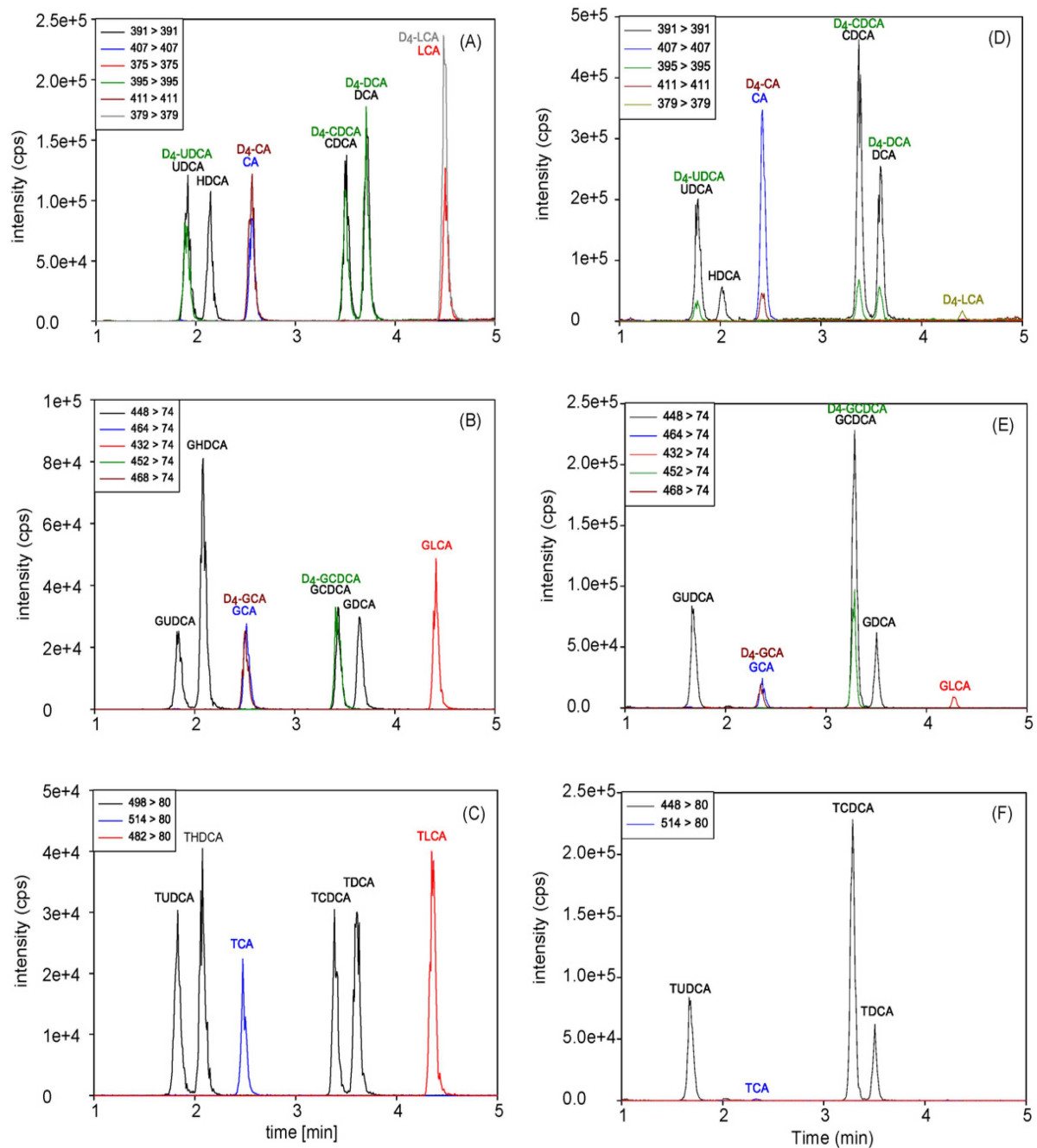
Fig. 2. Chromatogram of BAs. Displayed are representative mass chromatograms obtained using a bile acid standard mixture (A-C) and an extracted EDTA-plasma sample (D-F). (A and D) unconjugated, (B and E) glycin-conjugated and (C and F) taurin-conjugated BAs.

6.4.6 Quantitation of plasma and serum BAs

The method was applied to BA quantitation of plasma and serum samples of 29 healthy volunteers (11 females and 18 males), between 20 and 47 years of age (Tab. 3). Bile acid concentrations showed no notable differences between EDTA-plasma and serum samples (data not shown). The main species detected were CDCA and DCA and their glyco-conjugates, whereas glycol- and tauro-conjugates of HDCA were not detectable in most samples of healthy volunteers.

Table 3. Bile acid levels in human serum

Bile acid	Serum (n=29) Mean (S.D.; range) [µmol/L]
CA	0.2 (0.18; 0.053-0.68)
CDCA	0.34 (0.28; 0.065-1.19)
DCA	0.48 (0.34; 0.058-1.32)
LCA	0.030 (0.018; n.d.-0.084)
UDCA	0.11 (0.085; 0.021-0.33)
HDCA	0.21 (0.17; 0.030-0.67)
GCA	0.41 (0.36; 0.067-1.02)
GCDCA	1.71 (0.80; 0.47-3.21)
GDCA	0.38 (0.26; 0.048-0.88)
GLCA	0.068 (0.047; 0.009-0.165)
GUDCA	0.28 (0.15; 0.084-0.63)
GHDCA	n.d. (n.d.-0.0092)
TCA	0.048 (0.083; n.d.-0.35)
TCDCA	0.21 (0.23; 0.017-0.86)
TDCA	0.044 (0.037; n.d.-0.14)
TLCA	0.019 (0.016; n.d.-0.060)
TUDCA	0.007 (0.006; n.d.-0.025)
THDCA	n.d. (n.d.-0.023)

Mean values of healthy donors are expressed in µmol/L, S.D. and range are indicated in parentheses.

6.5 Discussion

In the last years BAs came under the spotlight due to their role as signaling molecules regulating their own as well as lipid and energy metabolism (1;3;4). In order to study BA function in detail, methods covering the full spectra of BA species are necessary. To use these methods in large clinical studies, these methods should require only a minimal sample preparation and a short analysis time. LC-MS/MS provides information about free and conjugated BAs together with an easy sample preparation.

However, up to now there are no LC-MS/MS methods published with a sufficient separation of isobaric BA species below 10min runtime ([5;6;8;9;11;14;16-19]). Therefore, we developed a LC-MS/MS method for simultaneous determination of free and conjugated BAs in plasma and serum with a runtime of 6.5min. Shortening of the run time was permitted by application of basic conditions (10mM NH_4Ac, 0.1% NH_3, pH 9; Fig. 1) and a small particles column. Changing to 1.8µm particle diameter not only allows fast baseline separation of isobaric species but also a 2-fold reduction of matrix suppression compared to a column with 2.5µm particles (data not shown).

To achieve reproducible and accurate results, a set of 7 stable isotope labeled BAs were used as internal standards (Tab. 1). This way we could show an excellent accuracy and overall imprecision below 11% CV for all analyzed BAs (Suppl.-Tab. 2.). Based on these data, we could conclude that the selected set of internal standards together with a matrix calibration were suitable to compensate matrix effects or other variations in analytical conditions. In contrast to most existing methods, this study shows a detailed validation according to FDA criteria including evaluation of matrix effects, extraction efficiencies and sample stability ([20]). Moreover, analysis of BAs in large clinical studies (>5000 samples) showed the robustness of our analytical set-up despite the use of crude samples.

We determined bile acid concentrations in serum and EDTA-plasma samples from 29 (11 females, 18 males) healthy volunteers. The concentrations for individual bile acid species were in a similar range as those recently reported by Burkard et al. ([8]).

6.6 Conclusion

In conclusion this study, presents a rapid LC-MS/MS method for the simultaneous determination of 18 bile acid species from serum (plasma). Improvements compared to previous LC-MS/MS methods were observed regarding run time and separation of isobaric BAs as a result of application of 1.8µm column particles and a mobile phase with basic pH. This novel LC-MS/MS method represents a valuable tool for screening bile acid profiles in routine diagnostics and clinical studies.

6.7   References

1. Thomas C, Pellicciari R, Pruzanski M, Auwerx J, Schoonjans K. Targeting bile-acid signalling for metabolic diseases. Nat Rev Drug Discov 2008;7:678-93.

2. Hofmann AF, Hagey LR. Bile acids: chemistry, pathochemistry, biology, pathobiology, and therapeutics. Cell Mol Life Sci 2008;65:2461-83.

3. Lefebvre P, Cariou B, Lien F, Kuipers F, Staels B. Role of bile acids and bile acid receptors in metabolic regulation. Physiol Rev 2009;89:147-91.

4. Houten SM, Watanabe M, Auwerx J. Endocrine functions of bile acids. EMBO J 2006;25:1419-25.

5. Ye L, Liu S, Wang M, Shao Y, Ding M. High-performance liquid chromatography-tandem mass spectrometry for the analysis of bile acid profiles in serum of women with intrahepatic cholestasis of pregnancy. J Chromatogr B Analyt Technol Biomed Life Sci 2007;860:10-7.

6. Tagliacozzi D, Mozzi AF, Casetta B, Bertucci P, Bernardini S, Di IC et al. Quantitative analysis of bile acids in human plasma by liquid chromatography-electrospray tandem mass spectrometry: a simple and rapid one-step method. Clin Chem Lab Med 2003;41:1633-41.

7. Ando M, Kaneko T, Watanabe R, Kikuchi S, Goto T, Iida T et al. High sensitive analysis of rat serum bile acids by liquid chromatography/electrospray ionization tandem mass spectrometry. J Pharm Biomed Anal 2006;40:1179-86.

8. Burkard I, von EA, Rentsch KM. Differentiated quantification of human bile acids in serum by high-performance liquid chromatography-tandem mass spectrometry. J Chromatogr B Analyt Technol Biomed Life Sci 2005;826:147-59.

9. Eckers C, New AP, East PB, Haskins NJ. The use of tandem mass spectrometry for the differentiation of bile acid isomers and for the identification of bile acids in biological extracts. Rapid Commun Mass Spectrom 1990;4:449-53.

10. Ikegawa S, Murao N, Motoyama T, Yanagihara T, Niwa T, Goto J. Separation and detection of bile acid 3-glucuronides in human urine by liquid chromatography/electrospray ionization-mass spectrometry. Biomed Chromatogr 1996;10:313-7.

11. Bootsma AH, Overmars H, van RA, van Lint AE, Wanders RJ, van Gennip AH, Vreken P. Rapid analysis of conjugated bile acids in plasma using electrospray tandem mass spectrometry: application for selective screening of peroxisomal disorders. J Inherit Metab Dis 1999;22:307-10.

12. Johnson DW, ten Brink HJ, Schuit RC, Jakobs C. Rapid and quantitative analysis of unconjugated C(27) bile acids in plasma and blood samples by tandem mass spectrometry. J Lipid Res 2001;42:9-16.

13. Mills KA, Mushtaq I, Johnson AW, Whitfield PD, Clayton PT. A method for the quantitation of conjugated bile acids in dried blood spots using electrospray ionization-mass spectrometry. Pediatr Res 1998;43:361-8.

14. Roda A, Gioacchini AM, Cerre C, Baraldini M. High-performance liquid chromatographic-electrospray mass spectrometric analysis of bile acids in biological fluids. J Chromatogr B Biomed Appl 1995;665:281-94.

15. Sakakura H, Suzuki M, Kimura N, Takeda H, Nagata S, Maeda M. Simultaneous determination of bile acids in rat bile and serum by high-performance liquid chromatography. J Chromatogr 1993;621:123-31.

16. Alnouti Y, Csanaky IL, Klaassen CD. Quantitative-profiling of bile acids and their conjugates in mouse liver, bile, plasma, and urine using LC-MS/MS. J Chromatogr B Analyt Technol Biomed Life Sci 2008;873:209-17.

17. Tessier E, Neirinck L, Zhu Z. High-performance liquid chromatographic mass spectrometric method for the determination of ursodeoxycholic acid and its glycine and taurine conjugates in human plasma. J Chromatogr B Analyt Technol Biomed Life Sci 2003;798:295-302.

18. Bentayeb K, Batlle R, Sanchez C, Nerin C, Domeno C. Determination of bile acids in human serum by on-line restricted access material-ultra high-performance liquid chromatography-mass spectrometry. J Chromatogr B Analyt Technol Biomed Life Sci 2008;869:1-8.

19. Perwaiz S, Tuchweber B, Mignault D, Gilat T, Yousef IM. Determination of bile acids in biological fluids by liquid chromatography-electrospray tandem mass spectrometry. J Lipid Res 2001;42:114-9.

20. U.S.Department of Health and Human Services Food and Drug Administration. Guidance for Industry
Bioanalytical Method Validation. 2001.

6.8 Data supplement

Suppl.-Table 1. Values represent the percent recovery of standards spiked before and after extraction.

| Bile acid	spiked concentration [µmol/L]	recovery [%]	found concentration [µmol/L]	Accuracy [%]
CA	0.22	92±2	0.24±0.014	107±6
	0.66	86±4	0.64±0.08	96±12
	1.33	88±4	1.29±0.11	97±8
CDCA	0.4	96±8	0.45±0.38	113±9
	1.2	101±9	1.27±0.1	105±8
	2.4	99±5	2.61±0.115	109±6
DCA	0.259	93±7	0.25±0.024	97±9
	0.776	85±6	0.75±0.046	96±6
	1.55	87±7	1.55±0.051	100±3
LCA	0.01	86±6	0.024±0.002	111±9
	0.03	97±7	0.065±0.005	110±9
	0.06	92±5	0.13±0.010	104±9
UDCA	0.24	97±8	0.23±0.018	98±8
	0.71	98±6	0.70±0.066	98±9
	1.41	100±7	1.41±0.076	100±5
HDCA	0.24	88±7	0.25±0.016	106±7
	0.71	95±4	0.72±0.060	102±8
	1.41	98±10	1.43±0.122	101±8
GCA	0.47	98±11	0.52±0.046	111±8
	1.41	95±8	1.47±0.098	105±7
	2.81	99±9	3.05±0.183	108±7
GCDCA	1.41	99±12	1.25±0.096	89±7
	4.23	99±5	4.53±0.41	92±6
	8.45	103±5	7.92±0.62	94±7
GDCA	0.166	92±9	0.17±0.015	103±10
	0.497	87±9	0.52±0.045	104±9
	0.994	96±7	1.06±0.052	107±7
GLCA	0.02	84±3	0.011±0.001	108±10
	0.06	81±9	0.028±0.002	96±6
	0.12	90±6	0.061±0.006	102±10
GUDCA	0.016	93±6	0.014±0.001	92±9
	0.048	86±3	0.045±0.004	95±9
	0.096	88±8	0.089±0.006	111±8
GHDCA	0.016	88±6	0.015±0.0007	96±5
	0.048	82±10	0.046±0.005	96±11
	0.096	90±6	0.089±0.007	93±7
TCA	0.14	79±9	0.14±0.01	102±6
	0.42	84±4	0.43±0.033	104±8
	0.84	80±9	0.88±0.051	105±6
TCDCA	0.46	87±5	0.45±0.04	98±8
	1.37	93±8	1.4±0.068	102±5
	2.75	85±4	2.84±0.14	103±5
TDCA	0.038	80±4	0.040±0.005	105±13
	0.115	85±3	0.115±0.004	100±3
	0.23	92±9	0.22±0.014	95±6
TLCA	0.01	83±4	0.008±0.0001	95±3
	0.03	84±10	0.027±0.003	90±10
	0.06	93±10	0.057±0.005	95±8
TUDCA	0.016	86±4	0.0017±0.0001	104±7
	0.048	79±12	0.044±0.004	91±10
	0.097	88.2±6	0.102±0.005	106±6
THDCA	0.016	81±6	0.014±0.001	90±6
	0.048	86±5	0.044±0.001	91±4
	0.096	83±10	0.087±0.006	91±6

Accuracy is displayed as the mean of the assayed concentration (corrected by endogenous bile acid concentrations in human serum) in percent of the spiked concentration. Each value represents the average of three determinations ± standard deviation.

Suppl.-Table 2. Precision of the BA species analysis.

Bile acid	Intraday- [µmol/L±S.D.]	CV [%]	Interday- [µmol/L±S.D.]	CV[%]
CA	0.065±0.004	6	0.077±0.006	8.5
	0.15±0.012	8	0.17±0.013	7.4
	0.348±0.025	7.2	0.33±0.032	9.9
CDCA	0.17±0.013	7.6	0.16±0.014	8.6
	0.18±0.014	7.7	0.20±0.018	9
	0.27±0.016	5.8	0.27±0.018	6.6
DCA	0.29±0.01	3.9	0.31±0.027	8.6
	0.20±0.017	8.5	0.25±0.01	4.8
	0.064±0.004	6.3	0.07±0.008	11
LCA	0.026±0.002	6.2	0.025±0.001	5.6
	0.025±0.002	5.2	0.025±0.002	8.3
	0.019±0.002	8.1	0.017±0.01	6.4
UDCA	0.068±0.002	2.8	0.06±0.004	7.7
	0.21±0.015	7.1	0.2±0.016	8
	0.567±0.032	5.6	0.055±0.06	10.2
HDCA	0.17±0.012	7.1	0.14±0.008	5.7
	0.1±0.005	4.8	0.11±0.009	8.8
	0.04±0.003	7.5	0.043±0.003	8.2
GCA	0.35±0.022	6.4	0.32±0.023	7.2
	5.62±0.7	8.2	6.0±041	6.8
	17±1.4	8.7	15.9±0.7	4.7
GCDCA	1.2±0.06	4.9	1.38±0.074	5.4
	4.82±0.38	7.8	5.06±0.49	9.6
	12.8±0.78	6	13.8±0.87	6.3
GDCA	0.36±0.025	7	0.42±0.038	9
	0.42±0.018	1.9	0.49±0.04	8.7
	0.62±0.045	7.3	0.58±0.039	6.7
GLCA	0.034±0.0018	5.2	0.03±0.002	6.6
	0.024±0.002	8.3	0.028±0.0015	5.3
	0.62±0.0045	7.3	0.07±0.0062	8.6
GUDCA	0.017±0.0009	5.4	0.21±0.01	4.8
	0.69±0.05	7.2	0.58±0.044	7.5
	2.3±0.18	7.6	2.51±0.04	6
GHDCA	-	-	-	-
TCA	0.055±0.004	7.2	0.42±0.038	9
	2.71±0.18	6.6	3.02±0.27	8.7
	9.13±0.74	8.1	9.45±0.62	6.6
TCDCA	0.247±0.0016	6.4	0.26±0.024	9.1
	3.06±0.19	6.2	3.1±0.17	5.4
	9.24±0.74	8.0	10.3±1.1	11.1
TDCA	0.065±0.0004	5.9	0.063±0.0005	9.1
	0.14±0.009	6.4	0.14±0.009	6.2
	0.3±0.024	8.0	0.24±0.026	7.7
TLCA	0.017±0.001	7.8	0.021±0.0002	10
	0.02±0.002	10.4	0.025±0.001	4
	0.031±0.002	6.5	0.024±0.002	9.2
TUDCA	-	-	-	-
	0.68±0.052	7.6	0.72±0.04	5.5
	2.67±0.083	3.1	2.3±0.15	6.5
THDCA	-	-	-	-

The displayed values are mean plasma concentrations in µmol/L and the coefficient of variation (CV) of 6 sample aliquots at 3 concentrations analyzed in series for intra-day and on 6 different days for inter-day precision.
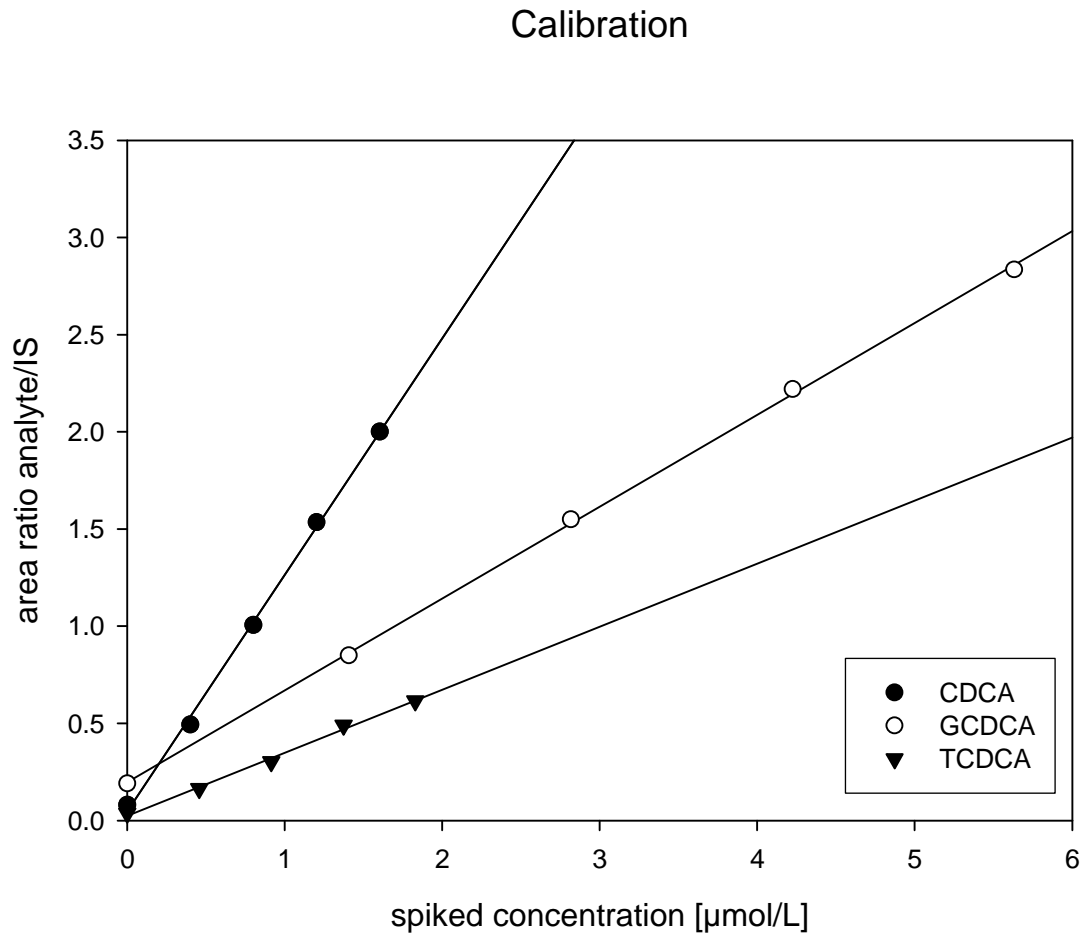
Calibration

Suppl.-Fig. 1. Calibration lines for CDCA, GCDCA and TCDCA.

Calibration lines were established by standard addition of BAs to plasma before extraction, yielding BA concentrations in a range of 0 - 28.2μmol/L. The corresponding calibration line statistics are shown in Table 2. The data shown were calculated from 4 independent samples. CDCA, GCDCA and TCDCA are representative for unconjugated, glycine- and taurine-conjugated BA species.

7   Summary

7.1   Summary in English

The crucial role of lipids in cells, tissues and body fluids is demonstrated by a large number of studies and human diseases that involve the disruption of lipid metabolic enzymes and pathways. Examples for such diseases include cancer, type 2 diabetes and atherosclerosis. Recent advances in research in the field of lipidomics has been driven by the development of new mass spectrometric (MS) tools and protocols for the identification and quantification of molecular lipid species in various biological matrices. However, the existing methods for minor sphingolipid (SL), glycerophospholipid (GP) and bile acid (BA) analysis show disadvantages like laborious sample preparation, time consuming LC-separation, high sample volumes or insufficient validation data, excluding these methods for high throughput analysis in huge clinical trials.

The present work presents fast, specific, sensitive and robust LC-MS/MS methods for the analysis of SL, GL and BA species. Chromatographic-separation should provide co-elution of analytes and internal standards within each lipid class. The latter is of major importance to compensate for matrix effects and varying ionization efficiencies. Additionally, these methods should provide automated data analysis tools to allow high sample throughput, a prerequisite for lipid species quantification in huge clinical trials. Finally, these methods should be applied for lipid species analysis in various biological matrices, including plasma, cell homogenates and tissue samples.

1. A method was developed for the simultaneous quantification of phosphatidic acid (PA), phosphatidylglycerol (PG), bis(monoacyl)glycerophosphate (BMP) and cardiolipin (CL) species using hydrophilic interaction chromatography (HILIC) coupled with ESI-MS/MS in positive ionization mode. GL extraction was performed in the presence of butanol. HILIC showed excellent peak shapes and the isobaric compounds PG and BMP were successfully baseline-separated. Furthermore, HILIC provides co-elution of lipid species and their internal standards. Since many lipid species differ only by their chain length and/or saturation

degree, co-elution may exhibit isotopic overlap which has to be corrected. Therefore, theoretically calculated isotope profiles were implemented into self programmed Excel Macros, which successfully corrected, for the first time, this complex isotopic overlap of an MS/MS experiment.

2. As one major achievement of this thesis, LC-MS/MS methods for the analysis of various low abundant SLs were developed. Separation of distinct SL classes and co-elution of analytes and internal standards was achieved by HILIC. MS/MS-analysis was either conducted in negative ionization mode for S1P and LPA quantification, or in positive ionization mode for the quantification of SPH and metabolites as well as for HexCer and LacCer. Since these methods use the same butanolic extraction and LC components, it is possible to analyze both sets of analytes from one extract. Treatment of fibroblasts with myriocin, which inhibits the first step of SL biosynthesis, and sphingosine-kinase inhibitor, demonstrated the importance of methods covering multiple instead of single sphingolipid metabolites. Additionally, SLs were quantified in plasma and in lipoprotein fractions prepared by fast performance liquid chromatography (FPLC). SLs showed a specific distribution across lipoprotein classes and the SL species profiles in separated lipoproteins may help to address the origin of plasma SLs.

3. BA species were quantified from human plasma/serum using ESI-MS/MS in negative ionization mode. LC-separation was performed with a reversed phase-C18 column and a gradient elution at basic pH was applied. Baseline-separation of eighteen BA species (free and conjugated) and a high sensitivity was achieved within 6.5 min runtime. The sample preparation procedure was based on protein precipitation with acetonitrile. Validation was performed according to FDA guidelines. This method provides a valuable tool for both, routine diagnostics and the evaluation of BAs as diagnostic biomarkers in large clinical studies.

7.2 Summary in German

Die äußerst wichtige Rolle von Lipiden in verschiedenen Zellen, Geweben und Körperflüssigkeiten wurde durch eine Reihe von Studien gezeigt. Viele Krankheiten stehen in engem Zusammenhang mit Störungen im Lipid-Stoffwechsel. Beispiele für solche Krankheiten sind unter anderem Krebs, Typ 2 Diabetes und Arteriosklerose. Neueste Ergebnisse im Bereich der „Lipidomics", wurde durch die Entwicklung neuartiger massenpektrometrischer Tools für die Identifizierung und Quantifizierung molekularere Lipid-Spezies in verschiedenen biologischen Materialien, vorangetrieben. Bereits existierende Methoden für die Analyse von gering konzentrierten Sphingolipiden (SL), Glycerophospholipide (GP) und Gallensäuren weisen deutliche Limitationen hinsichtlich aufwendiger Probenvorbereitungen, langen chromatographischen Trennungen, hohen Probenvolumina oder unzureichenden Validierungs-Daten auf. Aus diesem Grund sind diese Methoden nicht geeignet für Biomarker-Screening in großen klinischen Studien.

Die vorliegende Arbeit beschreibt schnelle, sensitive und robuste analytische Methoden für die Quantifizierung von SL, GL und Gallensäuren mittels Flüssigchromatographie Tandem-Massenspektrometrie (LC-MS/MS). Die chromatographische Trennung sollte hinsichtlich der Co-Elution von Analyten und internen Standards optimiert werden. Diese ist Voraussetzung um potentielle Matrix-Effekte und unterschiedliche Ionisationseffizienzen auszugleichen. Für den Einsatz in großen klinischen Studien, sollte die Datenauswertung automatisiert werden, um einen hohen Probendurchsatz zu gewährleisten. Neben Blutplasma sollten auch andere biologische Materialien, wie kultivierte Zellen und Gewebe eingesetzt werden.

1. Zunächst wurde eine Methode für die simultane Analyse von Phosphatidsäure (PA), Phosphatidylglycerol (PG), Bis(monoacyl)glycerolphsophat (BMP) und Cardiolipin (CL) entwickelt. Quantifizierung dieser Lipide erfolgte durch hydrophile Interaktionschromatographie (HILIC) gekoppelt mit ESI-MS/MS im positiven Ionisations-Modus. HILIC zeichnete sich durch optimale Peak-Qualitäten und Basislinien-Trennung der isobaren Komponenten PG und BMP aus. Zusätzlich wurde durch den Einsatz von HILIC eine Co-Elution der Lipid-Spezies und der zugehörigen internen Standards erreicht. Da sich viele Lipid-Spezies nur in ihrer Kettenlänge und/oder ihrem

Sättigungsgrad unterscheiden, führt Co-Elution zu einem Isotopen-Überlapp der korrigiert werden muss. Aus diesem Grund wurden theoretisch berechnete Isotopen-Profile in selbst-programmierte Excel-Makros implementiert. Der komplexe Isotopen-Überlapp wurde im Folgenden, zum ersten Mal, in einem MS/MS-Experiment erfolgreich korrigiert.

2. Als weiterer Schwerpunkt dieser Doktorarbeit sollten neue analytische Methoden für den Nachweis und für die Quantifizierung von verschiedenen Sphingolipiden entwickelt werden. Durch die Anwendung von HILIC wurden die verschiedenen SL-Klassen errfogreich getrennt, und gleichzeitige Co-Elution von Analyten und Internen Standards konnte erreicht werden. Charakterisierung mittels MS wurde für S1P und LPA im negativen Ionisationsmodus, für SPH und Metabolite sowie für HexCer und LacCer, im positiven Ionisationsmodus durchgeführt. Da beide Methoden die identische butanolische Extraktion, und die gleichen chromatographischen Komponenten verwenden, konnte das komplette SL Profil aus demselben Extrakt bestimmt werden. Ein Inkubations-Experiment von Fibroblasten mit Myriocin, einem Inhibitor des ersten Schrittes der SL-Biosynthese, und einem Sphingosinkinase-Inhibitor zeigte Veränderungen des SL Profils. Um weitere wichtige Erkenntnisse des SL-Stoffwechsels in Zusammenhang mit verschiedenen Erkrankungen zu gewinnen ist es daher wichtig, kombinierte Methoden, die eine Vielzahl von Metaboliten erfassen, anzuwenden. In einem zusätzlichen Experiment wurden SL in Plasma und in FPLC-getrennten Lipoprotein-Fraktionen quantifiziert. SLs zeigten eine spezifische Verteilung über die verschiedenen Lipoprotein-Klassen.

3. Gallensäuren wurden aus humanem Plasma/Serum mittels ESI-MS/MS in negativem Ionisations-Modus quantifiziert. Die chromatographische Trennung erfolgte mit einer Umkehrphase C18-Säule. Innerhalb von 6.5 min wurden 18 verschieden Gallensäuren mittels Gradienten-Elution unter basischen Bedingungen getrennt. Als Probenvorbereitung wurde eine Proteinfällung mit Hilfe von Acetonitril angewendet. Da diese Methode im Rahmen der Routinediagnostik und in großen klinischen Studien

eingesetzt wird, wurde eine Validierung auf Grundlage der FDA-Richtlinien durchgeführt.

8 Curriculum vitae

Personal Information

Name:	Max Benjamin Scherer
Date of birth:	January 15th , 1983
Place of birth	Hamburg, Germany

Tertiary Education

11/2007 – present	PhD thesis at the Institute of Clinical chemistry and laboratory medicine, University Hospital Regensburg Supervisor: Prof. Dr. Gerd Schmitz, Prof. Dr. Otto Wolfbeis
09/07	Diploma in chemistry and medicinal chemistry at the university of Regensburg
01/07-09/07	Diploma thesis at the Institute of Clinical chemistry and laboratory medicine, University Hospital Regensburg *Quantitative analysis of sphingosine-1-phosphate and lysophosphatidic acid by LC/MS-MS*
10/05-12/06	Main studies of chemistry with focus on medicinal chemistry at the university of Regensburg
09/04-08/05	Main studies of chemistry at the LMU Munich
08/04	Prediploma in chemistry at the LMU Munich
10/02-08/04	Basic studies of chemistry and biochemistry at the Ludwig-Maximilians-Universität (LMU) Munich

School Education

07/02	Abitur (eqv.: A-level)
09/93-08/02	Gymnasium Unterhaching
09/89-08/93	Basic school Unterhaching, Munich

9   Abstracts and publications

Parts of this thesis were published or presented as posters or oral lectures.

Original Publications

Scherer M, Schmitz G, Liebisch G. High-throughput analysis of sphingosine 1-phosphate, sphinganine 1-phosphate, and lysophosphatidic acid in plasma samples by liquid chromatography-tandem mass spectrometry. Clin Chem 2009;55:1218-22.

Scherer M, Gnewuch C, Schmitz G, Liebisch G. Rapid quantification of bile acids and their conjugates in serum by liquid chromatography-tandem mass spectrometry. J Chromatogr B Analyt Technol Biomed Life Sci 2009;877:3920-5.

Scherer M, Leuthaeuser-Jaschinski K, Ecker J, Schmitz G, Liebisch G. A rapid and quantitative LC-MS/MS method to profile sphingolipids. J Lipid Res 2010, 51:2001-11.

Ecker J, Liebisch G, **Scherer M**, Schmitz G. Differential effects of conjugated linoleic acid isomers on macrophage glycerophospholipid metabolism. J Lipid Res 2010 Sep; 51 (9):2686-94.

Scherer M, Böttcher A, Schmitz G, Liebisch G. Sphingolipid profiling of human plasma and FPLC-separated lipoprotein fractions by hydrophilic interaction chromatography tandem mass spectrometry. Biochim Biophys Acta 2010 (submitted).

Scherer M, Schmitz G, Liebisch G. Simultaneous quantification of cardiolipin, bis(mono)acylglycerophosphate and their precursors by hydrophilic interaction LC-MS/MS including correction of isotopic overlap. Anal. Chem. 2010 (accepted).

Sybille GE Meyer, Agnieszka E Wendt, **Max Scherer**, Gerhard Liebisch, Uta Kerkweg, Gerd Schmitz and Herbert de Groot. The inhibition of de novo synthesis of sphingolipids impairs the uptake of transferrin in mammalian cells. BMC Cell Biology 2010 (in revision)

Katharina Ruebsaamen, Gerhard Liebisch, **Max Scherer**, Alfred Boettcher, Gerd Schmitz
Sphingolipid metabolism of platelet senescence (in preparation).

Oral lectures

Max Scherer, Kerstin Leuthäuser-Jaschinski, Gerd Schmitz, Gerhard Liebisch, A rapid and qantitative LC-MS/MS method to quantify sphingolipids, *1st Steering Comitee Meeting of the EU-funded „LipidomicNet" project, Regensburg 2009*

Max Scherer, Gerd Schmitz, Gerhard Liebisch, Sphingolipid analysis in plasma and FPLC-separated lipoprotein fractions by LC-MS/MS, *2nd Steering Comitee Meeting of the EU-funded „LipidomicNet" project, Munich 2009*

Max Scherer, Gerd Schmitz, Gerhard Liebisch, Simultaneous analysis of PA, PG, BMP and CL by LC-MS/MS, *Midterm Reviewer Meeting of the EU-funded „LipidomicNet" project, Zurich 2010*

Poster presentations

Max Scherer, Gerd Schmitz, Gerhard Liebisch, High throughput analysis of sphingosine-1-phosphate, sphinganine-1-phosphate and lysophosphatididc acid on plasma samples by LC-MS/MS, 49th *International Conference on the biosience of lipids (ICBL), Maastricht 2008*

Max Scherer, Kertsin Leuthäuser-Jaschinski, Gerd Schmitz, Gerhard Liebisch, A rapid and validated LC-MS/MS method to quantify structural and regulatory sphingolipids, Frontier *Lipidology, Lipidomics in Health and Disease, Gothenburg 2009*

Max Scherer, Kertsin Leuthäuser-Jaschinski, Gerd Schmitz, Gerhard Liebisch, A rapid and validated LC-MS/MS method to quantify structural and regulatory sphingolipids, *6. Jahrestagung Deutschen Vereinten Gesellschaft für Klinische Chemie und Laboratoriumsmedizin (DGKL), Leipzig 2009*

Max Scherer, Gerd Schmitz, Gerhard Liebisch, Sphingolipid analysis in plasma and separated lipoproteins by LC-MS/MS, 50th *International Conference on the biosience of lipids (ICBL), Regensburg 2009*

Max Scherer, Gerd Schmitz, Gerhard Liebisch, Sphingolipid analysis in plasma and separated lipoproteins by LC-MS/MS, 50th *International Conference on the biosience of lipids (ICBL), Regensburg 2009*

Max Scherer, Gerd Schmitz, Gerhard Liebisch, Sphingolipid analysis in plasma and separated lipoproteins by LC-MS/MS, *1st Styrian Conference on Lipid Mass Spec, Graz 2009*

Max Scherer, Gerd Schmitz, Gerhard Liebisch, Quantitative analysis of sphingolipids in cells and plasma by LC-MS/MS, 1st International *Metabolomics Symposium, Munich 2010*

Max Scherer, Gerd Schmitz, Gerhard Liebisch, Sphingolipid analysis in plasma and separated lipoproteins by LC-MS/MS, 51th *International Conference on the biosience of lipids (ICBL), Bilbao 2010*

Eidesstattliche Erklärung

Ich erkläre hiermit an Eides statt, dass ich die vorliegende Arbeit ohne unzulässige Hilfe Dritter und ohne Benutzung anderer als der angegebenen Hilfsmittel angefertigt habe. Die aus anderen Quellen direkt oder indirekt übernommenen Daten und Konzepte sind unter Angabe des Literaturzitats gekennzeichnet. Weitere Personen waren an der inhaltlich-materiellen Herstellung der vorliegenden Arbeit nicht beteiligt. Insbesondere habe ich hierfür nicht die entgeltliche Hilfe eines Promotionsberaters oder anderer Personen in Anspruch genommen. Niemand hat von mir weder unmittelbar noch mittelbar geldwerte Leistungen für Arbeiten erhalten, die im Zusammenhang mit dem Inhalt der vorgelegten Dissertation stehen. Die Arbeit wurde bisher weder im In- noch im Ausland in gleicher oder ähnlicher Form einer anderen Prüfungsbehörde vorgelegt.

Regensburg, den _____   _____

                                                                    (Max Scherer)